2014

The Regulation of the Eight-Exon Isoform of the Coxsackievirus and Adenovirus Receptor (CAR^{EX8}) and Its Biological Relevance

Poornima Kotha Lakshmi Narayan
Wright State University

THE REGULATION OF THE EIGHT-EXON ISOFORM OF THE COXSACKIEVIRUS AND ADENOVIRUS RECEPTOR (CAR^{EX8}) AND ITS BIOLOGICAL RELEVANCE

A Dissertation submitted in partial fulfillment of the requirements for the degree of

Doctor of Philosophy

By

POORNIMA KOTHA LAKSHMI NARAYAN

B.Sc., Ethiraj College for Women, Chennai, India

M.S., Wright State University, Dayton, USA

2014

Wright State University

WRIGHT STATE UNIVERSITY

GRADUATE SCHOOL

July 10, 2014

I HEREBY RECOMMEND THAT THE DISSERTATION PREPARED UNDER MY SUPERVISION BY Poornima Kotha Lakshmi Narayan ENTITLED. The regulation of the eight-exon isoform of the Coxsackievirus and Adenovirus Receptor (CAR^{Ex8}) and its biological relevance BE ACCEPTED IN PARTIAL FULFILMENT OF THE REQUIREMENTS FOR THE DEGREE OF Doctor of Philosophy

Katherine J.D.A. Excoffon, Ph.D.
Dissertation Director

Mill W. Miller, Ph.D.
Director, Biomedical Sciences
Ph.D program

Robert E. W. Fyffe, Ph.D.
Vice President for Research and Dean of
the Graduate School

Committee on Final Examination

Katherine J.D.A. Excoffon, Ph.D.

David Goldstein, Ph.D.

Robert Putnam, Ph.D.

Dawn P. Wooley, Ph.D.

Julian Gomez-Cambronero, Ph.D.

Abstract

Poornima Kotha Lakshmi Narayan Ph.D. Biomedical Sciences Ph.D. Program. Wright State University, 2014. The regulation of the eight-exon isoform of the Coxsackievirus and Adenovirus Receptor (CAR^{Ex8}) and its biological relevance

The airway epithelium poses a formidable barrier for the entry of pathogenic viruses due to the formation of tight junctions between adjacent epithelial cells. The coxsackievirus and adenovirus receptor (CAR), a member of the Ig superfamily of cell junction adhesion proteins, is the primary receptor for adenovirus entry and infection. As a result of alternative splicing, two transmembrane isoforms of CAR are generated. While the seven-exon isoform of CAR (CAR^{Ex7}) is hidden on the basolateral surface of polarized epithelia, the eight-exon isoform of CAR (CAR^{Ex8}) localizes within the sub-apical region and at the air-exposed apical surface. Apical localization of CAR^{Ex8} makes it accessible to invading adenovirus entering the lumen of the airway and able to facilitate viral entry into the epithelium. Previous studies have shown that Interleukin-8 (IL-8), a proinflammatory cytokine and a neutrophil chemoattractant, increases the susceptibility of the airway epithelium to adenoviral infection. I hypothesized that the apical CAR^{Ex8} protein expression level and localization are responsible for the susceptibility of a polarized epithelium to viral infection. Moreover, I hypothesized that CAR^{Ex8} expression is tightly regulated by mediators of IL-8 signaling and the endogenous function CAR^{Ex8} is to tether neutrophils at the apical surface of the polarized epithelium. Finally, I hypothesized that adenovirus

has co-opted CAR^{Ex8} and neutrophil transmigration to enhance infection of the polarized epithelium.

Consistent with these hypotheses, I demonstrate that IL-8 increases the expression and the apical localization of CAR^{Ex8} in polarized airway epithelial cells. In addition, IL-8 differentially activates AKT/S6K and inactivates GSK3β to augment the protein synthesis of CAR^{Ex8}. Increased CAR^{Ex8} is able to mediate increased neutrophil binding at the apical surface of the epithelium that is completely abolished by competition with CAR-binding adenovirus fiber-knob. Finally, I also demonstrate that neutrophils adhering to the epithelial apical surface are able to promote adenoviral infection. Taken together, these data suggest that adenovirus has evolved to co-opt the host innate-immune response to the inflammation caused by molecules within inhaled droplets, pre-existing inflammation, or even adenovirus itself, in order to gain entry into the polarized epithelium by inducing the increased expression of endogenous apically localized CAR^{Ex8}.

Table of Contents

List of Figures

List of Tables

Abbreviations:

Ad	Adenovirus
AJ	Adherens junction
β-Gal	Beta-galactosidase
CF	Cystic Fibrosis
CAR^{EX7}	Coxsackievirus and Adenovirus receptor – Exon 7
CFTR	Cystic Fibrosis Transmembrane Conductance Regulator
COPD	Chronic Obstructive Pulmonary Disease
CAR^{EX8}	Coxsackievirus and Adenovirus receptor – Exon 8
CHX	Cycloheximide
DAF	Decay Accelerating Factor
DOX	Doxycyclin
eIF2B	Eukaryotic Initiation Factor 2B
FK	Fiber Knob
GAPDH	Glyceraldehyde 3- Phosphate Dehydrogenase
GSK3β	Gycogen Synthase Kinase Beta
HBSS	Hank's Balanced Salt Solution
ICAM-1	Intercellular Adhesion Molecule -1
IFN-γ	Interferon-gamma
IL-8	Interleukin -8
LAD-1	Leukocyte Adhesion Deficiency
MCP-1	Monocyte Chemoattractant Protein -1
MIP-1	Macrophage Inflammatory Protein -1
MOI	Multiplicity of Infection

MTOC	Microtubule-Organizing Center
PAR	Protease Activated Receptor
PMN	Polymorpho Nuclear Leukocytes
JAC	Junctional Adhesion Complex
JAML	Junctional Adhesion Molecule Like
S6K	Ribosomal S6 Kinase
TER	Transepithelial resistance
TGF-β	Transforming Growth Factor
TJ	Tight Junction
TNF-α	Tissue Necrosis Factor – Alpha
Vg	Viral genome
ZO-1	Zona Occludin -1

Acknowledgements

I first of all would like to thank God for being kind and blessing me with the strength and courage to accomplish my endeavors. I thank my mentor Dr. Katherine Excoffon for giving me an opportunity to work in her lab, for always believing in me and for caring. The faith that she had in my ability kept me going when I struggled to kick-start my project. She has always encouraged me and let me present my work at top-notch conferences around the United States. She never failed to spread the passion that she had for science by engaging everyone in the lab in thought provoking, scientific discussions. Working in her lab has helped me think and mature as a scientist. She was always open to the new ideas that I proposed and encouraged me to pursue them. I thank each and every committee member; Dr. Dawn P. Wooley, Dr. David Goldstein, Dr. Julian Gomez-Cambronero, and Dr. Robert Putnam. They have been extremely supportive and constructive in their suggestions towards helping me complete my thesis. They have been very flexible in accommodating my committee meetings.

I like to extend my special thanks to Dr. Cambronero and his lab members Karen Henkels and Madhu Mahankali for being very generous in sharing their reagents with our lab. I would like to thank all the present and past members of the Excoffon lab (Priyanka Sharma, Abimbola Kolawole, Kathy Frondorf, Trisha Brockman, Ran Yan, Sahar Kamel, Mahamoud S. Alghamri, Blake Spratski,

Jonathan Bowers, James Readler and Nathan Northern) who have always been sharing, available to help me with my project, available for scientific discussions and lot of fun indeed. In particular, I thank Priyanka Sharma for her support, for helping me with trouble shooting my experiments when needed and reviewing my documents. I thank Jonathan Bowers for editing my thesis. I thank Dr. Wooley for helping with the adeno-associated virus project. She made the AAV libraries she also provided me with the H9 cells and trained in isolating neutrophils. I thank my friends Madhu, Jerome, Bindu, Swathi, Divya, and Lakshmi for their support throughout my Ph.D and for making my stay in the US a memorable one. My special thanks to Madhu without whom I could not have completed my Ph.D. She was always there for me to lift my spirits. She built confidence in me whenever I lost faith in myself and thought of quitting. Meeting her and being her roommate has been one of the best things that happened to me at the Wright State University. She has been my emotional back-up and a pillar of support. We have also had loads of fun and I will cherish the memories forever. I thank my colleagues Geetha, Vishnu, Ramya, Dhawal, Hima, and Sriram for all the fun we had. Last but not the least, I would like to thank my wonderful parents and my brother, Ashwin who have made many sacrifices for me to have successful career. They have always supported me and have never failed to care for me.

Chapter 1: Introduction:

Our world is full of pathogens that prey on nutrient-rich organisms. All mammals, including humans, have evolved a complex set of innate barriers to prevent infection. The lung is one of the organs that comes into direct contact with the external environment and is a major portal of entry. The epithelium of the lung provides a first line of defense and is constantly exposed to inhaled pathogens that are normally cleared without causing inflammation or damage to the lung. However, there are times when susceptibility to infection is elevated. Much remains to be understood about factors that predispose us to the infection and how pathogens crack the epithelial barrier to gain entry into the host.

1.1. Junctional adhesion complex (JAC)

Epithelial cells line the mucosal surface of the airway. These are polarized cells with the apical surface facing the lumen of the airway tract and the basal surface facing the interstitium. One of the essential functions of the epithelium is to form a barrier thereby separating the harsh outside environment from the more fragile inside. Epithelial cells prevent the paracellular movement of inhaled particles into the interstitium. Likewise, it also prevents the loss of essential components into the airway lumen. This barrier function is accomplished by the JAC, which is composed of transmembrane and cytoplasmic tight junction proteins (TJ) and adherens junction (AJ) proteins (Figure 1A). Tight junction proteins are located at

the apico-lateral surface of the epithelial cells and form a zipper like structure that seals the space between the epithelial cells. Tight junction proteins include transmembrane proteins, cytoplasmic plaque proteins and cytoskeletal proteins [1]. Claudins are an example of tight junction transmembrane proteins that form homodimers with those on adjacent cells and form tight junction strands. Other transmembrane proteins including occludin and tricellulin are localized within or in close proximity to the tight junction strands. The cytoplasmic domains of both claudin and occludin bind to tight junction cytoplamic plaque proteins, which include: Zona occludin 1, 2 and 3 (ZO-1, ZO-2 and ZO-3) (Figure 1B) [2]. These are structurally related proteins that contain several functional domains (three PDZ domains, one SH3 domain and one GUK domain) through which they can interact with actin thereby linking the tight junctions to the actin cytoskeleton. In addition, tight junction proteins include junctional adhesion molecules (JAMs) and the coxsackievirus and adenovirus receptor (CAR), which belong to the immunoglobulin (Ig) superfamily of proteins. Although CAR is often classified as a tight junction protein, CAR is on the basolateral side of the tight junction and mainly overlaps with adherens junction proteins, such as epithelial cadherin (E-cadherin) [3, 4].

Adherens junctions are found beneath the tight junction seal (Figure 1B). These junctions serve to hold adjacent epithelial cells together as opposed to completely sealing the space between cells. Adherens junction proteins are comprised of the cadherin family of transmembrane proteins, Ig-like proteins and cytoplasmic plaque proteins such as α/β/δ-catenins [1]. The extracellular domain

of E-cadherin possesses five repetitive sub-domains called the extracellular cadherin or the ‘EC’ domain [5]. It is through these sub-domains that cadherins form homophillic interactions with those on the adjacent cells in a calcium-dependent manner. Treating the cells with calcium chelators, such as EDTA, disrupts the cadherin-cadherin interaction by removing calcium and allowing the junctions to fall apart. Subjacent to adherens junction are the desmosomal junctions, which aid in anchoring the neighboring cells. Similar to tight and adherens junction proteins, desmosomal junctions are also composed of transmembrane proteins and cytoplasmic plaque proteins. Transmembrane proteins include, JAM-C, desmoglein and desmocollin, while the plaque proteins include desmoplakin, plakophillin and γ-catenin. The cytoplasmic plaque proteins are connected to the intermediate filaments [1]. Therefore, the epithelial barrier integrity is maintained by the combination of these junctional proteins. Alteration in the expression and localization of these junctional proteins will tremendously impact the transepithelial resistance and permeability of the epithelial barrier.

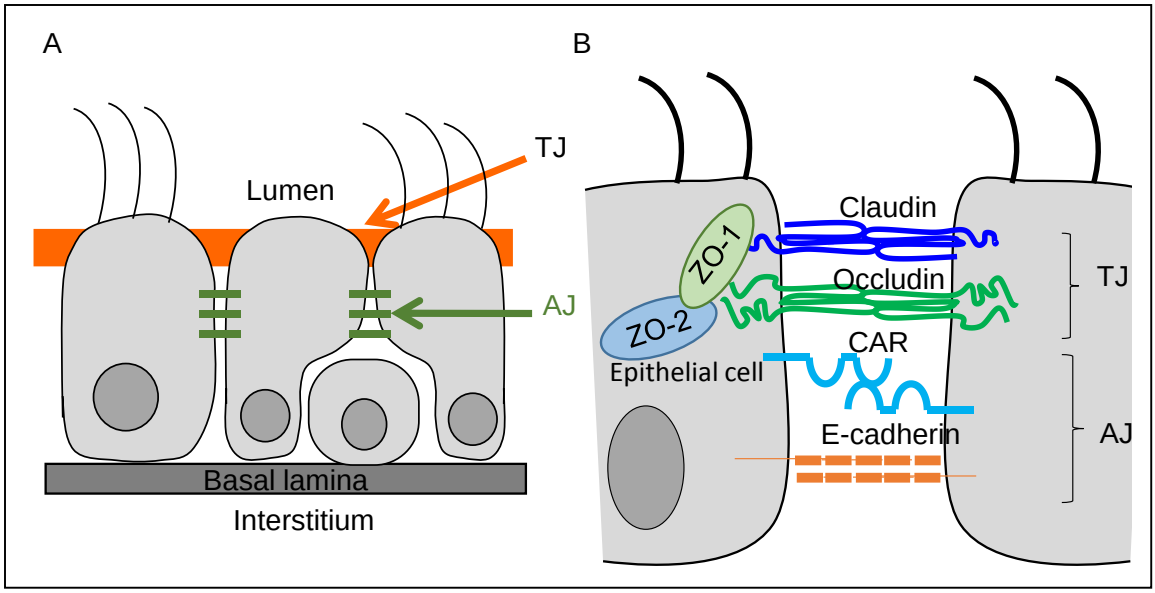

Adapted from Chin et al., 2007

Figure 1: Schematic of polarized epithelial cells. The apical surface of the cells faces the air-exposed airway lumen and the basolateral (basal) surface faces the interstitium. The cells are held together by the junctional adhesion complex (JAC) which is composed of apico-lateral tight junction (TJ) and basolateral adherens junction (AJ) proteins. B. A schematic of epithelial cells showing the different components of TJ and AJ. TJ proteins include transmembrane proteins such as claudin and occludin and cytoplasmic scaffolding proteins such as zona occludins (ZO-1 and -2). The adherens junction proteins include transmembrane proteins such as coxsackievirus and adenovirus receptor (CAR) and E-cadherin.

1.2. Regulation of adhesion proteins:

The expression and localization of various epithelial cell surface adhesion proteins are tightly regulated and are responsive to external stimuli, such as inflammation. For example, exposure of airway epithelial cells to tissue necrosis factor alpha (TNF-α) in combination with interferon gamma (IFN–γ) downregulates the gene expression and redistributes the tight junction proteins JAM and ZO-1 in airway epithelia. Likewise, in endothelial cells, gene expression and localization of CAR is downregulated in response to INF-γ and TNF-α. These cytokines also increase the permeability of both epithelial and the endothelial cells [6, 7]. As a result, the barrier integrity and the epithelial cell permeability is compromised by exposure to cytokines [7]. Tumor growth factor beta (TGF-β) and TNF-α negatively regulate the gene expression of occludin and claudin in testis. IFN-γ disrupts the epithelial barrier integrity by promoting macropinocytosis of the tight junction proteins occludin, claudin-1, and JAM-A [8, 9]. Intercellular adhesion molecule-1 (ICAM-1) relocates to the apical surface of intestinal epithelial cells in response to IFN-γ [10]. Interleukin-8 (IL-8), a proinflammatory cytokine relocalizes $\alpha_v\beta_3$ integrin and CAR at the epithelial apical surface. All these examples provide evidence for a profound effect of cytokines on the junctional proteins.

1.3. Junctional proteins as viral receptors:

The port of entry for many viruses has numerous barriers. When entering the respiratory tract, they first confront the mucus layer, above the apical surface of the epithelium that is constantly being swept out of the respiratory tract. Once through the mucus, the virus must find its receptor on the epithelium. While many

viruses utilize apical proteins as receptors for entry and infection (for example: influenza virus uses α 2-6 linked-sialic acid, rhinovirus uses ICAM-1), other viruses utilize junctional proteins as their primary receptor. For example: reovirus uses JAM-A [11], hepatitis C requires claudin and occludin [12], the measles virus depends on nectin-4, an AJ protein, as its primary receptor [13], and the coxsackie B virus along with most adenovirus serotypes utilize CAR as a primary receptor [14, 15]. The viruses that have adapted to utilize epithelial apical proteins as primary receptors are expected to find their receptors and bind to the apical surface of epithelial cells to initiate infection rather easily. However, if a virus has its primary receptor sequestered below the TJ, accessing the primary receptor to initiate an airborne infection appears to be more complicated and challenging. For a long time, it was believed that a mechanical break in the epithelial junctions was required to allow the virus to access its basolaterally localized primary receptor. Although this continues to serve as a potential mechanism for viral infection, recent studies have shown that viruses are astute in breaking into the intact epithelium. For example, Coxsackie B virus binds to DAF, an apical protein, which facilitates the translocation of the virus to the tight junction where it can interact with CAR and gain entry into the host cell [16]. Reovirus binds sialic acid at the apical surface which then mediates the binding of the virus to its primary receptor, JAM-A, allowing the virus to enter its host [17]. However, recent studies suggest that viral receptors once believed to be sequestered below the tight junctions might have alternatively spliced isoforms that can localize to the apical surface, facilitating the initial viral entry from the apical surface. Our lab has shown that adenovirus binds

to an alternatively spliced version of CAR (CAR^{Ex8}), which localizes to the apical surface, allowing adenovirus to gain entry into the airway epithelia from the air exposed apical surface [18-20].

1.4. Adenovirus

Adenovirus is a non-enveloped virus that is icosohedral in shape. Adenovirus is typically 80 nm in size and encloses a double stranded DNA genome. Over 50 human adenovirus types have been identified and are categorized into groups A through G. Adenoviruses most commonly cause mild and self-limiting upper and lower respiratory tract infections. However, in military recruits, pediatric patients, and in immunocompromised individuals, adenoviruses can cause fatal respiratory distress. Apart from respiratory infections, adenovirus can also cause conjunctivitis, gastroenteritis, and cystitis [21]. The virion has 12 triangular faces and 12 vertices. While the triangular faces are composed of a total of 240 hexons, the vertices are composed of pentons. From each penton base arises a trimeric fiberknob (FK) [21-23]. In order to infect, adenovirus first attaches to the host cell by binding to its receptor on the target cell via FK. The FKs of all adenovirus species, except group B, bind and utilize CAR as their primary receptor [15, 21, 23-27]. Several other important co-receptors, such as MHC class I [28], sialic acid [29], and coagulation factor X [30], have been described. Subsequently, the RGD motif on the Ad penton base binds to the $\alpha_v\beta_3$ or $\alpha_v\beta_5$ integrins, which function as co-receptors. Binding to these integrins activates downstream signaling, which facilitates clathrin-mediated endocytosis of the virus. Alternatively, the virus is also endocytosed through macropinocytosis or other non-clathrin mechanisms [31, 32].

After internalization, as the endosomes acidify, the Ad-FK dissociates from the capsid leading to a partial uncoating of the virus and release of protein VI. Protein VI aids in the lysis of the endosomal membrane and thereby facilitates viral escape into the cytoplasm [33]. Once in the cytoplasm, the virus interacts with dynein, a molecular motor protein, via the viral capsid protein, hexon, and is translocated along the microtubules to the microtubule organizing center (MTOC) near the nucleus [33]. From here the virus enters the nucleus via a mechanism that is not yet clearly understood.

1.5. Coxsackie and adenovirus receptor (CAR):

The first step for efficient infection by adenovirus is the attachment to the host cell and this is facilitated by the receptor on the host cell. As the name suggests, CAR was first identified as a receptor for both Coxsackie B viruses and most serotypes of adenovirus [15, 34-36]. It was shown that CAR is essential for the development of the heart, as knocking out CAR in mice proved embryonically lethal [37]. It was shown that CAR is required for the efficient development of both the heart and the lymphatic system [37, 38]. CAR is expressed in a variety of organs including the heart, brain, pancreas, lung, kidney, liver, small intestine, colon, and prostrate [37, 39, 40]. In polarized epithelia CAR is important for the maintenance of the epithelial barrier integrity [4]

CAR is a transmembrane protein that belongs to the immunoglobulin superfamily of proteins with two extracellular Ig-like domains. The most distal Ig-like domain, D1, mediates homophilic adhesion between CAR proteins on adjacent cells, heterophilic adhesion with adenovirus fiber knob and junction-adhesion

molecule like protein (JAML) found on leukocytes, such as neutrophils, all at an overlapping interface [7, 41] (Figure 2). The binding affinities of the different CAR interaction are listed in Table 1. CAR binds to Ad FK with nearly a 1000 fold greater affinity than with CAR itself. Therefore, adenovirus FK can outcompete CAR-CAR interactions. This was evident from viral egress studies that demonstrated that once adenovirus has infected the airway epithelium, FK is released into the basolateral extracellular space and breaks the CAR-CAR interactions and epithelial tight junctions to allow the virus to escape to the apical surface [4].

The gene for CAR, located on human chromosome 21 and named *CXADR*, consists of 8 separate exons. Alternative splicing of the exons results in 2 transcripts that encode 2 transmembrane isoforms. Both of the protein isoforms have identical extracellular and transmembrane domains, differing only in the extreme cytoplasmic carboxy-termini. The most abundant isoform originates from the splicing of the first seven exons of CAR (CAR^{Ex7}) (Figure 3A). CAR^{Ex7} localizes at the basolateral surface of polarized epithelial cells and is inaccessible to invading pathogens from the apical surface (Figure 3B) [4, 18-20, 42]. CAR^{Ex7} plays a key role in the maintenance of the epithelial barrier integrity via the formation of homodimers between adjacent epithelial cells. This isoform is also responsible for adenovirus egress after viral infection. The intact airway epithelium is largely resistant to CAR-mediated adenoviral infection because the major isoform is sequestered beneath the tight junction. The alternate transmembrane isoform is derived from mRNA splicing within the seventh exon to the eighth exon (CAR^{Ex8}). This splice event leads to a unique 13 aa c-terminus in CAR^{Ex8} that

replaces 26 aa unique to the c-terminus found in the CAR^{Ex7} isoform (Figure 3A). CAR^{Ex8} resides at the subapical/apical surface of the airway epithelium [18-20]. This apical localization creates a logical explanation as to how adenovirus infection can be initiated from the apical surface into intact epithelium [18]. It is important to understand the regulation of CAR^{Ex8} because any stimulus that either augments or decreases the levels of apically exposed CAR^{Ex8} is likely to be crucial for modulating the susceptibility of the airway to viral infection.

The heterophilic interaction of CAR with JAML on leukocytes is important for neutrophil transepithelial migration during inflammation and infection (explained in detail in the next section).

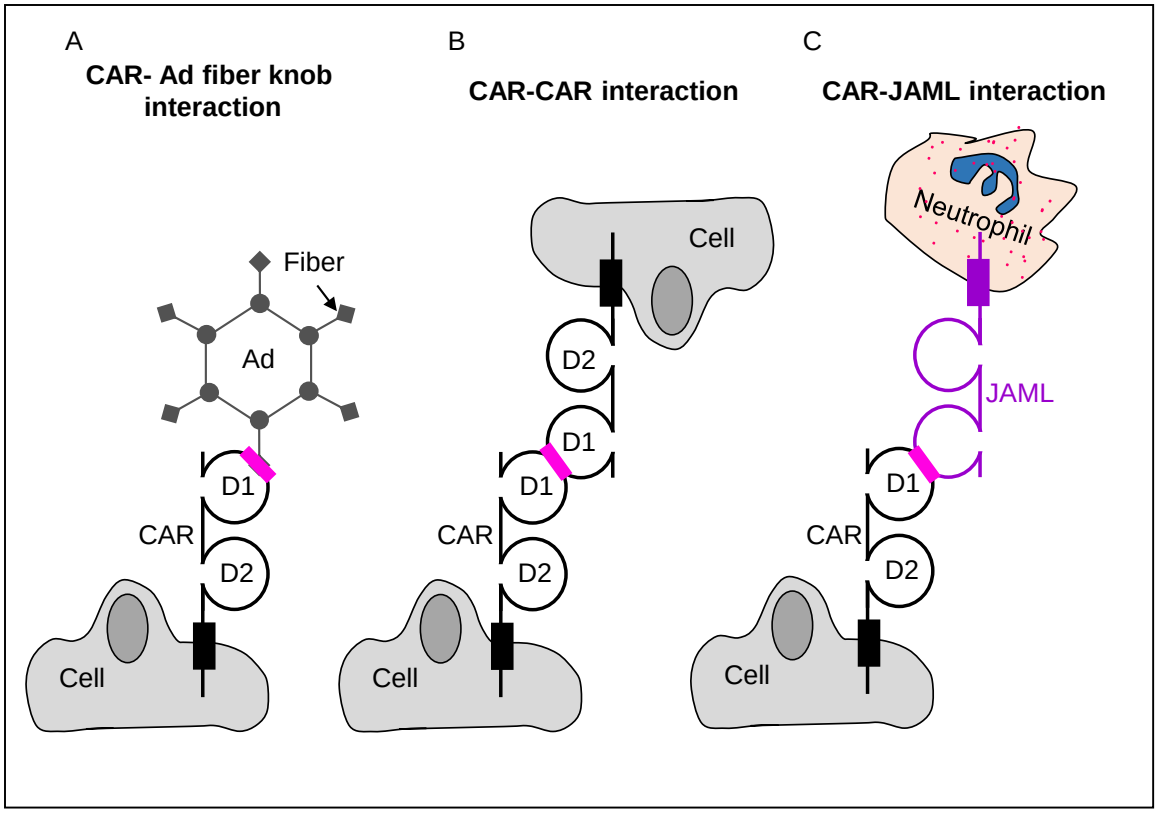

Figure 2: Schematic showing different CAR interactions. A) CAR interaction with adenovirus fiber knob at the CAR D1 domain. B) Hemophilic CAR-CAR interaction occurs between adjacent epithelial cells to hold them together. C) Heterophilic CAR-JAML interaction occurs between epithelial cells and neutrophils. Note that all three interactions occur at the same overlapping interface on CAR

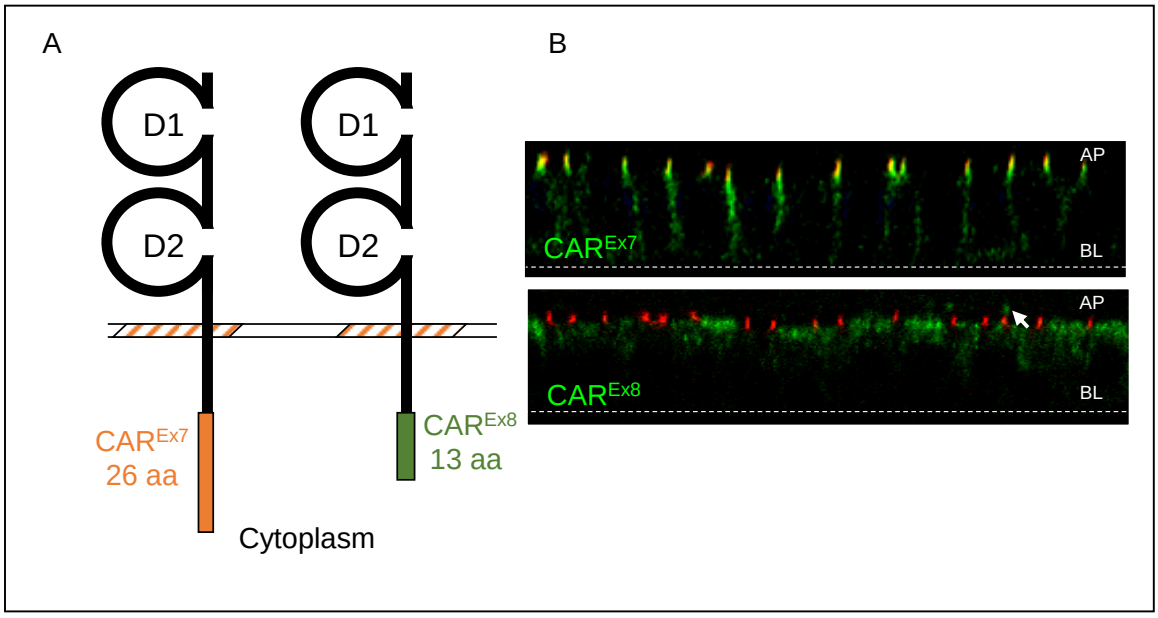

Figure 3: Transmembrane isoforms of CAR and their localization in polarized airway epithelia. A) Schematic of CAR^{Ex7} and CAR^{Ex8} that shows the extracellular region comprising the D1 and the D2 domains, the transmembrane region embedded into a lipid raft within the plasma membrane, and the C-terminus extending into the cytoplasm. The CAR^{Ex7} isoform has 26 aa that are unique to this isoform and CAR^{Ex8} has 13 unique aa due to alternative splicing from a cryptic splice site within the 7^{th} exon of the gene for CAR, CXADR. B) Immunofluorescence staining of the two transmembrane isoforms of CAR (green) and Zo-1 (red) in primary airway epithelial cells. CAR^{Ex7} (top panel) localizes at the basolateral surface and CAR^{Ex8} (bottom panel) localizes at the sub-apical and the apical surface (arrow).

1.6. Junctional adhesion molecule like (JAML)

Moog-Lutz et al., 2003, discovered JAML, a novel member of JAM family of proteins [43]. JAML is a transmembrane protein with extracellular, transmembrane, and intracellular domains. JAML belongs to the immunoglobulin superfamily as it contains two extracellular immunogloubulin (Ig) like domains called the D1 (membrane distal) and the D2 (membrane proximal) domains. One of the intriguing features of JAML is that, unlike other JAMs, it is exclusively expressed on the surface of leukocytes including neutrophils, macrophages, monocytes, γδ T-cells, and to a lesser extent on other human T lymphocytes. JAML interacts with CAR on epithelial cells and therefore is also called AMICA-1 (Adhesion molecule interacting with CAR antigen-1) [43-47]. The crystal structure of the JAML-CAR receptor-ligand pair reveals that the membrane distal D1 domain of JAML interacts with the membrane distal D1 domain of CAR [47].

As mentioned earlier, CAR normally forms homodimers by binding to another CAR molecule on an adjacent cell. This interface where one CAR molecule binds to another CAR molecule overlaps with the binding sites of both adenovirus FK and JAML. One CAR molecule can only bind to one molecule of CAR, JAML, or adenovirus at any one time. About 16 of 18 CAR amino acid residues that are involved in JAML binding overlap with the adenovirus FK binding site. The binding affinities of heterophilic and homophilic CAR interactions are in the order of CAR-adenovirus FK > CAR-JAML > CAR-CAR [24, 47, 48] (Table 1). Therefore, binding to adenovirus fiber knob will inhibit CAR binding to JAML.

Table 1: Binding affinities of CAR-mediated interactions.

Type of CAR interaction	Binding affinity (KD)	reference
CAR-CAR	16 µM	[24]
CAR- JAML	5 µM	[47]
CAR- Ad fiber knob	14 nM	[48]

1.7. Transepithelial migration:

In addition to serving as a barrier to the paracellular movement of large and small molecules, JAC also regulates the migration of polymorphonuclear leukocytes (PMNs), including neutrophils, across the epithelium. Neutrophils are the first leukocytes to arrive at the site of infection. Therefore, neutrophil transepithelial migration is crucial for clearing pathogenic infection. Defective neutrophil transmigration is seen in diseases such as leukocyte adhesion deficiency type-1 (LAD-1) and causes increased susceptibility to pathogens [49, 50]. In contrast, excessive and unregulated neutrophil infiltration can cause tissue damage and is the characteristic of a variety of inflammatory diseases such as inflammatory bowel disease in the gastrointestinal system, chronic obstructive pulmonary disease (COPD) and cystic fibrosis (CF) in the airway.

Upon stimulation, PMNs exit the vascular circulation, by migrating through the paracellular space found between adjacent endothelial cells (a process called transendothelial migration), and reach the connective tissue. PMNs further migrate through the paracellular space between the epithelial cells (transepithelial migration) before encountering the pathogen in the lumen of the airway. While PMN transmigration through the vascular endothelium has been extensively studied, transmigration through the epithelial barrier is not well understood. In addition, there are striking differences between the PMN transendothelial and transepithelial migration. For example: 1) Transendothelial migration occurs in the apical to basal direction, whereas transepithelial migration occurs from the basal surface to the apical surface. 2) The initial PMN-endothelial interaction occurs at

the endothelial apical surface. In contrast, the initial PMN-epithelial interaction occurs at the epithelial basal surface. 3) During transendothelial migration, PMNs migrate a relatively short distance, a few microns, as opposed to > 20 μm distance migrated during transepithelial migration [10, 51]. 4) The adhesive interactions occurring during the transendothelial migration are quite different from those involved in transepithelial migration. For instance, PMN transendothelial migration is dependent on the PMN CD11b/CD18 and CD11a/CD18 protein interaction with the endothelial cell surface ICAM-1 protein. Although CD11b/CD18 is important for transepithelial migration, CD11a/CD18 has not been shown to be involved in transepithelial migration. Moreover, upon stimulation with IFN-γ, ICAM-1 expression is localized to the epithelial apical surface and therefore is not accessible for infiltrating neutrophils. Once migrated ICAM-1 can however mediate adhesion of transmigrated neutrophils to the apical surface [10, 52, 53].

In vitro studies using model human epithelial cell lines have demonstrated that high-density PMN transepithelial migration disrupts the barrier integrity, whereas the low-density PMN migration does not [51, 54]. Low density PMN migration occurs during normal immune surveillance in a tightly regulated manner without compromising the barrier integrity. However, upon pathogenic invasion, intense PMN (including neutrophils) transmigration ensues. Epithelial cells sense the invading microbe through pathogen recognition and subsequently release a number of chemokines, which in turn recruit PMNs. During transepithelial migration, PMNs have to cross a relatively long paracellular path before they can reach the tight junction seal. In order to reach the apical surface, PMNs breach the

epithelial barrier either by loosening or disrupting the complex of junctional proteins supporting the epithelial barrier. The compromised junctional barrier is however, reformed upon the resolution of the infection. Our knowledge on neutrophil transepithelial migration is based on studies conducted in intestinal epithelia. There is currently a gap in the literature regarding this process in airway epithelia [51]. Although, some of the studies in the intestinal epithelium can be translated to the airway epithelium, one must recognize the important anatomical differences between these two systems. The upper airway is comprised of ciliated columnar epithelial cells, while the lower airway is comprised of squamous and cuboidal epithelial cells. On the other hand, the intestinal epithelia are non-ciliated cells and are modified into finger-like projections called microvilli.

Neutrophil transepithelial migration is a complex process that involves multiple interactions between the neutrophil and epithelial cells (Figure 4) [1, 55] and is not well understood. The process of neutrophil transepithelial migration can be broadly divided into early events and late events. During the early events, the physical interaction between the neutrophils and the basal surface of the epithelial cells is sufficient to increase the permeability of the junctional barrier. This event occurs prior to neutrophil transmigration. The increase in permeability occurs as a result of signaling that, without grossly affecting the expression and the localization of the junctional proteins, contracts the actomyosin ring that encircles the cytoplasmic side of epithelial cells. During the late events, which are characterized by the actual migration of neutrophils, remodeling of the junctional proteins is observed. Thus, the physical interaction between the epithelial cells and the

infiltrating neutrophils is essential during both the early and late events of epithelial transmigration [54].

Neutrophil transepithelial migration begins with the adhesion of the neutrophil proteins CD11b/CD18 to a yet unidentified ligand at the epithelial basal surface. There are differences between neutrophil migration in the gastrointestinal system and in the lung. For example, While, CD11b/CD18 is required for neutrophil transepithelial migration in the gastrointestinal system, this process can occur in the absence of CD11b/CD18 in lung epithelial tissue [1]. After initial attachment to the basal surface of the epithelium, neutrophils migrate through the paracellular space. This migration process is a stepwise process that involves various protein-protein interactions, some of which are as follows: 1) activation of epithelial protease-activated receptors 1 and 2 (PAR 1 & 2) by a family of PMN membrane bound proteases called the serposidins [56]; 2) interaction between epithelial CD47 and the PMN-expressed signal regulatory protein α (SIRP-α) [1]; 3) epithelial JAM-C binding to CD11b on neutrophils [57]; 4) interaction between epithelial basolateral CAR with PMN-expressed JAM-L [44]. Ultimately, the migrating neutrophils arrive at the epithelial apical surface where they remain attached transiently (Figure 4).

This attachment enables the PMNs to form a defensive barricade, achieve a critical concentration for maximal activity, and eradicate the invading pathogen. In order to enable PMN adhesion on the epithelial cell apical surface, PMNs should engage in an adhesive interaction with the epithelial cell. The interacting partners involved in this important step are now being recognized. For example DAF, a

glycosyl-phosphatidylinositol like protein, is important for detaching neutrophils from the apical surface. Blocking DAF diminishes the neutrophil transepithelial migration and promotes neutrophil accumulation at the apical surface [58]. Likewise, a variant of CD44 called CD44v6 was found to mediate detachment of neutrophils from the intestinal epithelial apical surface [59]. ICAM-1 has been shown to tether neutrophils at the apical-epithelial surface in both airway and gastrointestinal epithelial cell lines [10, 51, 52]. There is an apparent balance to neutrophil adhesion at the apical surface but how this is regulated and whether there are other major players is unknown.

Numerous human pathologies correlate with the intensity of neutrophil migration and the duration of neutrophil retention within the tissue or luminal space [1, 60]. In particular, several airway diseases, such as CF and COPD, are associated with persistent neutrophils at the epithelial surface [61, 62]. The vast majority of studies and therapeutic approaches have targeted neutrophils to combat neutrophilia. However, this has a global effect and predisposes for the secondary infection. In contrast, tissue-targeted approaches may yield improved disease-specific therapeutics with fewer side effects. For example proteins expressed on the epithelial cell surface, which are involved in recruiting or retaining neutrophils can be targeted in case of airway inflammatory diseases. The fact that CAR^{Ex8} localizes at the apical surface of the epithelial cells and that

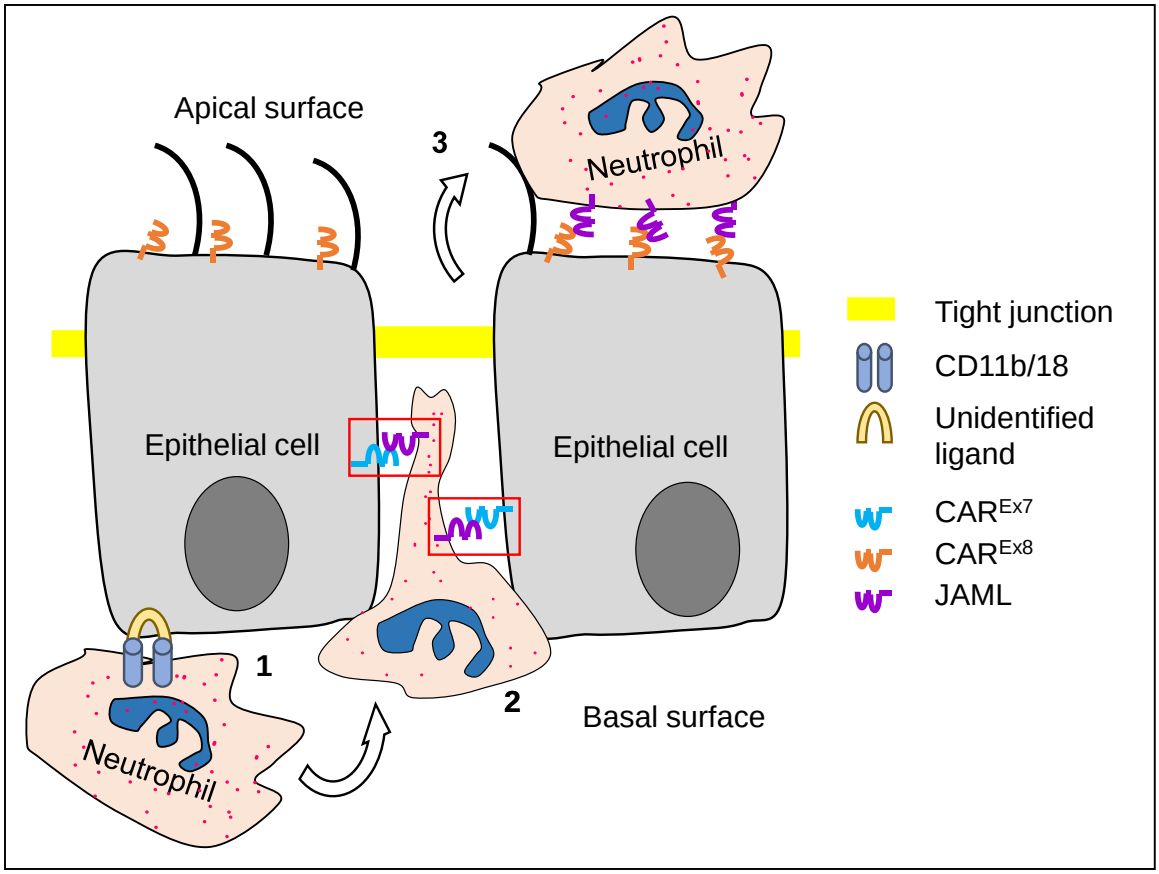

Figure 4 Schematic of the major steps of neutrophil transepithelial migration. 1. Migrating neutrophils attach to the basal surface of the epithelium via an interaction between neutrophil-CD11b/CD18 and epithelial ligand that is yet to be identified. 2. Attached neutrophils migrate through the paracellular space between the adjacent epithelial cells. Interaction between CAR^{Ex7} and JAML at the paracellular space is shown. 3. Finally, the neutrophils crawl up to the apical surface where they remain attached. I hypothesize that CAR^{Ex8} mediated interaction is important for adhesion at the apical surface.

the extracellular domain of CAR can bind to JAML on the neutrophils, suggests that CAR^{Ex8} might be involved in adhering neutrophils at the apical surface of epithelia.

1.8. Inflammatory diseases:

Inflammatory diseases are characterized by dysregulated inflammation, which results in the uncontrolled recruitment of PMN to the epithelial cell surface. Common examples of inflammatory diseases include inflammatory bowel disease, which affects the gastrointestinal system, and COPD, asthma, and CF, all of which affect airway epithelial tissues. CF is an inflammatory disease that affects around 30,000 individuals in the U.S. and 70,000 worldwide [63]. The disease ensues as a consequence of a mutation in the cystic fibrosis transmembrane conductance regulator (CFTR) gene. The CFTR gene codes for a cAMP regulated chloride channel that is crucial for maintaining homeostasis by controlling the osmotic balance and movement of water across the epithelium. As a result of a genetic mutation, CFTR malfunctions, which results in the hyperabsorption of water and the dehydration of the mucus. The resulting jelly-like mucus is sticky and adheres to the epithelial cell surface causing reduced mucociliary clearance, airway obstruction, inflammation, and pathogenic invasion [63-65].

CF lung is characterized by repeated infections (both bacterial and viral), increased inflammation and the excessive infiltration of neutrophils. Adenoviral infections are common in cystic fibrosis patients [66-68] and rank second in the respiratory viruses obtained from young CF patients [66]. Although some of the commonly detected viruses found in patients with cystic fibrosis (CF) include

rhinovirus, human corona virus and parainfluenza virus, these viruses do not contribute to the course of CF disease [67]. However, adenovirus infection is associated with deterioration of lung function in CF [68]. The predisposing factors that contribute for the high prevalence of viral infections in the patients with inflammatory disease is not well understood and is likely complex. The accumulation of neutrophils on the epithelial cell surface in inflammatory diseases causes considerable damage to the surrounding tissue [69]. All these facts suggest the importance of understanding the epithelial cell susceptibility to adenoviral infection in the presence of accumulated neutrophils*.*

1.9. Cytokines regulate viral infection:

The expression and localization of both apical and junctional adhesion proteins in epithelial cells are regulated by various factors including cytokines [53, 70, 71]. Cytokines are released by the epithelial cells themselves and by the resident macrophages [70, 71]. For example, TNF-α and IFN-γ induce ICAM-1 and subsequently enhance rhinovirus binding on airway epithelial cells [53]. Lutschg et al., 2010, demonstrated that IL-8 increases the airway epithelial cell susceptibility to adenoviral infection. They also demonstrated that IL-8 causes the translocation of $\alpha_v\beta_3$ integrin onto the apical surface of airway epithelia [71]. Integrins are adenovirus co-receptors that facilitate adenoviral entry into the cell by increased endocytosis and endosomal escape [25, 32]. However, CAR is the primary receptor that mediates efficient virus attachment, the crucial step that occurs prior to viral entry [15, 31, 72]. Even though, the cells that express integrins but not CAR are susceptible to adenovirus infection, addition of CAR increases infection by over

200-fold [73]. Since CAR^{Ex8} naturally localizes at the epithelial apical surface, it is likely that CAR^{Ex8} is downstream of IL-8 signaling. Also, very little is known about the regulation of CAR^{Ex8}. Understanding the regulation of CAR^{Ex8} is important because modulating the concentration CAR^{Ex8} at epithelial apical surface is predicted to have direct implications in epithelial cell susceptibility to adenoviral infection. Therefore, ***I hypothesized that IL-8 increases the expression and the apical localization of CAR^{Ex8} in polarized airway epithelial cells.***

The endogenous biological function of CAR^{Ex8} is not known. It is predicted that CAR^{Ex8} is localized at the apical epithelial cell surface to carry out an important biological function for the host cell rather than serving as a viral receptor. As mentioned earlier, CAR^{Ex7} (basal CAR) has been shown to interact with JAML, on the surface of neutrophils. Since the region that binds to JAML is identical between the two transmembrane isoforms of CAR, we predict that CAR^{Ex8} can tether neutrophils to the apical surface. Thus I hypothesized that ***CAR^{Ex8} tethers infiltrating neutrophils at the airway epithelial apical surface.***

Epithelial cells serve as a platform for the infiltrating neutrophils to adhere during inflammation. This enables the neutrophils to accomplish close encounters with pathogens leading to subsequent eradication of the pathogen. However, under pathological conditions, such as in inflammatory diseases, the accumulated neutrophils cause damage to the epithelial tissue, leading to secondary infections including viral infections. Thus I hypothesized that ***that adhered neutrophils at the epithelial surface promotes adenoviral infection.***

The overarching hypothesis of my thesis was that IL-8 increases the expression and the apical localization of CAR^{Ex8}, that CAR^{Ex8} tethers infiltrating neutrophils at the apical surface of the airway and that the adhered neutrophils augment adenoviral infection.

This overarching hypothesis was tested by 3 specific aims:

Specific Aims:

1) To test if IL-8 increases the expression and the apical localization of CAR^{Ex8} in polarized airway epithelial cells and to determine the mechanism underlying this increase.
2) To test if CAR^{Ex8} tethers infiltrating neutrophils at the epithelial apical surface
3) To test if the neutrophils adhered at the epithelial apical surface augment adenoviral infection.

Chapter 2: Materials and Methods:

2.1. Reagents

Antibodies specific for CAR, 1605p (total CAR) and 5678 (CAR^{Ex8}-specific) have previously been described [18, 20, 74]. Recombinant human IL-8 was purchased from Gold Biotechnologies, (St. Louis, MO). Anti-GSK3β, phosphospecific GSK3β-S9, anti-ribosomal subunit S6 kinase (S6K), phosphospecific S6K, anti-AKT, and phosphospecific AKT antibodies were purchased from Cell Signaling (Beverly, MA); anti-β-actin and anti-E-cadherin antibodies were obtained from Life Technologies (Grand Island, NY). CMV-driven Myc-S6K plasmid was a kind gift from Dr. Julian-Gomez Cambronero (Wright State University). Horseradish peroxidase-labelled secondary antibodies were purchased from Jackson ImmunoResearch (West Grove, PA). Adenovirus serotype 5 encoding β-galactosidase (Ad5-β-Gal) originated from the University of Iowa Gene Transfer Vector Core (Iowa City, IA).

2.2. Cell culture

The human airway epithelial cell line Calu-3 (ATCC HTB55) was cultured in RPMI 1640 media containing L-glutamine and 25mM HEPES, supplemented with 10% fetal bovine serum and penicillin/streptomycin. Cultured primary human airway tracheal epithelial cells were a kind gift from Dr. Joseph Zabner

(University of Iowa Cells and Tissue Core) and were isolated from the lungs of deceased healthy donors. The primary cells were propagated as described [75]. Briefly, human primary airway epithelial cells were co-cultured with irradiated 3T3-J2 feeder cells [76] in F-media (3:1(v/v) DMEM-F-12, 5% FBS, 0.4 µg/mL hydrocortisone, 5 µg/ml Insulin, 8.4 ng/ml cholera toxin, 10 ng/ml epidermal growth factor and 5 µM Y-27632 ROCK inhibitor). The cells were maintained at 37°C in a humidified incubator with 5% CO_2. The epithelial cells were spilt when they reached approximately 80-90% confluency; splitting the epithelial cells involved the use of differential trypsinization to first detach and remove the 3T3-J2 cells, followed by a PBS wash and fresh trypsinization to detach human primary airway epithelial cells. The airway cells were then resuspended in fresh F-media for passaging or polarization.

2.3. Cell polarization, TER, and conductance.

Cell polarization can be achieved in different ways. It is well accepted that cells able to polarize will do so once reaching 100% confluence in standard tissue culture dishes or on glass coverslips [16, 42, 77, 78]. Epithelial polarization upon reaching 100% confluency has been demonstrated by differential localization of apical and basolateral proteins, the formation of tight junctions, the restriction in viral entry via basolateral receptors, such as CAR, and selective movement of small molecules or ions. For polarization on plastic or glass, Calu-3 cells seeded at 40% confluence in regular growth media reach 100% confluence over the next 2-3 days. Experiments were performed at day 3 since cells allowed to continue to polarize become multi-layered. Primary human airway cells seeded at 60%

confluence were polarized in 1:1 v/v DMEM-F-12 supplemented with 2% ultroser G and penicillin/streptomycin, and routinely kept in culture as confluent epithelia for over 7-10 days before experiments were performed.

While polarization under standard conditions has some advantages, such as a larger surface area, high optic resolution for microscopy, and lower expense, experiments that require access to the basolateral surface or determination of transepithelial resistance are not possible. In this case, cells polarized on semipermeable membranes, such as millicells (Millipore, Bedford, MA) with 0.4 µm pores for standard hyperpolarization experiments or 3 µm pores for transmigration studies, were grown at the air-liquid interface. Epithelia grown at the air-liquid interface actively pump fluid off of the apical surface resulting in a “dry” appearance, with only a few µl of airway surface liquid covering the epithelium. This appearance is a surrogate marker for polarization and can be disrupted by molecules that break the junctions [42]. The same media as indicated above was used to polarize epithelia grown at the air-liquid interface on millicells. Any media on the apical surface of the cells was removed every alternate day in order to establish and maintain an air-liquid interface. Epithelia were considered polarized when the apical surface appeared “dry” and the transepithelial resistance (TER) was above 600 Ω/cm^2 [18, 79]. TER was measured using a millicell ERS meter with a chopstick electrode (Millipore, Bedford, MA), as previously described [42].

2.4. AdV-β-Gal infection and β-galactosidase assay.

Based on the needs of the experiment, either Calu-3 or MDCK cells were infected with AdV-β-Gal at a multiplicity of infection (MOI) of 100 plaque forming units (pfu)

per cell, or MOI as indicated in the text, for 1 h at 37°C. Virus inoculums were removed and cells were washed 2 times with PBS and incubated for additional 24 H prior to lysis. The protein concentration was determined by a Bio-Rad protein assay (Hercules, CA), and β-galactosidase expression was determined with a Galacto-Light Plus system (Applied Biosystems, Carlsbad, CA) as previously described [18].

2.5. Quantitation of viral entry

Based on the needs of the experiment, either Calu-3 or MDCK cells were polarized on a 24-well dish. The polarized cells were then treated as indicated in the text, washed three times with 1X PBS, infected with Ad5-βGal at MOI 100 for 1 H, washed with PBS, and incubated at 37^0C for 24 H. To determine viral entry based on viral genomes (Vg), total DNA was isolated from the cells using Qiagen DNeasy Blood and Tissue kit according to the manufacturer's protocol and Vg was quantitated by quantitative PCR (qPCR) using SYBRG with low ROX (Qunata, Gaithersburg, MD) in Stratagene's Real Time PCR system (Agilent Technologies, Santa Clara, CA) with primers for adenovirus-hexon gene, GAPDH, or MDCK actin, as previously described [20] and listed in Table 2.

A control experiment was performed to confirm that Ad5-β-gal Vg reflects actual entry of the virus into the epithelial cells rather than just attachment to the epithelial cell surface. Epithelial cells that were infected with Ad5-β-Gal, as above for 24 H, were treated with (or without) trypsin for 20 min at 37°C to cleave any adherent virus on the cell surface [80]. Genomic DNA was isolated and qPCR analysis was performed as described above. No difference in Vg was observed between the

Ad5-β-Gal infected epithelia with or without trypsin treatment (Figure 5) suggesting that viral genomes were protected within the epithelial cells.

Table 2: List of primer sequences used for qPCR

Primer Set	Forward primer 5' -> 3'	Reverse Primer 5' -> 3'
Ad Hexon specific primer	ACGCCTCGGAGTACCTGAG	GTGGGGTTTCTGAACTTGT
CAR^{Ex8}	TCGGCAGTAATCATTCATCCCTGG	ACTGTAATTCCATCAGTCTTGTAAGGG
CAR^{Ex7}	TCGGCAGTAATCATTCATCCCTGG	ACTATAGACCCATCCTTGCTCTGTG
E-cadherin	CCCAATAGATCTCCCTTCACAG	CCACCTCTAAGGCCATCTTTG
GAPDH	CACCCTGTTGCTGTAGCCAAA	CAACAGCGACACCCACTCCT
MDCK actin	AAGATCTGGCACCACACCTTCTAC	ATCTGGGTCATCTTCTCACGGTTG
CAR^{Ex8} (stable MDCK-CAR^{Ex8})	GTCCCTCCTTCAAATAAAGCTG	ACTGTAATTCCATCAGTCTTGTAAGGG
CAR^{Ex7} (stable MDCK-CAR^{Ex7})	GTCCCTCCTTCAAATAAAGCTG	CGGATCCCTATACTATAGACCCATC

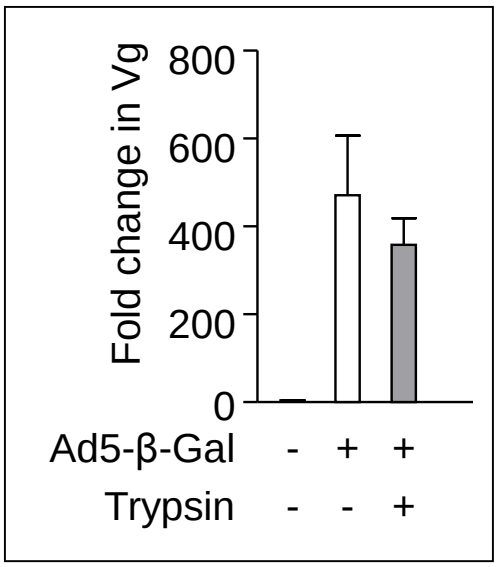

Figure 5: Quantitative PCR measurement of Ad5 viral genomes 24 hours post infection represents internalized DNA. MDCK cells were infected with Ad5-β-Gal for 1 H. Post infection, the epithelial cells were incubated at 37°C for 24 H. Next the cells were either treated or untreated with trypsin at 37°C for 20 min to cleave off any virus adherent on the cell surface. Cells were washed and genomic DNA was isolated for qPCR analysis. No significant difference was observed between the trypsin treated and untreated conditions.

2.6. Western blot analysis

Cells were seeded on a 6-well dish and grown to 100% confluency. The cells were then treated with the indicated amount of IL-8 for 4 H, unless otherwise stated. Post treatment, the cells were washed with ice-cold PBS, and lysed with lysis buffer (50 mM Tris pH 7.4, 150 mM NaCl, 1% Triton X-100, protease inhibitors (10 mg/ml) leupeptin, aprotinin, pepstatin, and 1 mM phenyl-methylsulfonyl fluoride) by rocking at 4°C. Cells were scraped, sonicated with five pulses, and centrifuged at 14,000 g for 10 min at 4°C in a microcentrifuge. Protein concentration was determined with the Bio-Rad protein assay (Bio-Rad, Hercules, CA). Equal amounts of protein were subjected to 10% polyacrylamide gel electrophoresis. Gels were transferred to a polyvinylidene difluoride (PVDF) membrane (Millipore, Bedford, MA), blocked with 5% BSA, washed with TBST, and probed with appropriate primary antibodies as described previously [18, 20, 74] and listed in Table 3. The secondary HRP conjugated antibodies were used at 1:3000 dilution.

Table 3: **Primary antibodies and the dilution at which they were used.**

Antibody	Dilutions used
Total CAR (1605)	1:1000
CAR^{Ex8} (5678p)	1:200
E-cadherin	1:4000
Actin	1:5000
GSK3β and phospho-GSK3β-S9	1:1000
AKT and phospho AKT	1:1000
S6K and phospo-S6K	1:1000
Myc	1:2000
FLAG	1:2000

2.7. RNA extraction, cDNA synthesis, and quantitative PCR (qPCR)

After the appropriate treatment of polarized cells with IL-8 for 4 H, total RNA was extracted with Trizol reagent, as per the manufacturer's directions (Life Technologies, Grand Island, NY). RNA concentration was estimated at 260/280nm and 1 µg was used to generate cDNA (Quanta Bioscience cDNA Synthesis kit). The cDNA generated was used for qPCR to specifically quantitate CAR^{Ex7}, CAR^{Ex8}, E-cadherin, and glyceraldehyde 3-phosphate dehydrogenase (GAPDH) RNA levels. Details of the specific primers used to determine the levels of CAR^{Ex7}, CAR^{Ex8}, and GAPDH have been previously described [20] and listed in table 2. qPCR was performed using SYBR Green with low ROX (Quanta, Gaithersburg, MD) in Stratagene's Real Time PCR System (Agilent Technologies, Santa Clara, CA). Abundance relative to GAPDH gene expression was calculated for each gene of interest and the expression of target genes was quantified via comparative delta delta Ct analysis by using Mx4000p software v5 for data analysis.

2.8. Cell surface biotinylation

Cell surface biotinylation was performed as previously described [18-20]. Briefly, after IL-8 treatment for 4 H, polarized cells were treated with 1 mg/ml Sulfo-NHS-SS-biotin (Thermo Scientific, Rockford, IL) for 1 H at 4°C with rocking, washed with ice cold PBS, and then any remaining free Sulfo-NHS-SS-biotin quenched with ice cold 100 mM glycine for 20 min at 4°C. The cells were then washed three times with PBS including Ca^{2+} and Mg^{2+} (PBS +/+) and lysed with lysis buffer as described above. NeutrAvidin beads (Thermo Scientific, Rockford, IL) were added to the clarified cell lysate and incubated at 4°C for 2 H with rotation. The

NeutrAvidin beads were then collected by centrifugation at 1,000 g at 4°C for 3 min and washed three times with ice-cold wash buffer. The sulfo-NHS-SS-biotin-labeled proteins were eluted from the NeutrAvidin beads with SDS-PAGE sample buffer at 65°C for 10 min. This was followed by SDS-PAGE and Western blotting using appropriate antibodies.

2.9. Generation of MDCK stable cells

To generate MDCK stable cells, the Lenti-X Tet-On advanced inducible expression system was used (Clontech. Cat no: 632162) according to the manufacturer's protocol. First, the gene encoding FLAG-tagged human CAR^{Ex8} or FLAG-tagged human CAR^{Ex7} or mCherry (Clontech) was cloned into the pLVX-tight-puro vector using the infusion cloning kit (Clontech). pLVX-Tet-on advanced, as well as the pLVX-tight-puro plasmid, were then packaged separately into the lentivirus by transfecting the plasmids into the 293T packaging cell line along with the Lenti-X HTX packaging system using X-fect transfection reagents (Clontech). The Lenti-X HTX packaging system contains the plasmid mixture that expresses the necessary lentiviral packaging components such as Pol, Tat, Rev, and Gag proteins. The lentiviruses produced via this process were called either tet-on, CAR^{Ex8}, CAR^{Ex7}, or m-Cherry lentivirus. MDCK cells were first infected with the tet-on virus in the presence of a neomycin antibiotic drug that selects for tet-on transduced cells. The neomycin resistant clones were used for further selection. The selection process was carried out in a 96-well dish in order to obtain clones of single cells expressing the tet-on gene. The neomycin resistant clones obtained were serially diluted such that when seeded on a 96-well plate there was only one cell per well. The wells

that had one positive cell each were selected and allowed to expand and replicate. Such clones were further screened for the stable expression of pLVX-tet-on, morphology similar to parental cells, and the ability to form an epithelium. This newly created MDCK cell line was named MDCK-tet-on cells. Next, the MDCK tet-on cells were transduced with an additional pLVX-tight-puro lentivirus carrying our gene of interest in the presence of puromycin (a drug that selects for the pLVX-tight-puro transduced cells). The resulting clones were selected and screened, as described above, for the stable expression of FLAG-CAR^{Ex8}, FLAG-CAR^{Ex7}, or mCherry. These new cell lines based on MDCK-tet-on were named MDCK-CAR^{Ex8}, MDCK-CAR^{Ex7}, or MDCK-mCherry. They will also be collectively referred to as the MDCK stable cells. The MDCK stable cells were characterized for no obvious changes in transepithelial resistance (TER) or changes in the expression of the different junctional proteins (e.g. both CAR isoforms, ZO-1, E-cadherin) both by Western blot and immunocytochemistry prior to use in later experiments.

2.10. Isolation of primary neutrophils

To isolate primary neutrophils, 50 ml of blood was drawn from healthy donors in EDTA sprayed 10 ml vacutainers under IRB SC# 4765. The blood was equally distributed between two 50 ml conicals each containing 7.5 ml of 6% dextran prepared in a saline solution. After securely closing the lid, the tubes were inverted twice to allow thorough mixing. The tubes were then allowed to incubate at room temperature for 30 min. Next, the top phase was removed and transferred into another fresh 50 ml conical and centrifuged at 4000 rpm for 3 min at room temperature (the remaining bottom phase was bleached). After centrifugation the

pellet was gently resuspended in 1 ml of saline and then diluted with up to 35 ml of additional saline. To this, 8 ml of ficoll was added to the bottom of the tube using a sterile glass pasteur pipette. The mixture was then centrifuged at 740 x g at 4^0C for 15 min with the breaks turned off. After centrifugation, a white ring was visible in the interphase that contained monocytes and lymphocytes. This phase was aspirated along will the rest of the supernatant leaving the pellet found at the bottom of the centrifuged container (the pellet contains neutrophils). The pellet was resuspended in 1 ml of saline and placed on ice. To lyse the contaminating red blood cells, 20 ml of ice cold water was added to the resuspended pellet and mixed well by pipetting up and down twice. The tube was then placed on ice for no more than 40 seconds. Immediately after, 20 ml of ice cold 1.8% NaCl was added, mixed gently and centrifuged at 740 x g at 4^0C for 4 min. The supernatant was discarded and the pellet was resuspended in 1ml HBSS-/- (Hanks balanced salt solution without calcium and magnesium) followed by the addition of another 9 ml of HBSS-/-. The neutrophil cell count was determined by using a hemocytometer.

2.11. Purification of adenovirus fiber knob

The plasmid encoding the His-tagged Ad5 FK protein was kindly provided by Dr. Glen Nemerow (The Scripps Research Institute). The Ad5 FK plasmid was transformed into Rosetta (BL21) *Escherichia coli* cells (EMD Chemicals, Gibbstown, NJ), which were grown in LB broth to an optical density of 0.75 at 600nm (OD600), induced with 0.3 mM isopropyl-D-1-thiogalactopyranoside (IPTG), and subsequently incubated for an additional 4 h at 32°C. The cells were then harvested by centrifugation, and the pellets were resuspended in bacterial

lysis buffer (5 mM Sodium ohosphate, 100 µM sodium orthovanidate, 300 µg/ml lysozyme, 10 mM imidazole, 1% triton-X 100, 20% glycerol and 2X protease inhibitor cocktail (Sigma-Aldrich)). The resuspended cells were sonicated on ice for 6 min with 30 s pulses and centrifuged at 14,000 X g at 4°C for 20 min. 2 ml of HisPur Ni-NTA superflow agarose (Thermo Scientific) was added and incubated at 4°C with rotation for 1.5 H to allow the His-tagged protein to bind to the resin. Next, the resin was centrifuged to remove the supernatant and the resin was washed thrice with the wash buffer (50 mM sodium phosphate pH 7.0, 10 mM imidazole). After washing, the resin was resuspended in the elution buffer (50 mM sodium phosphate, 500 mM NaCl and 300 mM imidazole), incubated for 5 min at 4°C, and centrifuged. After centrifugation, the supernatant was saved. This step was repeated 3-5 times. The elutes were pooled, concentrated, and dialyzed into a buffer containing 20 mM Tris and 100 mM NaCl. The protein concentration was measured using Bradford's (BioRad) method according to the manufacturer's protocol. Routinely ~10 µg/ml concentration of the purified protein was obtained.

2.12. Neutrophil adhesion assay

MDCK-CAR^{Ex8}, MDCK-CAR^{Ex7} and MDCK-mCherry cells were seeded on a 24-well dish at 1X10^5 cells per well, a concentration that allows these cell lines to reach 100% confluence by day 3. Once at 100% confluence and polarized, the cells were induced with increasing concentration of DOX (0 to 1000 ng/ml) for 24 H to allow the overexpression of FLAG-CAR^{Ex8}, FLAG-CAR^{Ex7}, or mCherry respectively. The following day, neutrophils were isolated from the peripheral blood of healthy donors and resuspended in HBSS-/-. The neutrophils were then stained with 1.5 µM

calcein green for 30 min at 37°C. The stained neutrophils were washed once with HBSS-/- and resuspended in HBSS+/+ (HBSS with calcium and magnesium). The required number of stained neutrophils were then added to the MDCK apical cell surface. To block neutrophil adhesion, the epithelial cells were incubated with either purified Ad5 FK or purified control Ad type 3 FK (a group B adenovirus FK that does not bind CAR) for 10 min at room temperature prior to the addition of the neutrophils. After the addition of the neutrophils, the culture plates were spun down at 140 x g for 4 min with the breaks of the centrifuge turned off. The epithelial cells were then incubated for 15 min at 37°C to allow for neutrophil adhesion. Next, the epithelial cells were washed 3 times with HBSS+/+ to remove the unbound neutrophils. The bound neutrophils were imaged using fluorescence microscopy and the fluorescence intensity was quantitated using Metamorph software. Additionally, Calu-3 cells were seeded on the 24 well dish at 2 X 10^5 cells/well and allowed to reach confluency on the dish. On the day of the adhesion assay, these Calu-3 cells were treated with IL-8 (30 ng/ml) for 4 H. Post treatment, a neutrophil adhesion assay was performed as described above.

2.13. Polarization of MDCK stable cells for transmigration assay

To perform the neutrophil transmigration assay, the MDCK-stable cells were polarized on millicells in an inverted fashion. Millicells of 3µM pore size were purchased from Millipore (Cat no: PITP01250). First the Millicells were placed in a 12-well dish in an upright fashion. 4.5 ml of media was added to the well (at this point the millicell will be fully submerged). Then, the millicells were inverted (membrane facing up) using a sterile glass pipette. It was then necessary to make

sure that no air bubbles were trapped inside the millicell. Next, 1.7 ml of the media was removed from the 12-well dish (leaving the membrane of the millicell exposed to air). Slowly, the millicell was moved to the center of the well using the glass pipette. Now 1 X 10^5 of MDCK stable cells, resuspended in 80 ul of the media were added to the membrane. This set up was then incubated at 37°C for 72 H. Next, the TER of the cells was measured. To measure the TER, the millicells were transferred to a 24-well dish containing 600µl of HBSS+/+. 400µl of the HBSS+/+ was then added to the inside of the millicell (the equivalent of the basal surface). The cells were allowed to equilibrate by incubating at 37°C for 30 min. The TER was then measured and epithelia were considered polarized if the TER was at least 600 Ω/cm^2. After attaining appropriate TER, the millicells were transferred to 24-well dish containing media with or without DOX (200 ng/ml) for additional 24 H in the upright direction. The media was added both on the apical and the basolateral surfaces. Next day, the neutrophil transmigration assay was performed.

2.14. Neutrophil transmigration assay

The setup used for the transmigration assay is shown in the model in (Figure 27). Briefly, to perform the neutrophil transmigration assay, the MDCK-stable cells that were polarized on millicells (3 µM pore) in an inverted fashion were used. Before performing the neutrophil transmigration assay, the MDCK-stable cells were washed once with HBSS+/+, allowed to equilibrate at 37°C for 30 min and were measured with a chopstick ohmmeter to determine the TER. The millicells were then transferred to a fresh 24-well dish that contained 500 µl of 100 nM fMLP

(formyl-methionyl-leucyl-phenylalanine, a neutrophil chemoattractant) in HBSS+/+ (i.e the fMLP containing HBSS+/+ is on the apical surface of the epithelial cells). 1 X 10^6 neutrophils, fluorescently stained with calcein green and resuspended in HBSS+/+, were added to the basal surface of the epithelial cells (i.e. inside of the millicell cup) and allowed to transmigrate through the epithelium towards the apical surface for 60 min at 37°C. Post neutrophil transmigration, the neutrophils that successfully transmigrated to the bottom chamber were imaged under a fluorescent microscope and quantitated using MetaMorph software.

2.15. Identifying neutrophils adhered to the epithelial apical surface

After performing the neutrophil transmigration assay, the neutrophils that remained adhered to the epithelial apical surface were detached using the following protocol: First the millicells were transferred to a fresh 24-well dish that contained 500µl of HBSS+/+. The basal surface of the millicells were washed 3 times with HBSS+/+ in order to remove any neutrophils that failed to migrate into or through the epithelium. Next, the millicells were centrifuged at 50 X g for 5 min. The millicells were discarded and the neutrophils that detached from the epithelial apical surface were imaged under a fluorescent microscope and quantitated using MetaMorph software.

2.16. Adenoviral transduction in the presence of neutrophils

MDCK-CAR^{Ex8}**,** MDCK-CAR^{Ex7} and MDCK-mCherry cells were either induced or mock-induced with DOX or diluent, respectively. A neutrophil adhesion assay was then performed as described earlier. Subsequently, the unbound neutrophils were washed off and the epithelial cells were infected with the indicated MOI of Ad5-β-

Gal for 1 H. After 24 H of incubation the DNA was extracted and the viral genomes were quantitated to determine the fold change in viral entry.

2.17. Statistical analysis

All experiments were performed at least three times. Microsoft Excel and Graph Pad Prism V5 (La Jolla, CA) were used to perform statistical analyses. Significant differences were analyzed using one-way or two-way ANOVA tests, followed by T-test to determine individual differences between control and experimental conditions. Results were considered to be statistically significant if a $p<0.05$ was obtained.

Chapter 3: IL-8 regulates the protein expression and the localization of CAR^{Ex8} via differential activation of AKT/S6K and inactivation of GSK3β

Epithelial cells pose a formidable barrier to the invading pathogens including adenoviruses. Viruses have evolved to break the barrier using mechanisms that are just starting to be understood. Some viruses use the junctional proteins that are sequestered beneath the epithelial tight junctions, other utilize the apical proteins. Adenoviruses use CAR for entry into polarized epithelial cells. The alternatively spliced isoform, CAR^{Ex8}, is able to localize at the apical surface. Thus adenovirus is provided with an opportunity to bind and enter the epithelial cells from the apical surface. Therefore, any changes in the levels of CAR^{Ex8} expression will have a direct implication for the susceptibility of a polarized epithelium to adenoviral infection. The expression and the localization of several epithelial junctional and apical proteins are regulated by proinflammatory cytokines. IL-8 has been shown to increase the apical localization of $\alpha_v\beta_3$ integrin and increase the susceptibility of a polarized epithelium to adenovirus infection. Therefore, *I hypothesized that IL-8 increases the apical localization and expression of CAR^{Ex8} in airway epithelial cells.* This hypothesis was tested through three specific aims:

3.1. *To test if IL-8 increases CAR^{Ex8} expression and apical localization in the human airway epithelial Calu-3 cell line*

3.2. *To validate that IL-8 increases CAR^{Ex8} expression and apical localization in primary human airway epithelial cells*.

3.3. *To determine the molecular mechanism underlying the IL-8 mediated increase in CAR^{Ex8} expression.*

3.1. IL-8 increases CAR^{Ex8} expression and apical localization in the human airway epithelial Calu-3 cell line.

3.1.1. Rationale:

Proinflammatory cytokines are released by the resident macrophages during viral infection in the lung. Previous studies have shown that IL-8, a proinflammatory cytokine and neutrophil chemoattractant, increases the airway susceptibility to adenoviral infection [71]. However, the mechanism underlying this increase in susceptibility remains unclear. IL-8 has been shown to relocalize integrins to the epithelial apical surface. Integrins are adenoviral co-receptors that aid in the steps of viral entry that occur after viral attachment to the host cell. Viral attachment on the epithelial cell surface is accomplished when the virus binds to its primary receptor. For most adenoviruses, CAR is the primary receptor. Lutschg et al., 2010 [71] demonstrated that IL-8 increases the airway epithelial cell susceptibility to adenoviral infection. The focus of their study was integrins which are co-receptors for adenoviral entry. However, CAR is the primary receptor for adenoviral infection and they provided limited evidence that CAR localizes at the apical surface post IL-8 treatment. Moreover, this study did not differentiate between the two isoforms of CAR, CAR^{Ex7} (the basolateral isoform) and CAR^{Ex8} (the apical isoform).

Therefore, we hypothesized that IL-8 upregulates CAR^{Ex8} expression and apical localization in airway epithelial cells. To test this hypothesis we used Calu-3 cells an accepted model system for studies of human airway epithelia [81]. Although Calu-3 cells are derived from human lung adenocarcinoma [82], Calu-3 cells are able to differentiate and polarize into an electrically tight epithelium that resembles the broncho-alveolar epithelium [81].

3.1.2. Results:

IL-8 increases airway epithelial cell susceptibility to adenoviral infection and CAR^{Ex8} protein expression.

We first tested the effect of IL-8 on the susceptibility of Calu-3 airway epithelial cells to adenoviral infection. Polarized Calu-3 epithelia were treated with increasing concentrations of IL-8 (ranging from 0 ng/ml to 100 ng /ml (0 – 12.5 nM)) for 4 H, followed by apical infection with Ad5-βGal. Consistent with Lutschg et al., 2010, [71] quantitative PCR analysis showed that adenovirus entry was increased in response to IL-8 treatment in a dose-dependent manner (Figure 6). Viral entry reached its maximum at 3, 10 and 30 ng/ml of IL-8 with ~5-fold increase in viral genomes (Vg) when compared to 0 ng/ml IL-8. At 100 ng/ml, viral entry was decreased when compared to 30 ng/ml IL-8. Explanations for this could be that signaling is saturated or the cell is no longer able to respond to the higher concentration of IL-8 as a result of desensitization of the receptors, receptor internalization, or receptor degradation.

I then asked how IL-8 promotes adenoviral infection in these polarized cells. Since the primary receptor for Ad5 is CAR, we tested the expression of CAR in the

presence of IL-8. In particular, we examined the expression of the apical isoform of CAR, CAR^{Ex8}. IL-8 treatment stimulated CAR^{Ex8} expression in a dose-dependent manner with the maximal effect at a concentration of 30 ng/ml (Figure 7). More intriguingly, the IL-8-mediated effect appeared to be CAR^{Ex8}-specific. Analysis of total CAR, which is predominantly composed of the CAR^{Ex7} isoform [18, 19], and E-cadherin (another junctional protein) did not show a significant change in protein expression (Figure 7). IL-8 had the maximal effect on CAR^{Ex8} expression between 4-12 H of treatment (Figure 8). Based on these data, further experiments were carried out with 30 ng/ml IL-8 for 4 H, at time point where the change in CAR^{Ex8} protein expression was obvious and amenable to experimental analysis.

IL-8 stimulates apical CAR^{Ex8} protein localization.

In order to determine whether IL-8 enhances the apical localization of CAR^{Ex8}, we performed apical-surface biotinylation of polarized Calu-3 epithelia. IL-8 significantly increased the apical localization of CAR^{Ex8} in polarized Calu-3 cells in a dose-dependent manner (Figure 9). In addition, actin, a negative control, was not detected with apical proteins. Together, the above data indicates that IL-8 stimulates CAR^{Ex8} protein expression at the apical surface of airway epithelial cells and that the effect is dose-dependent.

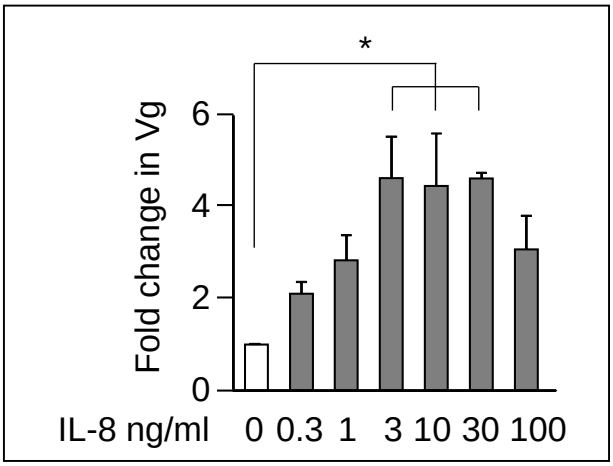

***Figure 6: IL-8 increases the susceptibility of polarized airway epithelia to adenovirus entry*.** The apical surface of polarized Calu-3 cells was treated with increasing concentrations of IL-8 for 4 H and then transduced with Ad5-β-Gal. Total genomic DNA was analyzed for the fold change in viral genomes (Vg) relative to GAPDH by qPCR. Statistical significance was evaluated using one-way ANOVA and Tukeys post hoc test, * P<.05.

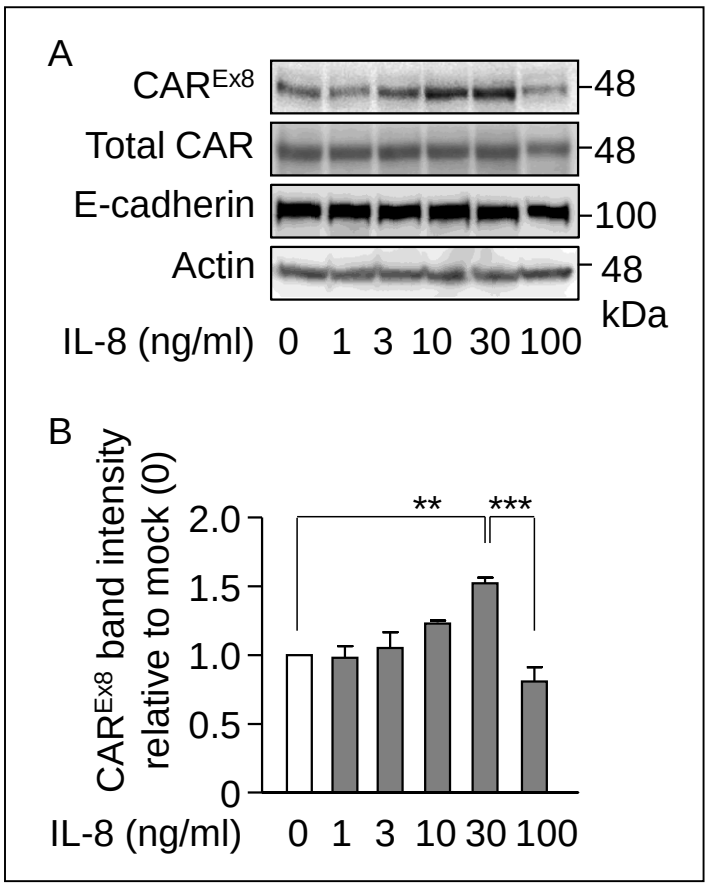

Figure 7: IL-8 stimulates CAR^{Ex8} expression. A) Polarized Calu-3 epithelia were treated with increasing concentration of IL-8 for 4 H. Whole cell extracts were then analyzed by Western blot for the expression of CAR^{Ex8}, total CAR, E-cadherin, and actin. B) Band intensity of CAR^{Ex8} relative to mock treated (0 ng/ml IL-8) (Average of 3 individual experiments). The reported values are mean and standard error of the mean (SEM), calculated from at least three independent experiments. Statistical significance was evaluated using one-way ANOVA and Bonferroni post hoc test. ** P<.01, ***P<0.001.

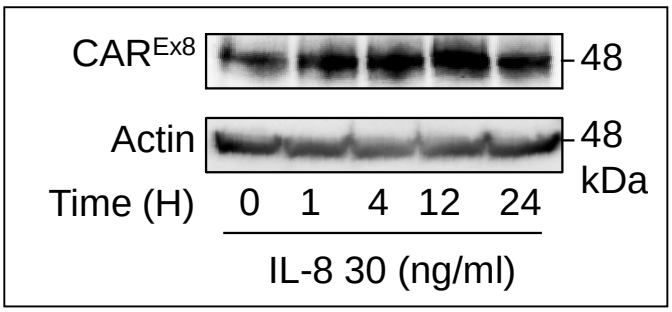

Figure 8: IL-8 has its maximal effect of CAR^{Ex8} expression between 4 and 12 H. Polarized Calu-3 epithelia were treated with 30 ng/ml IL-8 for varying lengths of time (0 to 24 H). Post treatment, CAR^{Ex8} protein expression was analyzed by Western blot analysis

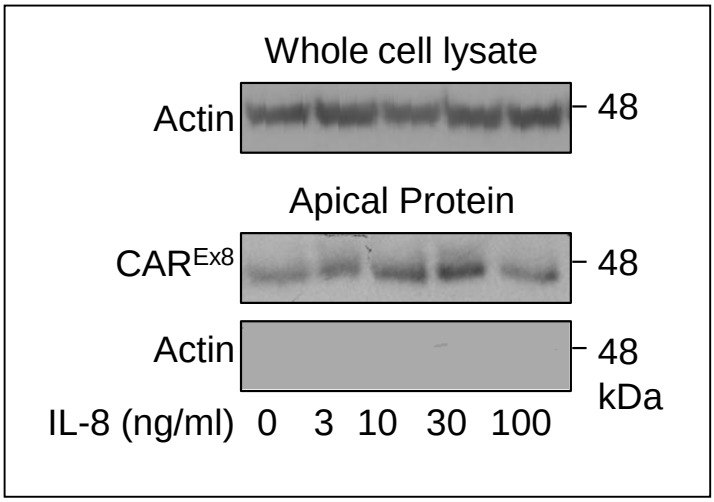

Figure 9: IL-8 stimulates enhanced localization of CAR^{Ex8} at the apical surface of polarized epithelia. Polarized Calu-3 cells were treated with increasing concentrations IL-8 for 4 H prior to apical surface biotinylation. Biotin-labeled proteins were pulled down using neutravidin beads and analyzed for the expression of CAR^{Ex8} by Western blot. As a control, the cytosolic protein actin was probed for in the total lysate (present) and after the apical-biotin/neutravidin pull down (absent).

3.2. IL-8 increases CAR^{Ex8} expression and apical localization in primary human airway epithelial cells.

3.2.1. Rationale:

Although the Calu-3 cell line is an excellent model of an airway epithelium, this cell line is derived from human lung adenocarcinoma and immortalized [81, 82]. Therefore it is important to validate the IL-8-mediated effect on CAR^{Ex8} expression and localization in primary airway epithelial cells. In order to facilitate these studies, a new technique that allows the expansion of primary airway cells and subsequent differentiation into well-differentiated primary airway epithelia was used [75]. **I hypothesized that IL-8 will augment the expression and the apical localization of CAR^{Ex8} in polarized primary airway epithelial cells obtained from the trachea of the healthy donors.**

3.2.2. Results:

Primary human airway epithelial cells can be cultured indefinitely in the presence of 3T3-J2 feeder cells and ROCK inhibitor. Primary airway epithelial cells from three different donors were successfully cultured in the presence of irradiated 3T3-J2 feeder cells and ROCK inhibitor, as described [75] (Figure 10). Upon removal of the feeder cells and the ROCK inhibitor the epithelial cells differentiated and polarized. Of the three donors tested, the cells from donor 2 were chosen because of their ability to form a highly polarized electrically-tight epithelium (TER reached nearly 2000 Ω/cm^2). Moreover, the immunofluorescence staining revealed the expected localization of junctional proteins.

IL-8 augments CAR^{Ex8} protein expression and apical localization in primary human airway epithelial cells. To validate that IL-8 stimulates CAR^{Ex8} protein expression and apical localization as was observed with Calu-3 cells, the experiments in primary airway epithelial cells were repeated. Similar to Calu-3 epithelia, apical treatment with 30 ng/ml IL-8 for 4 H resulted in a robust increase in CAR^{Ex8} protein expression (Figure 11A and B) and apical localization (Figure 11C). As negative controls for apical surface biotinylation, intracellular actin and basolateral E-cadherin were investigated by Western blot. As expected, both were present in total lysate but absent from the apical surface. The epithelial barrier integrity in the presence of IL-8 was also tested. We observed that IL-8 treatment did not alter the TER of the polarized primary airway epithelial cells (Figure 12).

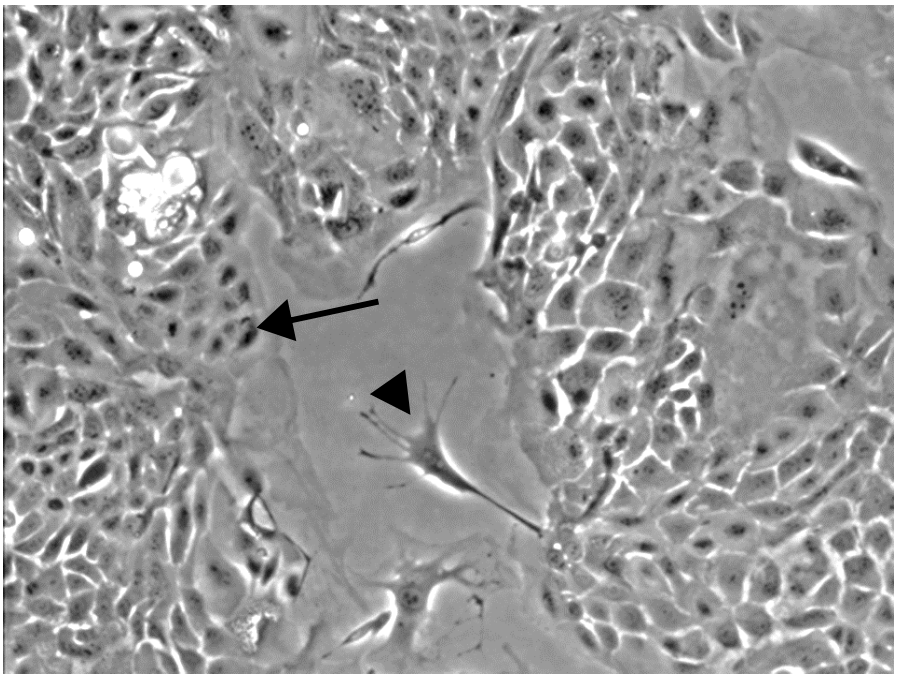

Figure 10: Primary airway epithelial cells co-cultured with the irradiated 3T3-J2 cells. The bright field image shows the primary airway epithelial cells (arrow) growing in the presence of irradiated 3T3-J2 cells (arrowhead).

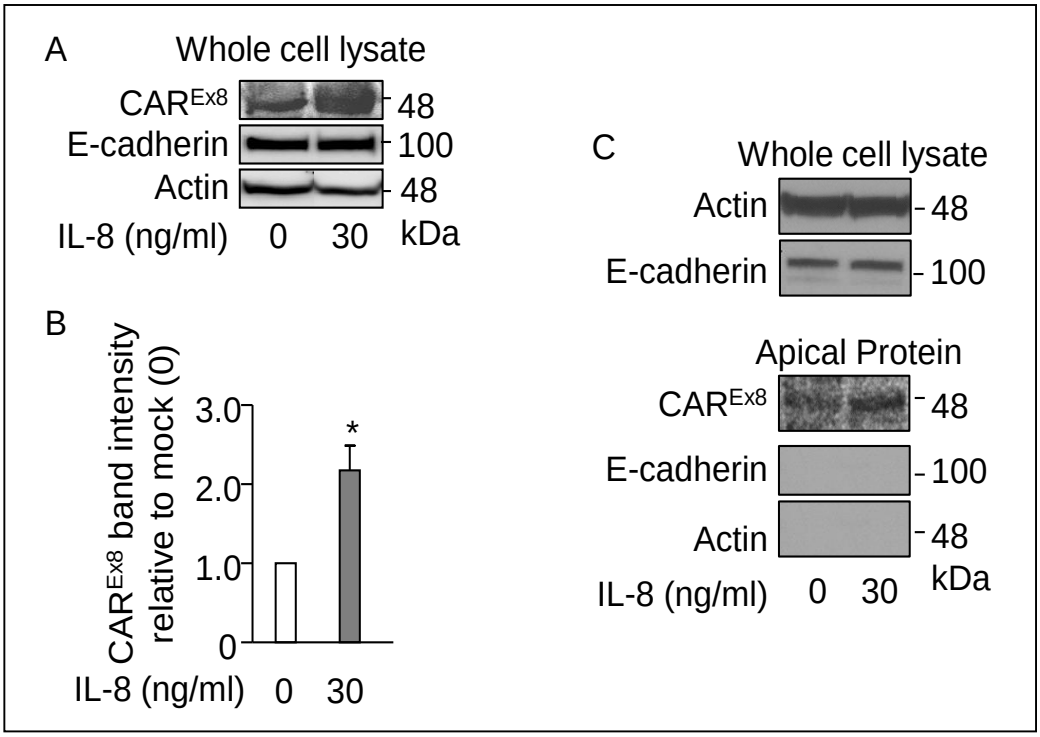

Figure 11: IL-8 stimulates CAR^{Ex8} expression and apical localization in polarized primary airway epithelial cells A) Whole cell extracts of polarized primary human airway epithelial cells mock treated (0 ng/ml IL-8) or treated with 30 ng/ml IL-8 were analyzed for the expression of CAR^{Ex8}, E-cadherin, and actin. B) Band intensity of CAR^{Ex8} (30 ng/ml IL-8) relative to mock treated (0 ng/ml IL-8) (Average of 3 individual experiments). C) Polarized primary airway epithelial cells were either mock (0 ng/ml IL-8) treated or treated with IL-8 at 30 ng/ml for 4 H. Post-treatment apical surface biotinylation was performed. Biotin-labeled proteins were pulled down using neutravidin beads and analyzed for the apical expression of CAR^{Ex8} and the negative control proteins actin and E-cadherin. The values reported are the mean and the standard error of the mean (SEM) of 3 individual experiments. Statistical significance was evaluated using student t-test, * P<.05.

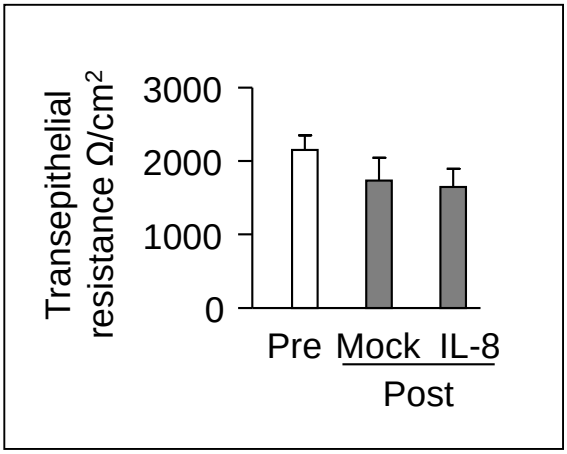

Figure 12: IL-8 treatment does not affect the transepithelial resistance of polarized airway epithelia. Polarized primary airway epithelial cells were either mock treated (0 ng/ml) or treated with IL-8 (30 ng/ml). TER measurements were taken pre- or post-treatment.

3.3. The molecular mechanism underlying the IL-8 mediated increase in CAR^{Ex8} expression.

3.3.1. Rationale:

Protein expression can be regulated in multiple different ways. Two major mechanisms involve regulation at the transcriptional level (e.g. mRNA copy number) or at the translational level (e.g. the efficiency of converting mRNA to protein). I asked whether IL-8 regulates CAR^{Ex8} protein expression by one of these two mechanisms. Previous studies have shown that in response to IL-8, AKT is activated and causes activation of ribosomal S6 kinase (S6K). S6K in turn regulates protein synthesis by phosphorylating and activating ribosomal S6 protein, a key component of active ribosomes [83]. Moreover, our lab has demonstrated that GSK3β negatively regulates CAR^{Ex8} expression [20]. GSK3β is a ubiquitously expressed serine/threonine kinase which plays a crucial role in various cellular processes including glucose metabolism, protein synthesis, cell motility, and proliferation. GSK3β negatively regulates transcription factors including TCF and LEF. Inhibition of GSK3β via phosphorylation at serine 9 renders GSK3β inactive, which allows transcription factors to enter the cell nucleus and activate target-gene transcription [84]. GSK3β has also been shown to negatively regulate protein translation by inhibiting eukaryotic initiation factor 2B (eIF2B) by inducing phosphorylation at Ser 340. eIF2B is a guanine nucleotide exchange factor (GEF) for the small GTPase eIF2. When GSK3β is inhibited, eIF2B is activated as a result of dephosphorylation at Ser 340. Activated eIF2B further activates eIF2 (GTP coupled) by recruiting the initiator methonyl tRNA to

the mRNA and beginning translation [85-89]. I hypothesized that, in addition to activating AKT, IL-8 inactivates GSK3β to augment CAR^{Ex8} expression.

3.3.2. Results:

IL-8 regulation of CAR^{Ex8} expression is post transcriptional

To understand the molecular mechanism underlying the IL-8 mediated increase in CAR^{Ex8} expression, I sought to first examine whether IL-8 stimulates CAR^{Ex8} expression at the transcriptional and/or at the post transcriptional level. I first tested the hypothesis that the CAR^{Ex8} increase was via increased transcription. CAR^{Ex8}-specific mRNA levels were examined in IL-8 treated or untreated polarized primary airway epithelia. IL-8 treatment did not alter the mRNA levels of CAR^{Ex8}, even at time points earlier than 4 H when a transcriptional increase would be expected in order to facilitate the protein increase observed by 4 H (Figure 13A). As expected, the mRNA levels of CAR^{Ex7} and E-cadherin also showed no significant change upon IL-8 treatment (Figure 13A). In addition, CAR^{Ex8} mRNA levels did not change in IL-8-exposed Calu-3 epithelia (Figure 13B). These data suggest that IL-8 might stimulate CAR^{Ex8} protein synthesis without altering its mRNA levels. To further confirm this, the protein synthesis inhibitor, cycloheximide (CHX) was used. Remarkably, CHX abolished the IL-8-mediated increase in CAR^{Ex8} expression both in polarized Calu-3 (Figure 14A) and polarized primary airway epithelial cells (Figure 14B). Taken together, these data show that IL-8 stimulates de novo CAR^{Ex8} protein synthesis that does not require an increase in CAR^{Ex8} mRNA levels.

IL-8 activates AKT and S6K to increase CAR^{Ex8} protein expression.

Next, the roles of the previously mentioned signaling proteins were investigated in IL-8-mediated increased CAR^{Ex8} expression. Previous studies have shown that activation of AKT leads to the downstream activation of ribosomal S6 protein

kinase (S6K) [83]. In agreement, we observed a robust activation of AKT (pAKT-T308) upon IL-8 treatment (Figure 15A). Moreover, inhibition of AKT using chemical inhibitor Ly294002 (30 µM) blocked the IL-8-mediated increase in CAR^{Ex8} expression (Figure 15B) and attenuated adenovirus infection (Figure 15C). Likewise, we also observed that IL-8 stimulation caused an increase in the activated form of S6K, phospho-S6K T389 (Figure 16A). Inhibition of S6K using chemical inhibitor RO318220 (300 nM) blocked the IL-8 mediated increase in CAR^{Ex8} (Figure 16B) and completely blocked the increase in adenovirus infection (Figure 16C). Taken together these data show that upon stimulation of airway epithelial cells with IL-8, AKT and S6K are activated and both these signaling proteins regulate the expression of CAR^{Ex8} (Figure 21).

Given the large effect of the S6K inhibitor on adenovirus infection and to further validate these results, we tested whether overexpression of S6K in Calu-3 (Figure 17A) or COS7 cells (Figure 17B) had an effect on CAR^{Ex8} protein expression. Overexpression of S6K resulted in a robust increase in the CAR^{Ex8} expression both in Calu-3 cells and COS7 cells. These data indicate that both AKT and S6K play an important role in stimulating CAR^{Ex8} expression in response to IL-8 treatment.

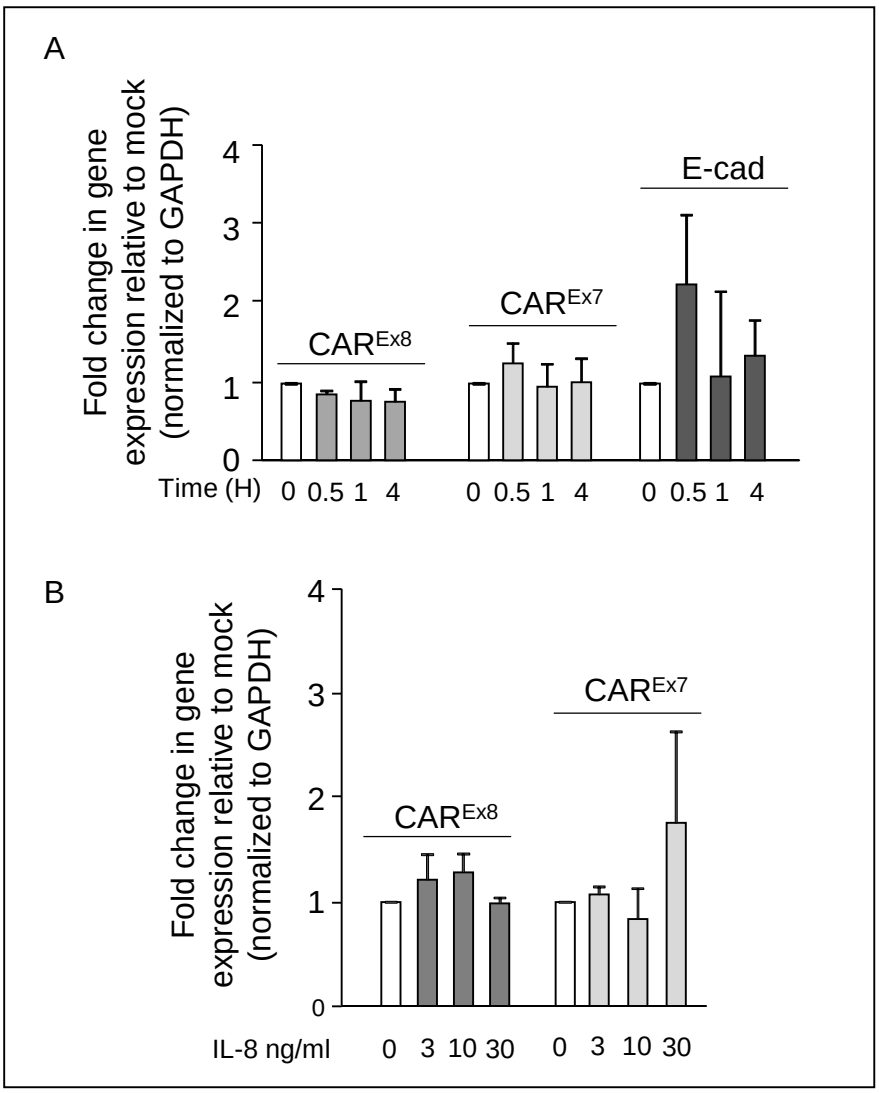

***Figure 13: IL-8 does not alter CAR^{Ex8} mRNA levels*.** A) Polarized primary airway epithelia cells were treated with IL-8 for varying lengths of time before RNA extraction and qPCR analysis were performed to quantitate the fold change in the gene expression of CAR^{Ex8,} CAR^{Ex7} and E-cadherin relative to 0 H control. An average of 3 experiments is shown. B) Polarized Calu-3 cells were treated with increasing concentration of IL-8 for 4 H before RNA extraction and qPCR analysis were performed to quantitate the fold change in the gene expression of CAR^{Ex8} and CAR^{Ex7} relative to untreated (0 ng/ml IL-8) control. The values reported are the mean and the standard error of the mean (S.E.M.) of 3 individual experiments. No significant difference was detected by ANOVA.

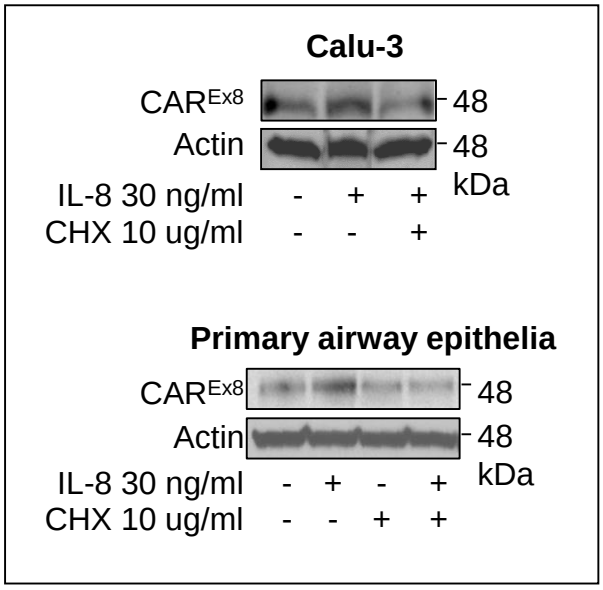

Figure 14: IL-8 increases new CAR^{Ex8} protein synthesis. A) Polarized Calu-3 cells, or B) polarized primary airway epithelial cells were either untreated or treated with IL-8 30ng/ml for 4 H in the absence or presence of cycloheximide (CHX). CAR^{Ex8} expression in cell lysates was analyzed by Western blot.

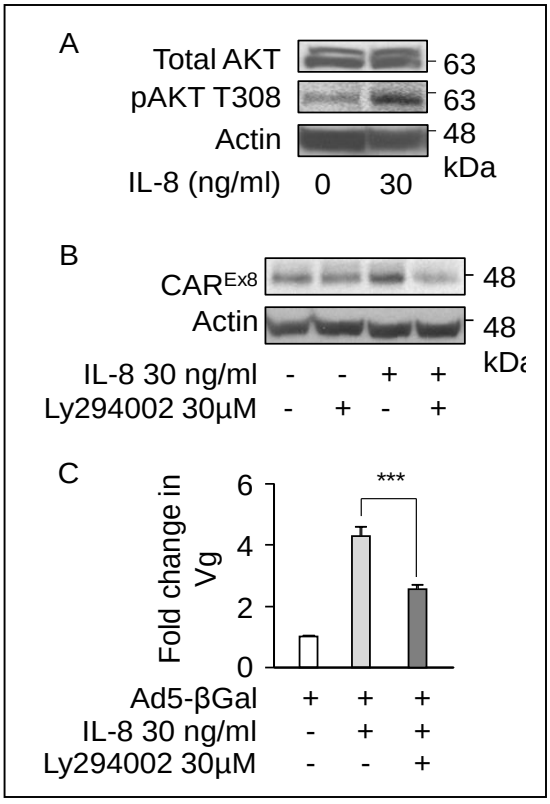

Figure 15: IL-8 stimulates activation of AKT and augments CAR^{Ex8} expression and adenoviral infection. A) Polarized Calu-3 epithelia were either untreated or treated with 30 ng/ml IL-8 for 4 H. pAKT T308 is the activated form of AKT. B) Polarized Calu-3 epithelia were either untreated or treated with IL-8 in the presence or absence of the AKT inhibitor Ly294002 (30 µM) for 4 H Quantitation of relative CAR^{Ex8} band intensity normalized to actin is shown below the blot. C) Polarized Calu-3 epithelia were either untreated or treated with IL-8 30 ng/ml in the presence or absence of AKT inhibitor Ly294002 (30 µM) for 4 H followed by infection with Ad5-βGal. Genomic DNA was isolated 24 H post infection to determine the fold change in viral genomes (vg; viral entry) using qPCR. Statistical significance was evaluated using one-way ANOVA and Bonferroni post hoc test, ***P<.001.

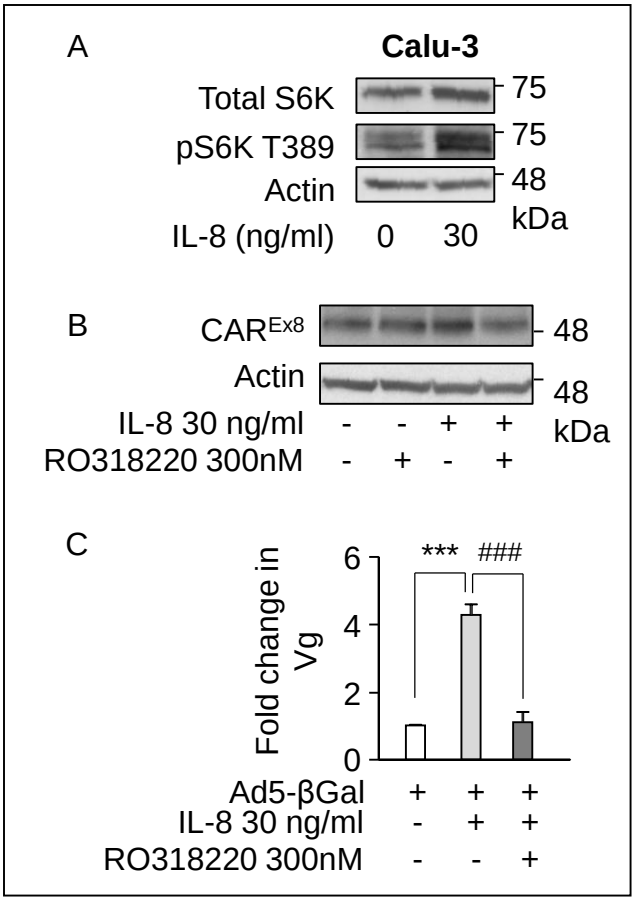

Figure 16: IL-8 stimulates the activation of ribosomal S6 kinase (S6K) and augments CAR^{Ex8} expression and adenovirus infection. A) Polarized Calu-3 cells were either untreated or treated with IL-8 30 ng/ml for 4 H. Whole cell extracts were analyzed by Western blot for the expression of total S6K and pS6K T389, the activated form of S6K. B) Polarized Calu-3 cells were either untreated or treated with IL-8 30 ng/ml in the presence or absence of S6K inhibitor RO318220 (300 nM) for 4 H, Post treatment the whole cells extracts were analyzed by WB for CAR^{Ex8} expression or C) infected with Ad5-βGal, followed by genomic DNA extraction and quantitation of the fold change in viral genomes (vg; viral entry) using qPCR. Statistical significance was evaluated using one-way ANOVA and Bonferroni post hoc test, ***P<.001.

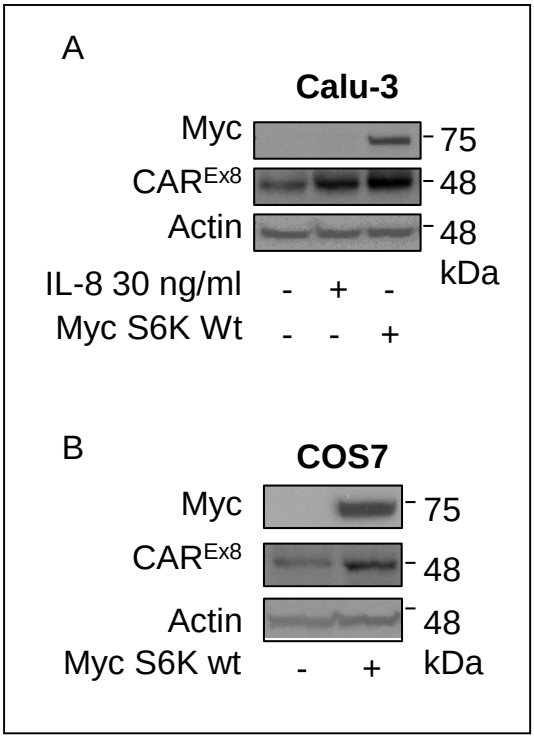

Figure 17: S6K augments CAR^{Ex8} protein expression. A) Polarized Calu-3 cells were either untreated or treated with IL-8 30 ng/ml and compared to polarized Calu-3 cells that were transfected with a Myc-tagged S6K plasmid. B) COS7 cells were either untransfected or transfected with Myc tagged S6K plasmid. Whole cell extracts were prepared form both Calu3 and COS7 cells and analyzed by Western blot for expression of myc-tagged S6K, CAR^{Ex8}, and actin.

IL-8 signaling inactivates GSK3β which negatively regulates CAR^{Ex8} expression.

Our lab has previously shown that GSK3β negatively regulates CAR^{Ex8} expression [20]. Therefore, to further decipher the signaling downstream of IL-8-stimulation, the activity of GSK3β was investigated. IL-8 treatment of either Calu-3 cells (Figure 18A) or primary airway epithelial cells (Figure 18B) resulted in an increase in the phosphorylated form of GSK3β at serine 9 (GSK3β-S9). Phosphorylation at S9 inactivates GSK3β [90, 91]. To further validate the involvement of GSK3β, primary airway epithelial cells were treated for 4 H with SB415286 or LiCl which are known GSK3β inhibitors [92]. We observed that both GSK3β inhibitors increased CAR^{Ex8} expression to a level similar to that observed with IL-8 treatment (Figure 19A) and increased airway epithelial cells susceptibility to adenoviral infection (Figure 19B). To our knowledge, this is the first time that IL-8 signaling has been shown to inhibit GSK3β. Taken together these data indicate that IL-8 regulates CAR^{Ex8} protein expression by inhibiting GSK3β.

AKT/S6K and GSK3β increase CAR^{Ex8} through parallel pathways

The data above shows that inhibition of GSK3β and over expression of S6K each increase apical CAR^{Ex8} to a similar degree. To determine whether GSK3β- and S6K-mediated regulation of CAR^{Ex8} are within the same pathway, polarized Calu-3 cells were either untreated or treated with IL-8 30 ng/ml for 4 H in the presence GSK3β inhibitor (SB415286, 45 μM) or S6K inhibitor (RO318220, 300 nM) or in a combination of both SB415286 and RO318220. I predicted that if S6K was a downstream target of GSK3β, inhibition of S6K would prohibit increased

CAR^{Ex8} protein levels when GSK3β was inhibited. However, a standard increase in CAR^{Ex8} protein levels (Figure 20) was observed indicating that the GSK3β and S6K pathways do not overlap.

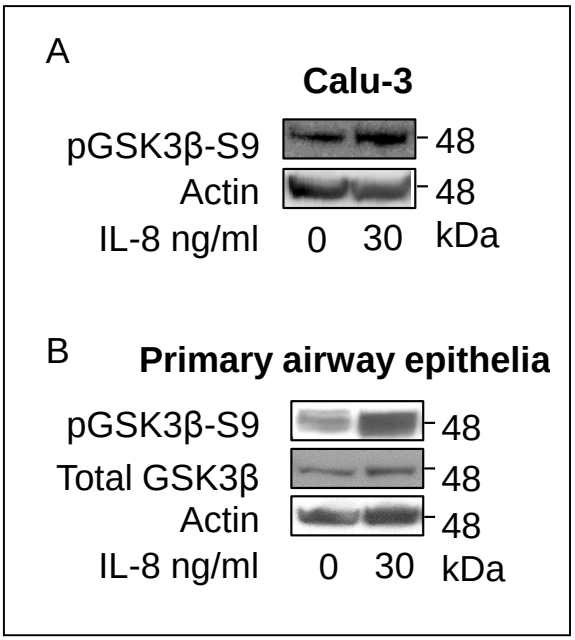

Figure 18: IL-8 treatment results in the inactivation of GSK3β. A) Polarized Calu-3 cells and B) polarized primary airway epithelial cells were treated with IL-8 30 ng/ml for 4 H. The expression of GSK3β-S9 (inhibited form of GSK3β) was analyzed by Western blot. Protein expression of whole GSK3β and actin were also determined as controls.

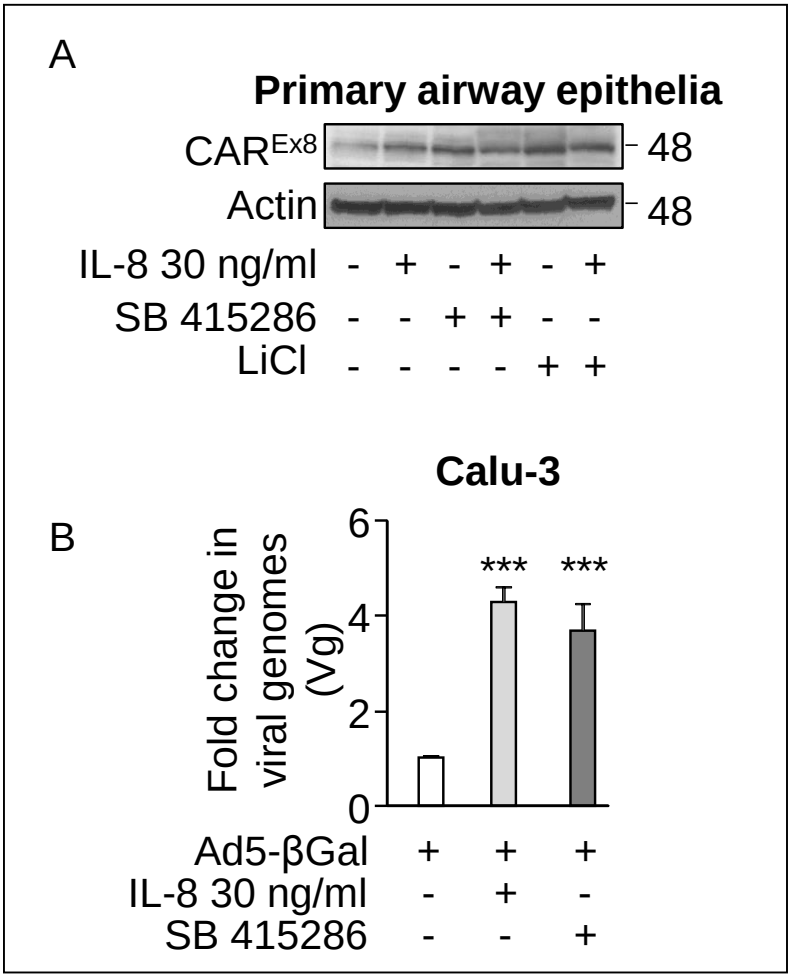

Figure 19: GSK3β negatively regulates CAR^{Ex8} expression and adenoviral infection. *A) Primary airway epithelial cells were treated with GSK3β inhibitors and CAR^{Ex8} expression was analyzed by Western blot. B) Calu-3 cells were either untreated, treated with IL-8 30 ng/ml, or treated with the GSK3β inhibitor SB 415286 for 4 H, followed by infection with Ad5-β-Gal. The cells were analyzed 24 H post infection. Experiments were repeated at least 3 times; representative Western blot experiments are shown and quantified.* Statistical significance was evaluated using one-way ANOVA and Bonferroni post hoc test, ***P<.001.

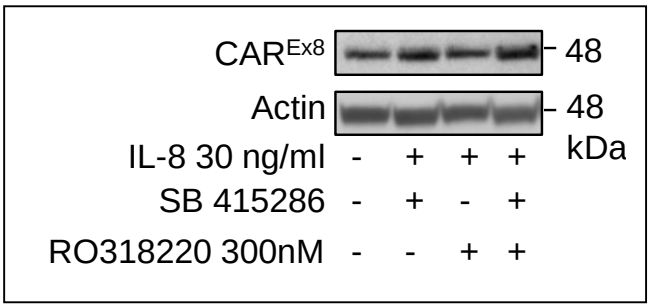

Figure 20*: *AKT/S6K and GSK3β increase CAR^{Ex8} through parallel pathways. Polarized Calu-3 cells were either untreated or treated with IL-8 30 ng/ml for 4 H in the presence GSK3β inhibitor (SB415286, 45 μM) or S6K inhibitor (RO318220, 300 nM) or in a combination of both SB415286 and RO318220. Whole cell lysates were analyzed by Western blot analysis for expression of CAR^{Ex8} and actin.

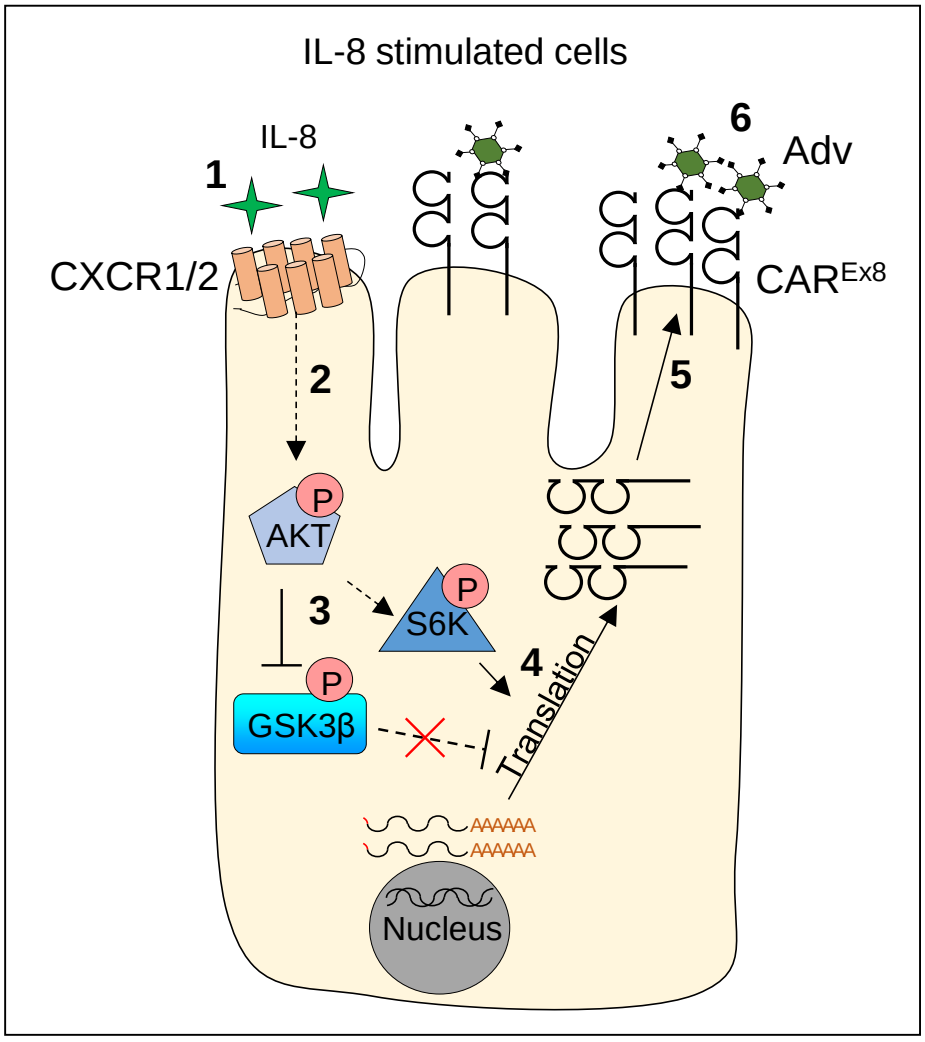

Figure 21: Schematic model of the pathway by which IL-8 stimulates an increase in CAR^{Ex8} protein expression summarizing results. 1) IL-8 binds to the IL-8 receptor (CXCR1/2). 2) AKT is activated and GSK3β is inhibited downstream of AKT. 3) Activation of AKT in turn activates S6K to increase CAR^{Ex8} protein expression. Inhibition of GSK3β relieves its inhibition of CAR^{Ex8} protein synthesis. 4) Both of these pathways stimulate CAR^{Ex8} protein synthesis, 5) which increases CAR^{Ex8} localization at the apical surface of the epithelial cell, and 6) augments adenoviral infection.

3.4. Discussion

We show for the first time that IL-8 stimulates the expression of CAR^{Ex8} at the apical surface of the polarized airway epithelial cells without altering the mRNA levels for CAR^{Ex8} (Figures 7, 9, 11, 13 and 14). Consequently, this increases the susceptibility of the apical surface of the epithelium to adenovirus infection. We demonstrate a novel signaling cascade downstream of IL-8, wherein exposure of airway epithelial cells to IL-8 results in the inhibition of GSK3β (Figure 18). Additionally, we also observed that IL-8 treatment caused robust activation of AKT and S6K, which enhance CAR^{Ex8} protein levels leading to increased adenovirus infection (Figures 15, 16 and 17). The same mechanism is found in both Calu-3 cells and well-differentiated primary airway epithelial cells. Primary airway epithelia are powerful models since they closely reflect an *in vivo* airway epithelium [93, 94]. These data elucidate a novel signaling mechanism underpinning the regulation of the "apical" adenovirus receptor, CAR^{Ex8}, and bridge a gap in our knowledge of how host cytokines enhance viral entry from apical epithelial surfaces.

Pathogens have developed multiple ways to break into host cells. Many pathogens like *E. coli* and *H. pylori* breach the epithelial barrier integrity before it can infect the cells [95]. Viruses, on the other hand, are sophisticated in that they often infect epithelial cells without causing much damage to the barrier integrity [16, 17]. For example, Coxsackie B virus binds to DAF which causes translocation of the virus to the tight junction where it can interact with CAR and gain entry into the cells [16]. Reovirus binds sialic acid at the apical surface which then, mediates binding of the virus to its receptor JAM-A in order to enter into the cells [17]. Many

inflammatory factors have been shown to modulate viral infections. For example, IL-26 increases adsorption of vesicular stomatitis virus onto target cells [96]. In fact, viral infections are quite common in inflammatory respiratory diseases such as COPD [97], cystic fibrosis [66, 98], and asthma [99]. Our work improves the understanding of the mechanisms behind the effect of cytokines on viral infection.

The proinflammatory cytokine IL-8 belongs to CXCL family of cytokines and is one of the first cytokines released by a variety of host cells during a pathogenic insult. IL-8 is a neutrophil chemoattractant and modulates numerous cellular signaling proteins in a variety of cell types, including epithelial cells [100]. Cytokines regulate the expression of various cell surface proteins. For example, ICAM-1 is shown to localize at the intestinal epithelial apical surface in response to IFN–γ [10]. IFN-γ also disrupts the epithelial barrier integrity by promoting macropinocytosis of tight junction proteins including occludin, claudin-1, and JAM-A [8, 9]. Exposure of airway epithelial cells to TNF-α in combination with IFN-γ downregulates the expression and delocalizes tight junction proteins JAM and ZO-1 in airway epithelia, and CAR in endothelial cells [6, 7]. For the first time, we show that the stimulation of polarized Calu-3 and primary airway cells with IL-8 augments the protein, but not the mRNA levels of CAR^{Ex8}. Interestingly, the IL-8-mediated effect did not affect the expression of CAR^{Ex7} or E-cadherin, indicating that the regulation may be specific to CAR^{Ex8}. IL-8 also has an acute effect that stimulates maximal CAR^{Ex8} expression between 4-12 H. There might be several reasons for the acute effect of IL-8 on CAR^{Ex8} expression. For example, CAR^{Ex8} might be crucial in mediating early innate immunological responses. Prolonged signaling

may lead to adverse immunological complications due to prolonged inflammation. It is also possible that IL-8-mediated signaling undergoes negative feedback to inhibit IL-8 signaling by downregulating the IL-8 receptor [101]. Future work will focus on these possibilities and the speculation that adenovirus entering into the lung on air-suspended droplets may take advantage of the temporary increase in apical CAR^{Ex8} to invade the epithelium. It is also demonstrated that IL-8 increases the CAR^{Ex8} protein expression without affecting its mRNA transcript levels. Moreover, blocking protein synthesis with CHX, blocked the IL-8-mediated effect suggesting that IL-8 signals protein synthesis of CAR^{Ex8}. In the future, pulse-chase experiments using radiolabeled methionine will be more conclusive to prove the direct effect of IL-8 on CAR^{Ex8} protein synthesis.

Further evidence indicates that IL-8 triggers activation of AKT and its proximal target, S6K (Figures 15 and 16). This is consistent with the previous studies demonstrating IL-8/AKT/S6K-mediated upregulation of cyclin D1 protein synthesis [83, 102]. Active S6K directly stimulates protein translation via phosphorylation of ribosomal S6 protein. S6K is also known to be activated by mTOR [102]. Interestingly, we did not observe an increase in the active form of mTOR, phospho-mTOR-S2448, when Calu-3 or primary airway epithelial cells were treated with IL-8 (data not shown). Whether alternative activated forms of mTOR, such as phospho-mTOR-S1261 [103], or other potential players, such as PDK1 [104], might be involved in S6K activation are currently under investigation.

In addition, we demonstrate for the first time that IL-8 signaling results in the inhibition of GSK3β, as determined by the increase in phospho-GSK3β-S9 protein

(Figure 18). GSK3β is a ubiquitously expressed constitutively active serine/threonine kinase that regulates multiple signaling pathways, such as gene transcription, protein translation, cell-cycle regulation, and apoptosis [105]. Our data indicate that GSK3β negatively regulates CAR^{Ex8} expression and is consistent with our previous studies [20]. GSK3β is known to regulate protein translation by modulating the activity of eIF2B, a guanine nucleotide exchange factor for a protein translation initiation factor, eIF2 [85-87]. The results of this study, however, do not address the possibility of an indirect effect that may result from the inhibition of AKT/S6K or GSK3β, which is a limitation in this study.

We propose a model through which the protein levels of CAR^{Ex8} are stimulated by IL-8 and this model summarizes our results (Figure 21). Treatment of airway epithelial cells with IL-8 results in the activation of AKT which has two differential downstream targets: 1) S6K, which is activated, and 2) GSK3β, which is inactivated [91, 106]. Both these signaling proteins culminate in augmenting *de novo* CAR^{Ex8} protein synthesis and in turn susceptibility to adenoviral infection. The reason why one external stimulus differentially activates two pathways is not clear. However this is not an uncommon phenomenon. For example, coxsackievirus binding at the apical surface of gut epithelial cells is shown to activate Abl and Fyn kinase differentially and both of these signaling proteins, and their respective pathways, are crucial for the efficient infection of polarized gut epithelial cells by group B coxsackieviruses [16].

Why are CAR^{Ex8} levels increased at the apical epithelial cell surface in response to IL-8? I hypothesize that CAR^{Ex8} localizes at the apical surface of

epithelial cells to retain leukocytes, such as neutrophils, in the region of inflammation by interacting with the leukocyte-specific junctional adhesion molecule-like protein (JAML). The basolateral CAR-JAML interaction is for efficient neutrophil transmigration [43, 44]. Upregulated apical CAR^{Ex8} may retain infiltrating neutrophils in the region of inflammation and limiting distant, spurious inflammation. The following aim is focused on testing the hypothesis that CAR^{Ex8} tethers neutrophils at the epithelial apical cell surface.

Chapter 4: CAR^{Ex8} tethers infiltrating neutrophils at the epithelial apical surface

The data presented so far demonstrates that exposure of an airway epithelium to IL-8 stimulates CAR^{Ex8} protein levels in the cell and at the apical surface of the epithelium. Adenovirus is then able to take advantage of increased apical CAR^{Ex8} to efficiently enter the airway epithelium. However, why would the cell increase CAR^{Ex8} levels in response to IL-8 stimulation if it might be detrimental for the cell? One possible answer to this question is that CAR^{Ex8} might be crucial for an innate function. It is well accepted that viruses have evolved to exploit essential proteins and cellular biology to enhance infection and survival of the virus. It is likely that invading adenovirus has simply taken advantage of an important physiological cell function in order to gain entry into the epithelium. By exploiting an evolutionary conserved physiological function, adenovirus has found a niche that the host has not eliminated through natural selection. ***We hypothesize that the endogenous function of CAR^{Ex8} in a polarized epithelium is to tether infiltrating neutrophils at the apical surface of polarized airway epithelial cells.***

This hypothesis was tested through three specific aims:

4.1. ***To generate stable MDCK cells expressing inducible human CAR^{Ex8}, human CAR^{Ex7}, or m-Cherry.***

4.2. To show that CAR^{Ex8} mediates neutrophil adhesion at the epithelial apical surface.

4.3. To show that infiltrating neutrophils adhere to the apical surface in a CAR^{Ex8} dependent manner

4.1. Generation of stable MDCK cells expressing inducible human CAR^{Ex8}, or human CAR^{Ex8}, or m-Cherry.

4.1.1. Rationale:

I hypothesized that CAR^{Ex8} mediates neutrophil adhesion at the epithelial cell surface. If this hypothesis is true, then increasing the cellular apical levels of CAR^{Ex8} will increase neutrophil adhesion at the apical cell surface. To test this, we developed MDCK cells that stably express human CAR^{Ex8} under the regulation of a doxycyclin (DOX) inducible promoter. This system enables the manipulation of the levels of CAR^{Ex8} expressed within an established epithelium. Additionally, control cells stably expressing either human CAR^{Ex7} or the red fluorescent protein, m-Cherry, were also developed.

4.1.2. Results:

Inducible MDCK stable cells expressing CAR^{Ex7}or CAR^{Ex8}, or mCherry

MDCK cells were chosen because these cells are well characterized, grow fast, and most importantly, polarize rapidly into an epithelium with the expected distribution of cellular proteins. To generate MDCK stable cells, cells were first infected with lentivirus carrying the Tet-on gene that is required for inducible expression from the pLVX-tight-puro promoter. Clonal cell lines from single cells

were compared to the parental MDCK to identify the Tet-on cell line most similar to parental. This MDCK-Tet-on cell line was the parental cell line for creating the Dox-inducible pLVX-tight-puro cell lines carrying the gene encoding FLAG-tagged human CAR^{Ex7}, or FLAG-tagged human CAR^{Ex8}, or m-Cherry. Clones from single cells stably expressing Dox-inducible CAR^{Ex8}, CAR^{Ex7} and mCherry were selected and expanded. These clones are from now on referred to as either MDCK-CAR^{Ex8}, MDCK-CAR^{Ex7}, or MDCK-mCherry cells. The stable integration of CAR^{Ex8}, CAR^{Ex7}, or m-Cherry was confirmed using PCR (Figure 22). The primers used in the PCR analysis of DNA from these cells were specific to exogenous CAR^{Ex8} or CAR^{Ex7}, respectively, and did not detect the endogenous gene. To accomplish this specificity, the forward and the reverse primer used to detect exogenous CAR^{Ex7} overlapped the junction between exon 6 and exon 7 for the upstream primer while the downstream primer was in the CAR^{Ex7}-specific sequence. PCR for CAR^{Ex8} used the same upstream primer but the downstream primer overlapped the splice site between exon 7 and exon 8. Using such primers eliminates the possibility of detecting the endogenous CAR^{Ex7} or CAR^{Ex8} gene in which the exons are interspersed with long introns. Several clones positive for the exogenous expression of CAR^{Ex7}, CAR^{Ex8}, or mCherry respectively were expanded and subjected to further characterization.

Characterization of MDCK- CAR^{Ex7}, CAR^{Ex8} and mCherry

The clones were chosen on the basis of their ability to form junctions, polarize into an epithelium and be infected by adenovirus. These properties of the MDCK stable cells in the absence of DOX was compared to the parental MDCK cell line. Of the

multiple different colonies and clones picked for gene, MDCK-CAR^{Ex8} clone #1, MDCK-CAR^{Ex7} clone #3, and MDCK-mCherry clone #1 were chosen after careful characterization and comparison with the parental MDCK (data not shown) in the absence of DOX. We analyzed the exogenous expression of CAR^{Ex8} and CAR^{Ex7} in the presence of increasing concentration of DOX using WB analysis (Figure 23A). We observed that with increasing concentration of DOX there was a dose-dependent increase in the expression of FLAG-CAR^{Ex8} and CAR^{Ex7}. In addition, apical surface-specific biotinylation was performed and we observed a dose-dependent increase in the apical localization of CAR^{Ex8} (Figure 23B). In contrast, in the presence of DOX we observed little or no CAR^{Ex7} at the apical surface, as predicted.

MDCK-CAR^{Ex8} shows an increased susceptibility to adenovirus infection.

To characterize the susceptibility of the polarized MDCK stable cells to adenovirus infection, cells were polarized and infected with Ad5-β-Gal from the apical surface. Consistent with the WB, we observed a rapid dose-dependent increase in adenoviral entry for the MDCK-CAR^{Ex8} stable cell line followed by a plateau in viral transduction (Figure 23C) and viral genomes (Figure 23D). This cell line had a 2-8 fold increase in adenoviral entry, as measured by viral genomes, when compared to MDCK-CAR^{Ex7} and mCherry stable cells. This data strongly suggests that CAR^{Ex8} increased the polarized airway epithelial cell susceptibility to adenoviral infection. This property is attributed to the apical localization of CAR^{Ex8} since MDCK-CAR^{Ex7} did not show any significant difference when compared to the control MDCK-mCherry cells. These experiments confirmed the successful

development of MDCK stable cells that express DOX inducible FLAG-CAR^{Ex8}, FLAG-CAR^{Ex7}, and mCherry. These stable cell lines were critical for many of the remaining experiments in my thesis.

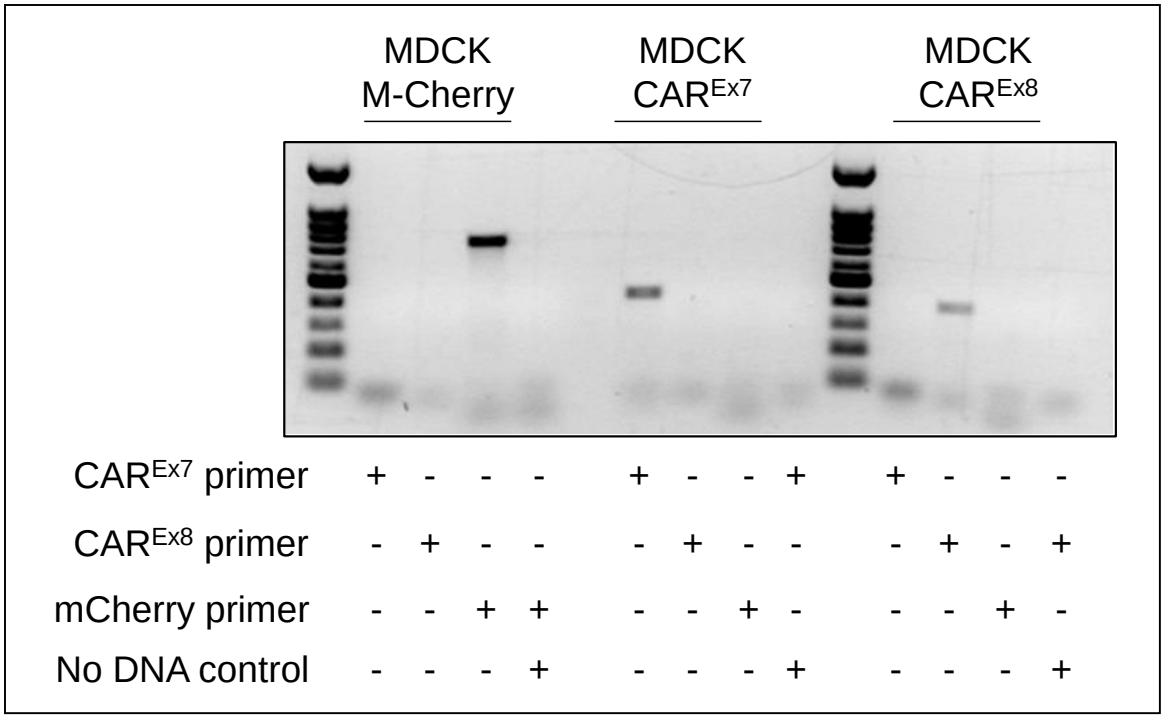

Figure 22: MDCK cells that have stably incorporated m-Cherry, CAR^{Ex7}, or CAR^{Ex8} exogenous tet-inducible genes. The DNA isolated from the MDCK-mCherry, MDCK-CAR^{Ex7} and MDCK-CAR^{Ex8} cells was PCR amplified to determine the presence of stably incorporated mCherry, CAR^{Ex7} and CAR^{Ex8} DNA, respectively.

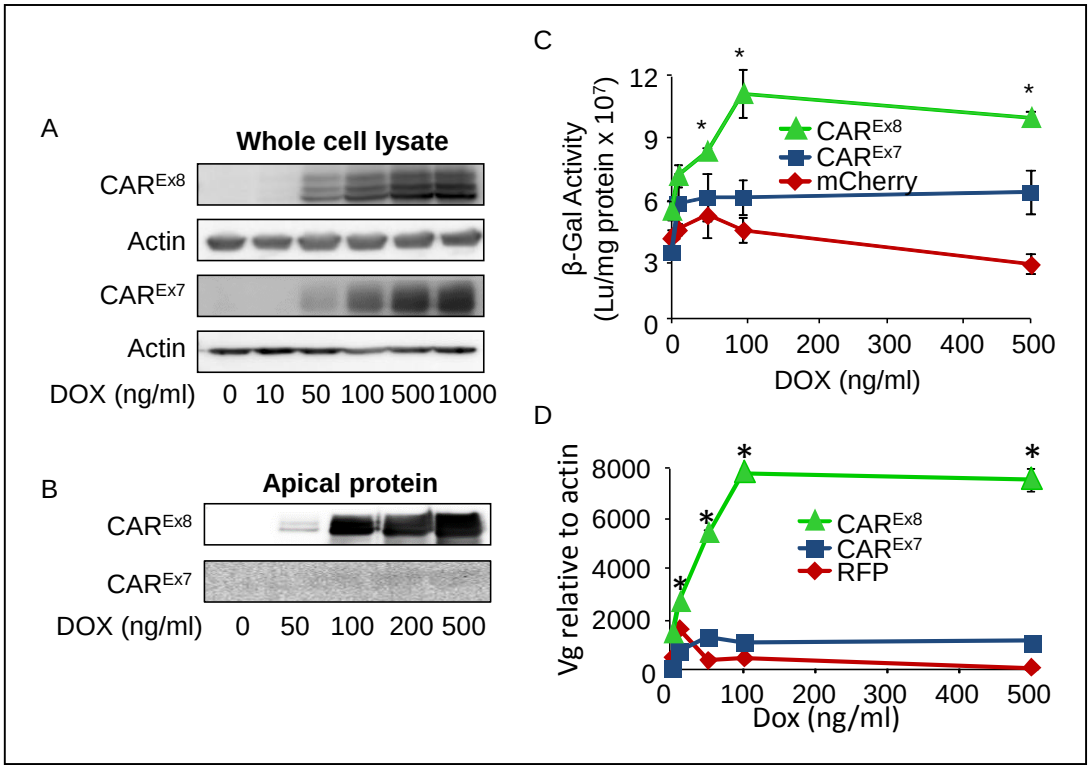

Figure 23: Doxycycline dose response in MDCK cells stably expressing DOX-inducible CAR^{Ex8}, CAR^{Ex7}, or mCherry polarized epithelia. A) Increasing DOX increases CAR^{Ex8} or CAR^{Ex7} protein levels but not actin. B) Apical-surface selective biotinylation of CAR^{Ex8} and CAR^{Ex7} shows the presence of FLAG-tagged CAR^{Ex8} but not CAR^{Ex7}. C) MDCK stable cells treated with increasing DOX shows a dose-dependent increase in apical Ad-β-Gal activity (which correlates with viral transduction) and D) viral genomes (Vg), (which correlates with the amount of viral entry). The dramatic increase is not seen in the MDCK-CAR^{Ex7} cells and the negative control MDCK-mCherry cells. Statistical significance was evaluated using one-way ANOVA *P<.05.

4.2. CAR^{Ex8} mediates neutrophil adhesion at the epithelial apical surface.

4.2.1. Rationale:

Unlike CAR^{Ex7}, which localizes basolaterally, the CAR^{Ex8} isoform localizes apically in polarized airway epithelial cells. Zen et al., 2005 showed that blocking the basolateral CAR-JAML interaction reduces the rate of neutrophil transmigration by 50% [44]. JAML has been shown to interact with CAR at its extracellular D1 domain. The CAR D1 domain is identical between the CAR^{Ex7} and CAR^{Ex8} isoforms. Therefore, I hypothesized that while CAR^{Ex7} is crucial for neutrophils migrating through the paracellular space, CAR^{Ex8} tethers neutrophils at the epithelial cell surface. Therefore, I further hypothesized that increasing CAR^{Ex8} expression should promote neutrophil adhesion at the epithelial apical surface. The CAR-JAML interface overlaps with the region where CAR interacts with Ad FK. Thus, blocking CAR using Ad FK will further confirm CAR^{Ex8} mediated adhesion of neutrophils at the epithelial apical surface. As shown earlier, IL-8 stimulates CAR^{Ex8} protein expression and apical localization. Therefore, we predicted that treatment of airway epithelial cells with IL-8 would stimulate neutrophil adhesion at the epithelial apical surface.

4.2.2 Results:

MDCK-CAR^{Ex8} tethers neutrophils at the epithelial apical surface.

MDCK-CAR^{Ex8}, CAR^{Ex7} and mCherry cells were polarized on a tissue culture dish and induced with increasing concentrations of DOX for 24 H to enable dose-dependent increase in the expression of the exogenous genes. This was followed by a neutrophil adhesion assay using freshly isolated, fluorescently labelled

neutrophils from the peripheral blood of healthy donors. Increasing the CAR^{Ex8} protein levels in MDCK-CAR^{Ex8} cells correlated directly with increased neutrophil adhesion on the epithelial cell surface in a dose-dependent manner (Figure 24). In contrast, the MDCK-CAR^{Ex7} and mCherry cells only showed a baseline neutrophil adhesion both in the presence and absence of DOX (Figure 24). This data suggests that MDCK-CAR^{Ex8} cells tether neutrophils at the epithelial cell surface.

Neutrophil adhesion is CAR^{Ex8} mediated:

It is hypothesized that MDCK-CAR^{Ex8} tethers neutrophils at the apical surface via CAR^{Ex8}-mediated interaction. To directly test this hypothesis, the Ad5 FK was used to outcompete the putative interaction between epithelial apical CAR^{Ex8} and neutrophil JAML. Ad5 FK specifically binds to CAR to attach to the host cell and although the binding site overlaps the CAR-CAR and CAR-JAML binding sites, the CAR-FK affinity is 1000 and 500 times greater, respectively. CAR^{Ex8} was first blocked with purified Ad5 FK in polarized MDCK-CAR^{Ex8} cells that were either not induced or induced with DOX for 24 H. Fluorescently-labeled neutrophils were added to the apical surface and allowed to bind in the presence or absence of Ad5 FK for 15 min. In the presence of increasing Ad5 FK, there was a dose-dependent decrease in neutrophil adhesion (Figure 25). Moreover there was complete knock down of neutrophil adhesion at the highest Ad5 FK concentration (192 ug, nearly 10^6 times greater Ad5 FK than the predicted number of CAR receptor on the epithelial cell surface of uninduced cells) that was used. In contrast, the neutrophil adhesion could not be blocked in the presence of Ad3 FK, a control group B Ad that does not bind to CAR as the primary receptor (Figure 24). The primary

receptor for Ad3 is desmoglein 2 [107]. These data strongly suggest that CAR^{Ex8} tethers neutrophils at the apical epithelial cell surface.

IL-8 treatment of primary airway epithelial cells allows increased neutrophil adhesion on the apical surface of the Calu-3 cells.

I have previously shown that the treatment of both Calu-3 cells and primary airway epithelial cells with IL-8 stimulates CAR^{Ex8} at the epithelial apical surface with little or no effect on the basolateral CAR^{Ex7} protein levels. Thus, to confirm that IL-8-induced CAR^{Ex8} mediates neutrophil adhesion, we performed neutrophil adhesion assays on Calu-3 cells treated with IL-8 for 4 H. We observed that IL-8 treatment resulted in a significant increase in neutrophil adhesion (Figure 26).

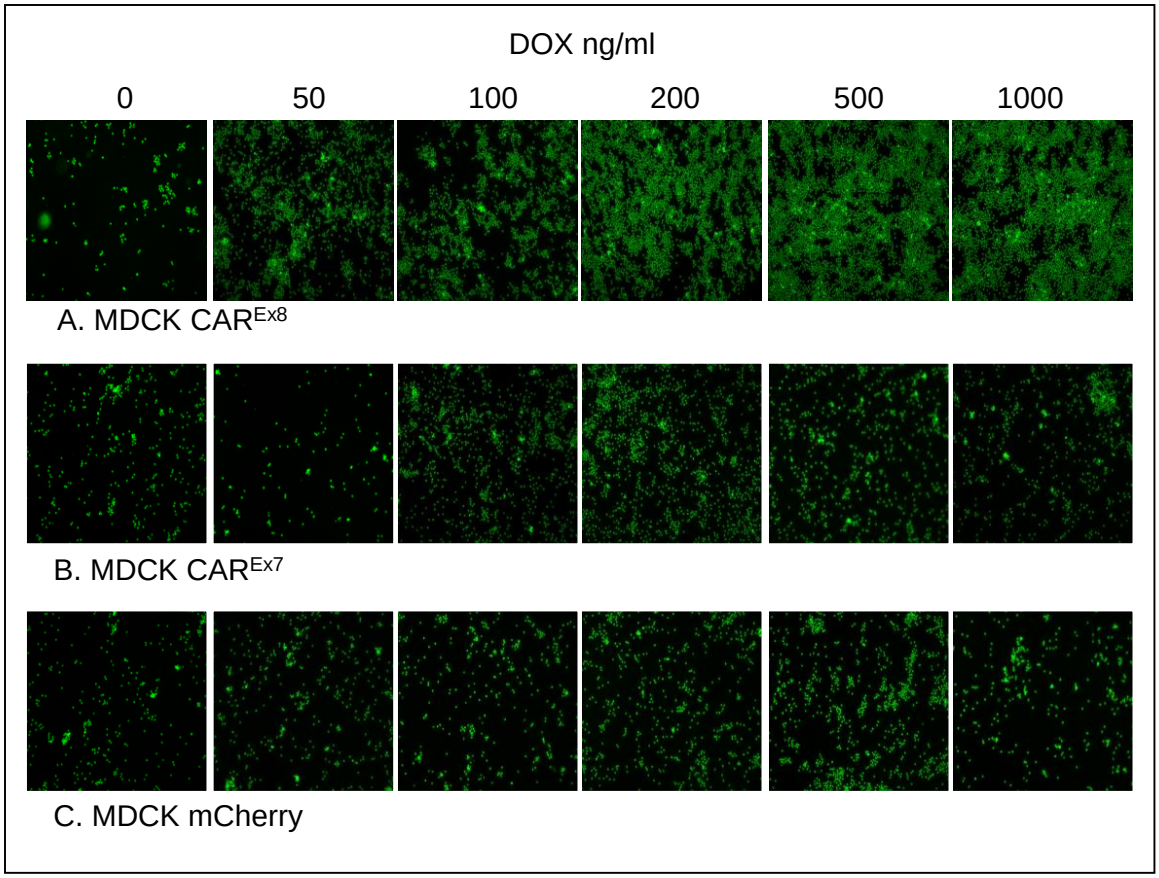

Figure 24: CAR^{Ex8} tethers neutrophils at the epithelial apical surface. Neutrophil adhesion assays were performed on DOX induced stable cells A) MDCK-CAR^{Ex8}, B) MDCK-CAR^{Ex7}, and C) MDCK-mCherry cells. Neutrophils (green) that adhered to the epithelial apical surface were imaged. Each panel is a representative image of the respective DOX concentrations used in this experiment.

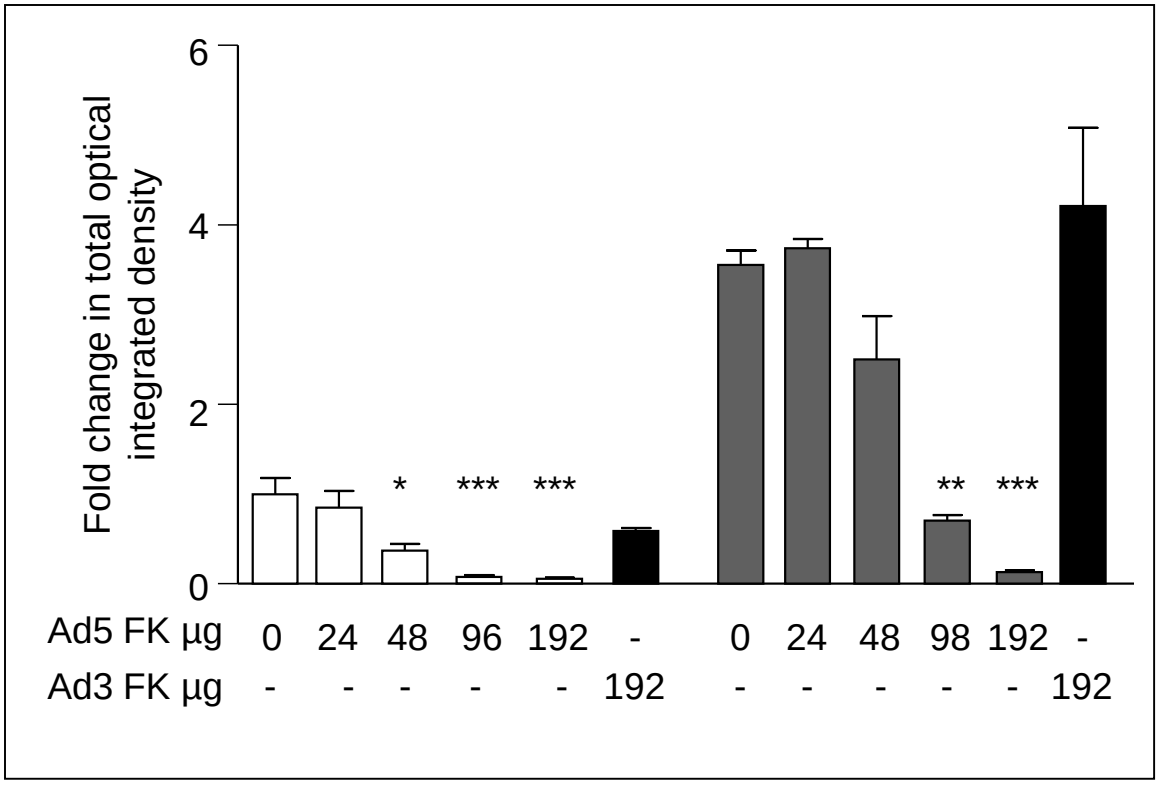

Figure 25: CAR^{Ex8} tethers neutrophils at the epithelial apical cell surface. A) MDCK-CAR^{Ex8} either uninduced or induced with DOX were treated with increasing concentrations of Ad5 FK (gray bars) or 640 ug/ml Ad3 FK (black bars). Neutrophil adhesion assays were performed with the freshly isolated, fluorescently labelled neutrophils. The adhered neutrophils were imaged and the fluorescence intensity was quantitated. Fold changes in the fluorescence intensity in comparison to uninduced and untreated controls are shown. Statistical significance was evaluated using one-way ANOVA and Bonferroni post hoc test. *P<.05, ** P<.01 and ***P<.001

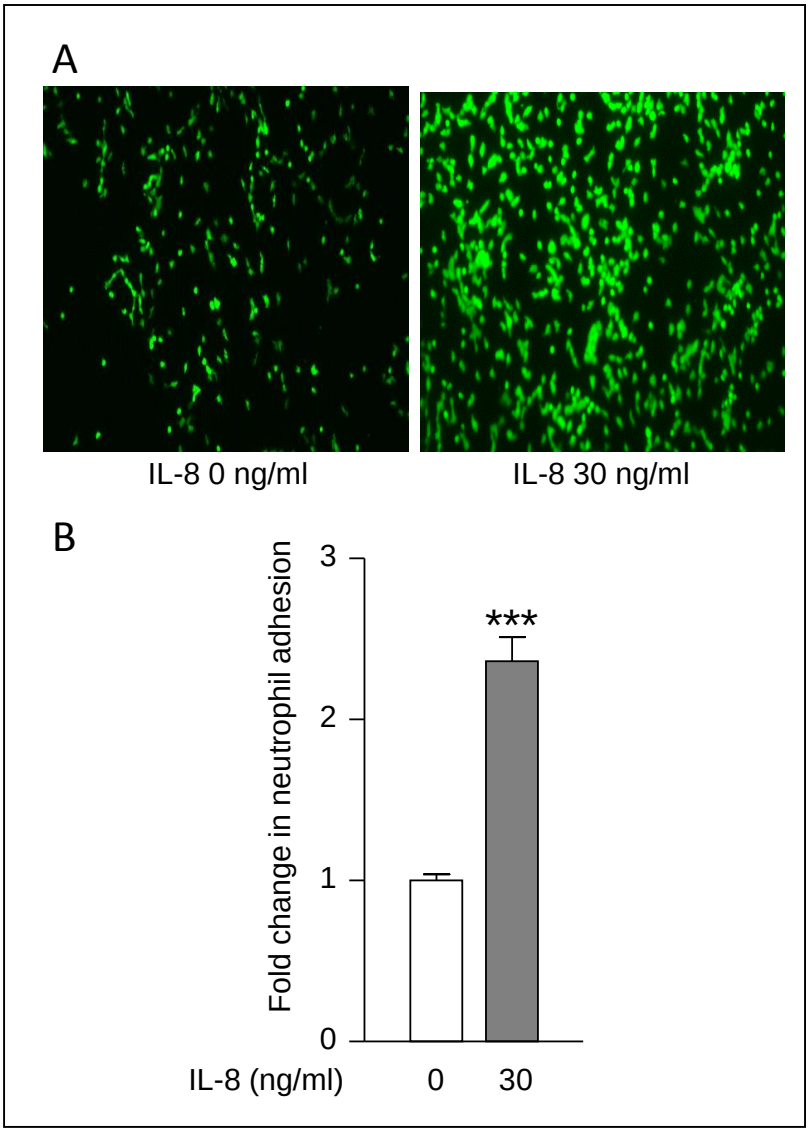

Figure 26: IL-8 treatment in Calu-3 cells increases neutrophil adhesion. IL-8 treatment in Calu-3 cells increases neutrophil adhesion. A) Calu-3 cells were either uninduced or induced with IL-8 30 ng/ml for 4 H. Post-treatment a neutrophil adhesion assay was performed. Bound neutrophils were imaged and B) quantitated using MetaMorph software. Statistical significance was evaluated using student t test, ***P<.001

4.3. Infiltrating neutrophils adhere to the apical surface in a CAR^{Ex8} dependent manner

4.3.1. Rationale:

Section 4.2 indicates that CAR^{Ex8} is able to tether neutrophils at the epithelial cell surface. However, *in vivo,* the neutrophils migrate from the basal surface of the epithelium, through the paracellular space and finally to the apical surface. At the apical surface the neutrophils remain adhered before detaching into the lumen of the airway. Therefore, I asked whether CAR^{Ex8} can tether the infiltrating neutrophils that transmigrate through the epithelium space to the apical surface in a physiologically relevant polarized basal to apical surface model system. Based on the results above it is predicted that CAR^{Ex8} will adhere the infiltrating neutrophils at the epithelial apical surface. On the other hand, because CAR^{Ex7} is shown to be important for neutrophil transmigration [44], it is predicted that overexpressing CAR^{Ex7} will promote neutrophil transmigration across the epithelium CAR^{Ex7}. It is also expected that induced mCherry cells will remain similar to baseline.

4.3.2. Results:

CAR^{Ex8} tethers infiltrating neutrophils at the epithelial cell surface.

To determine the fate of infiltrating neutrophils in the presence of increased CAR^{Ex8} concentrations, I performed a neutrophil transmigration assay (Figure 27). After allowing the neutrophils to migrate, 2 populations of cells were quantitated 1) neutrophils that completely transmigrated through the paracellular space and had entered the apical lumen (the outer well in the model system (Figure 27) and 2) neutrophils that remain adhered to the epithelial apical surface. I observed that

DOX treatment induced neutrophil adhesion at the apical surface of MDCK-CAR^{Ex8} cells (Figure 28C). However there was no change in neutrophil transmigration (Figure 28D). In contrast, Dox treatment induced neutrophil transmigration across the polarized epithelium of MDCK-CAR^{Ex7} cells without affecting neutrophil adhesion on the apical surface (Figure 28F). Neutrophil adhesion at the epithelial apical surface was not affected in MDCK-CAR^{Ex7} cells (Figure 28E). The MDCK-mCherry cells that served as a negative control had baseline neutrophil adhesion and migration (Figure 28A and B).

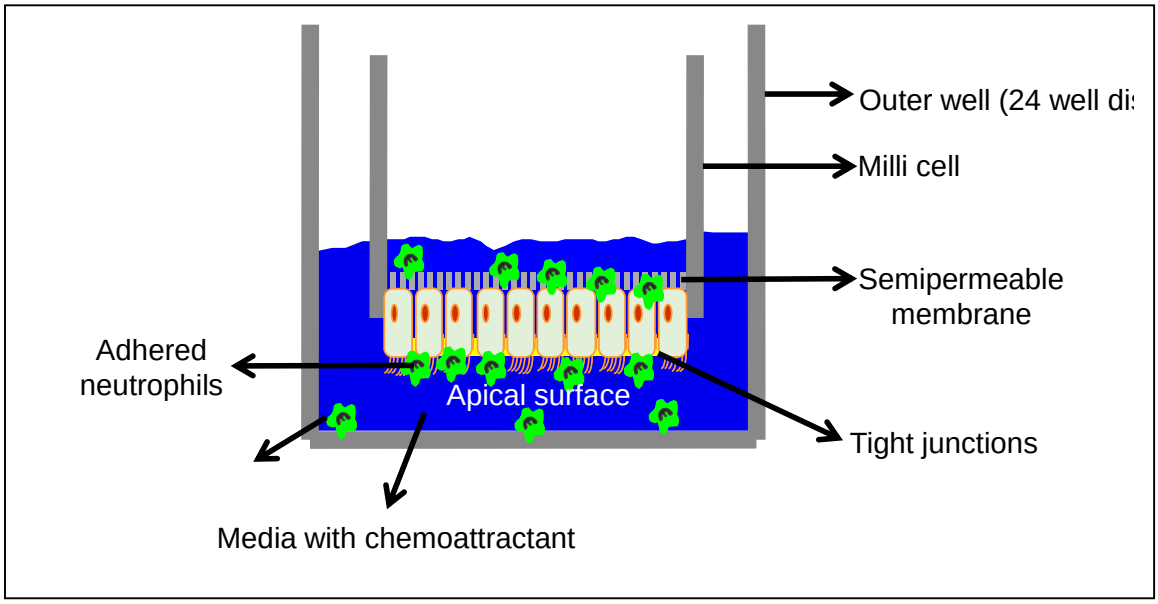

Figure 27: A model showing the system used for neutrophil transepithelial migration. The system contains an outer well with a millicell placed inside. The epithelial cells are polarized in an inverted fashion such that the apical surface is facing the bottom of the outer well. Fluorescently labelled neutrophils are chemically (chemoattractant) driven to transmigrate from the basal to the apical surface. After transmigration, neutrophils that remain adhered to the epithelial cells and those that transmigrated to the bottom of the outer well were quantitated.

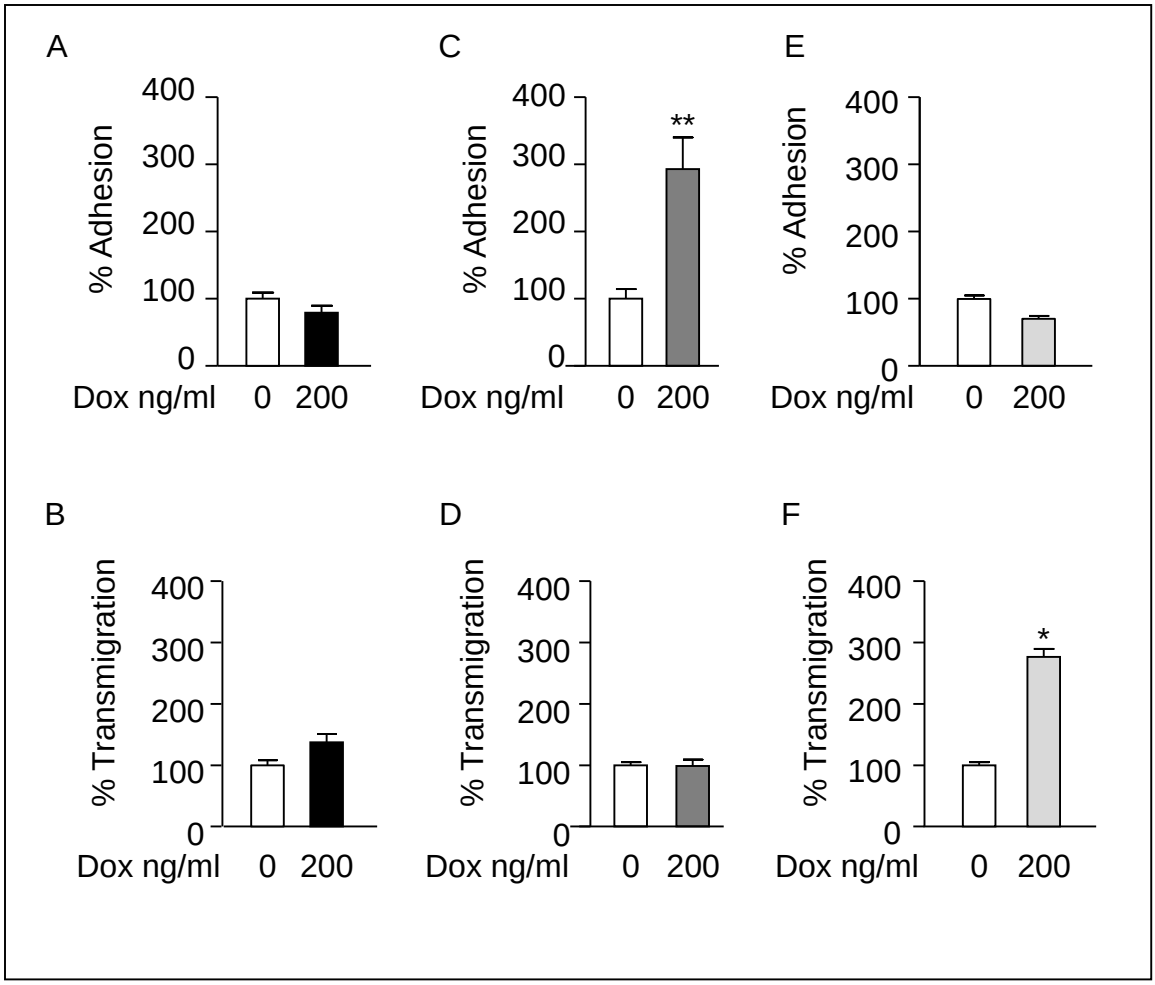

***Figure 28: CAR^{Ex8} tethers infiltrating neutrophils at the apical surface of the polarized epithelium*.** Neutrophil transmigration assays were performed in a physiologically relevant manner (basal to apical surface) in (A, B) MDCK-mCherry, (C, D) MDCK-CAR^{Ex8} and (E, F) MDCK-CAR^{Ex7} cells that were either uninduced or induced with DOX. % neutrophil adhesion (A, C, E) and % neutrophil transmigration (B, D, F) were quantitated by measuring the fluorescent intensity using metamorph software. Statistical significance was evaluated using student t test, *P<.05, **P<.01

4.4. Discussion

Upon pathogenic encounter, neutrophils are the first amongst the immune cells to arrive at the site of inflammation or infection. Neutrophils transmigrate through the endothelium into the interstitium and finally arrive at the airway lumen via transepithelial migration. Subsequently, via a combination of enzymatic and cytotoxic events, neutrophils aid in the clearance of pathogens. Therefore neutrophil transmigration is an important phenomenon in the innate immune response of the host. Deficiency in the neutrophil recruitment leads to several diseased conditions, such as LAD-1, and predisposal to infections [49]. On the other hand, uncontrolled neutrophil transepithelial migration and accumulation at the mucosal surface of the airway or gut is a hallmark of inflammatory diseases. For example, the accumulation of neutrophils in the alveolar space and intestinal crypts is observed in cystic fibrosis and inflammatory bowel diseases, respectively. The severity of the inflammatory disease directly correlates with the extent of PMN accumulation. Based on the type of cytokine present, different leukocytes are recruited. Monocyte Chemotactic Protein (MCP1), Macrophage Inflammatory Protein 1 alpha (MIP1α), and Regulated on Activation, Normal T cell Expressed and Secreted (RANTES; aka CCL5) recruit monocytes, T cells, natural killer cells, and eosinophils [108] The proinflammatory cytokine IL-8 recruits neutrophils preferentially [109].

The process of neutrophil transepithelial migration compels the constant formation and destruction of interactions between the neutrophil and the epithelium. After extravasation from the blood vessel and migration through the

interstitial tissues, it begins with the adhesion of neutrophils to the epithelial basal surface, followed by migration through the paracellular pathway, ultimately arriving at the apical surface (Figure 4). The different proteins that are involved in neutrophil adhesion at the apical surface and the importance of these molecules are finally being identified. For example, proteins, such as CD44 and DAF, are crucial for the detachment of neutrophils into the gastrointestinal lumen [58, 59]. However, less is known about neutrophil adhesion and detachment in the airway.

For the first time, a novel biological function for CAR^{Ex8} is described in this study. It has been shown that IL-8 augments apical CAR^{Ex8} expression in polarized airway epithelia (Figures 7, 9, 11). In addition, apically localized CAR^{Ex8} can tether neutrophils (Figure 24). This is supported by the finding, that blocking CAR^{Ex8} using adenovirus type 5 FK completely inhibits neutrophil adhesion, underscoring the importance of CAR^{Ex8} in tethering neutrophils (Figure 25). Interestingly IL-8 treatment of airway epithelia increased neutrophil adhesion (Figure 26). Since it is proven that IL-8 stimulates CAR^{Ex8} expression, it is very likely that IL-8 stimulated neutrophil adhesion might be via CAR^{Ex8}. Moreover, apical CAR^{Ex8} proves to be adhesive for infiltrating neutrophils, without grossly affecting neutrophil transmigration (Figure 28). It was also observed that CAR^{Ex7}, which localizes at the basolateral surface of polarized epithelia, promotes neutrophil transmigration but not apical adhesion (Figure 28). This data is in agreement with the previous study that shows blocking basolateral CAR affects the rate of neutrophil transepithelial migration [44]. It is speculated that the difference in the function of the two isoforms of CAR is attributed to its localization within the epithelium. In

addition the fact that neutrophil transmigration is not affected in MDCK-CAR^{Ex8} cells induced with DOX suggests that CAR^{Ex8} might not be involved in neutrophil transmigration.

Considering these lines of evidence, it is envisioned that IL-8 secreted during a pathogenic intrusion sets off an innate immune response by recruiting neutrophils to the apical surface. At the same time, IL-8 also increases the expression and the apical localization of CAR^{Ex8}, which serves to tether the recruited neutrophils. Adhesion of neutrophils to the epithelial apical surface could serve several essential biological functions such as: 1) To achieve the critical neutrophil concentration required for the efficient killing of invading pathogens; 2) To help maintain focused inflammation, thereby preventing unnecessary damage to the neighboring cells; 3) To form a defensive barricade that prevents further infection of the epithelium; and 4) To prevent neutrophils from being washed away into the airway lumen.

Expression of ICAM-1 has been shown to be upregulated in response to IFN-γ and TNF-α in both airway [53] and gastrointestinal epithelium [10, 52]. Also, increased ICAM-1 expression is evident in CF [110] and inflamed intestinal mucosa [10]. ICAM-1 has been shown to tether neutrophils at the apical surface of both the airway [110] and the intestinal epithelium. However, blocking ICAM-1 only partially reduced neutrophil adhesion suggesting the involvement of additional proteins [52, 110, 111]. Whether CAR^{Ex8} is involved in neutrophil tethering in the inflammatory diseases is yet to be determined. Uncontrolled secretion of proinflammatory cytokines, including IL-8 [110] and TNF-α, is evident in

inflammatory diseases. TNF-α, via activation of NFκB, is known to induce IL-8 secretion [112]. Therefore, it is very likely that CAR^{Ex8} is involved in tethering neutrophils at the apical surface. In the future, it will be intriguing to determine how the expression of CAR^{Ex8} differs in pathological tissues from patients with CF compared to healthy tissue from the general population.

Current therapeutic options for the treatment of chronic inflammation and neutrophilia in inflammatory diseases are largely ineffective [63, 110, 113-115]. A greater understanding of the mechanisms that govern neutrophilia is required in order to identify novel strategies and therapeutics for the treatment of excessive or prolonged neutrophil recruitment and retention. The vast majority of studies and therapeutic approaches have focused on neutrophils to combat neutrophilia. In contrast, tissue-targeted approaches may yield improved disease-specific therapeutics with fewer side effects. Therefore, there is a pressing need for the elucidation of various adhesive interacting partners and the mechanism underlying PMN retention at the epithelial apical surface. This will further enable the design of organ specific drugs for the treatment of inflammatory diseases. Thus, the findings of this study have direct implications in the development of interventions for the treatment of inflammatory diseases.

Chapter 5: Neutrophils tethered to the airway epithelial cell surface benefit adenovirus entry

Background: Currently there are no specific treatments for adenovirus infection and supportive care is insufficient. Particularly in military recruits, pediatric patients, and in immunocompromised individuals, adenovirus infection can cause fatal respiratory distress. Several studies have shown that for infants and adults with bronchitis and lower respiratory tract infections, adenovirus contributes to about 5-15% of total viral infections [116-120]. In a study conducted by Gem et al., adenovirus, detected either as a sole pathogen or in combination with other respiratory virus, accounts for nearly 20% of the viral infections in infants in urban areas, who are at a higher risk for wheezing illness and asthma [99].

Although many contributing factors, such as demographic characteristics, environmental factors, and allergen exposure, may influence the development of asthma, exposure to viral pathogen is also a critical factor for the development of asthma. In particular adenovirus infection is of interest because early exposure to the virus can further the development of asthma [121]. The development and severity of COPD has also been associated with adenovirus infections [21, 122]. In CF, the factors that modulate viral infection remain elusive. CF is characterized by accumulation of neutrophils at the epithelial apical surface. The

accumulation of neutrophils is detrimental to the epithelium. The reactive oxygen species generated by the neutrophils injure the surrounding tissue [123]. Therefore, I hypothesized that neutrophils adhered at the epithelial apical surface will augment adenoviral infection.

This hypothesis will be tested by 2 aims:

5.1. To test if neutrophils tethered on the epithelial apical surface augment adenoviral infection

5.2 To test if neutrophil adhesion alters transepithelial resistance

5.1. Neutrophils tethered on the epithelial apical surface increase the susceptibility of the epithelium to adenoviral infection

5.1.1. Rationale:

In the previous aim I demonstrated that CAR^{Ex8} tethers neutrophils at the epithelial apical cell surface. *In vivo* this function of CAR^{Ex8} might be essential because the adhered neutrophils form a defense barricade at the apical surface that is very important in normal healthy individuals. However, under pathological conditions the neutrophils that have accumulated at the epithelial apical surface might cause damage to surrounding tissue as a result of the chemicals released by the neutrophils. Therefore ***it is hypothesized that adhered neutrophils at the apical surface of the epithelium will aid in adenoviral infection***.

5.1.2. Results:

Tethered neutrophils augment viral entry in polarized epithelia.

In order to understand the contribution of neutrophils to viral infection, a neutrophil adhesion assay was performed with increasing concentrations of neutrophils (0 – 1 X 10^7) on polarized uninduced or induced MDCK-CAR^{Ex8} cells. The unbound neutrophils were washed off and the epithelia (with neutrophils adhered on the apical surface) were infected with adenovirus for 1 H, washed, and returned to the incubator. 24 H post infection, cells were lysed and viral entry was quantitated using qPCR analysis for viral genomes (vg). Consistent with the hypothesis I observed a significant 2-3 fold increase in adenoviral entry when more adhered neutrophils were present (Figure 29). Adenoviral entry was increased by an additional 2-fold when this same neutrophil adhesion assay was performed on MDCK-CAR^{Ex8} cells treated with DOX (Figure 29). This latter effect is attributed to increase in CAR^{Ex8} that is induced upon DOX treatment.

Next we used an alternate approach to test the hypothesis. A neutrophil adhesion assay was performed with one constant concentration of neutrophils on MDCK-CAR^{Ex8} cells, which were either induced or not induced with DOX. Post neutrophil adhesion, these epithelial cells were infected with increasing MOI of Ad5-β-Gal (Figure 30). To determine the baseline infection, uninduced MDCK-CAR^{Ex8} cells having no neutrophils were infected with increasing Vg. Interestingly, we observed that in the presence of neutrophils there was a significant 3-10 fold increase in adenoviral entry that was further amplified by at least 3 fold in the presence of DOX (Figure 30). In the case of uninduced MDCK-CAR^{Ex7} (Figure 31) and mCherry cells (Figure 32) there was a significant increase in adenovirus entry in the presence of neutrophils as observed in the uninduced

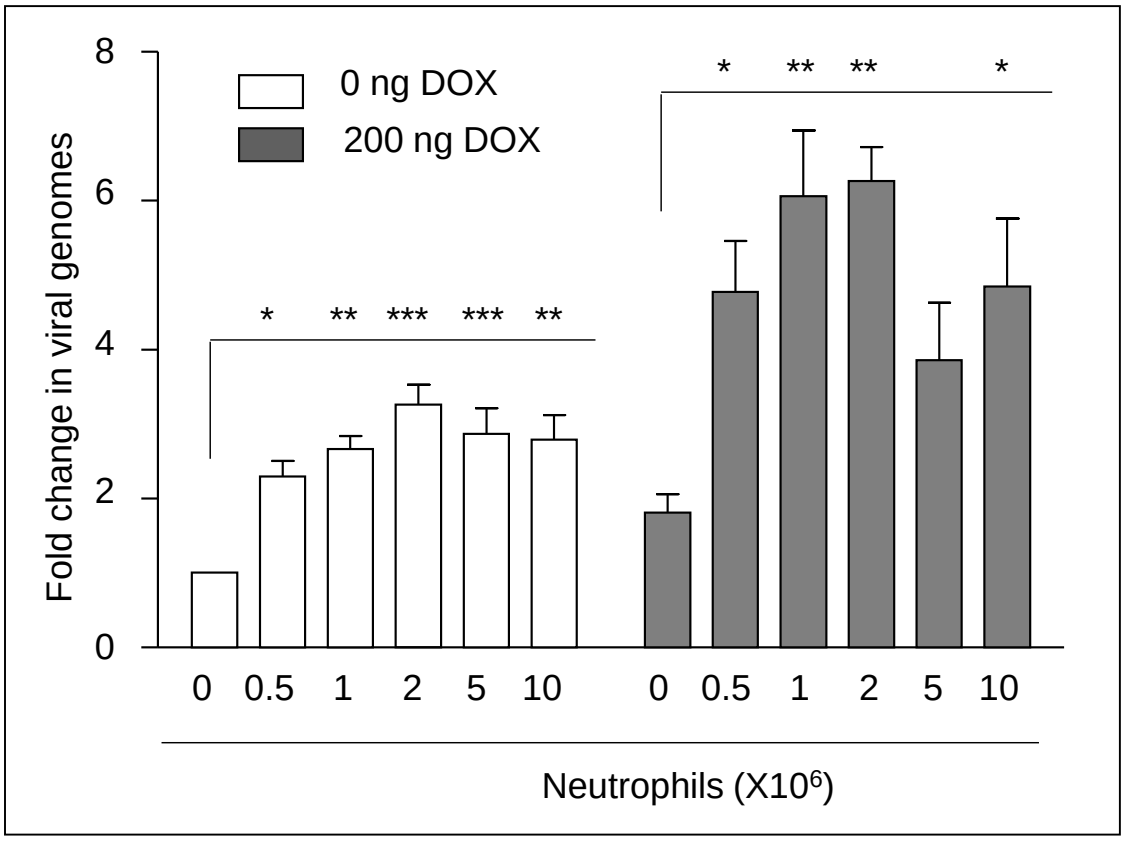

Figure 29: Doxycycline induction promotes adenoviral infection in MDCK-CAR^{Ex8} cells in the presence of adhered neutrophils. *MDCK-CAR^{Ex8} cells were either uninduced (white bars) or induced (shaded bars) with DOX. A neutrophil adhesion assay was performed with increasing number of neutrophils as indicated in the figure. Post neutrophil adhesion, the MDCK-CAR^{Ex8} cells were infected with Ad5-β-Gal for 1 H. 24 H later, viral entry was determined by quantitating viral genomes (Vg) using qPCR analysis. Fold change in viral genome entry is shown.* Statistical significance was evaluated using one way ANOVA and Dunnetts post hoc test, *P<.05, **P<.01, ***P<0.001.

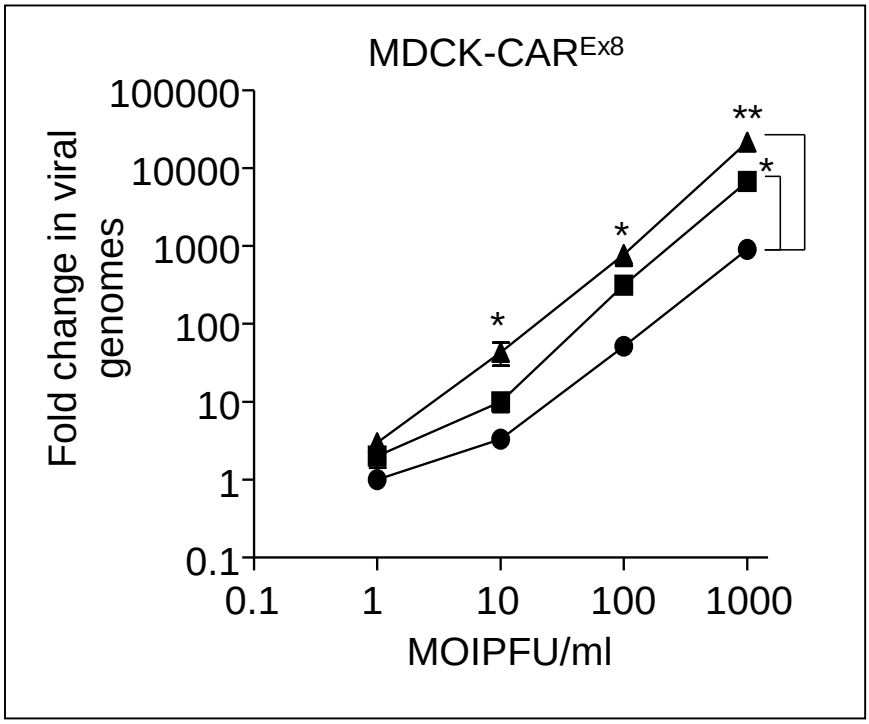

Figure 30: Neutrophils adhered on the apical surface of the epithelial cells promote adenoviral entry. Adenovirus entry was quantitated by qPCR analysis in uninduced MDCK-CAR^{Ex8} cells (circle) and compared with uninduced MDCK-CAR^{Ex8} cells with adhering neutrophils (square) and DOX induced MDCK-CAR^{Ex8} cells with adhering neutrophils (triangle). Statistical significance was evaluated using one way ANOVA and Bonferroni post hoc test, *P<.05, **P<.01,

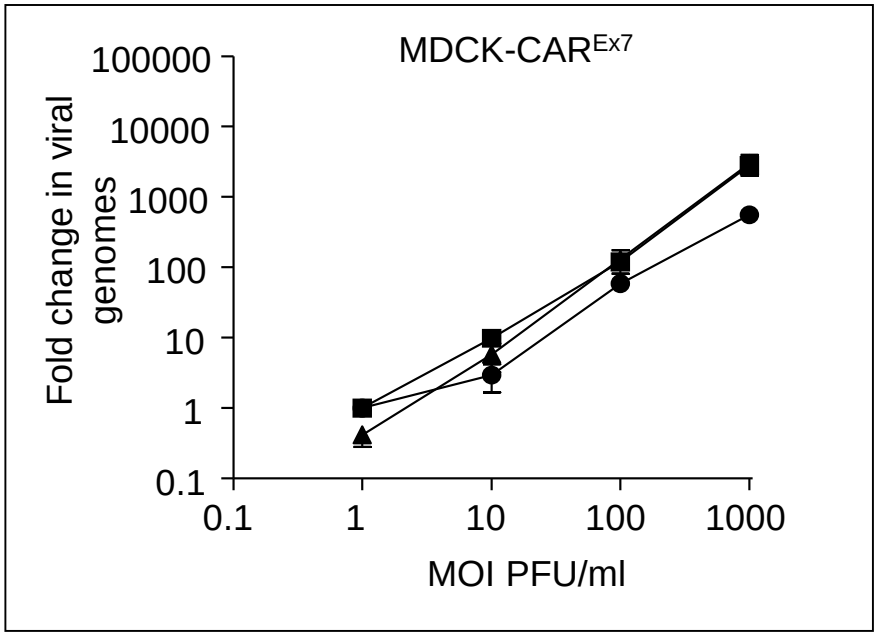

Figure 31: Neutrophils enhance adenovirus entry into polarized epithelia but CAR^{Ex7} does not. Adenovirus entry was quantitated by qPCR analysis in uninduced MDCK-CAR^{Ex7} cells (circle) and compared with uninduced MDCK-CAR^{Ex7} cells with adhering neutrophils (square) and DOX induced MDCK-CAR^{Ex7} cells with adhering neutrophils (triangle). DOX induced MDCK-CAR^{Ex7} cells with adhered neutrophils had the greatest adenovirus susceptibility

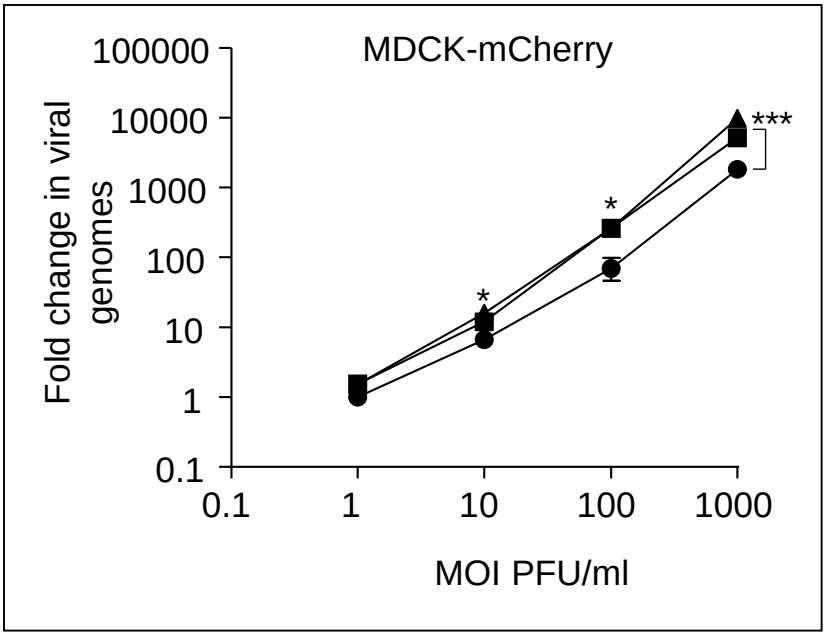

Figure 32: Neutrophils enhance adenovirus entry into polarized epithelia but mCherry and Dox treatment does not. Adenovirus entry was quantitated by qPCR analysis in uninduced MDCK-mCherry cells (circle) and compared with uninduced MDCK-mCherry cells with adhering neutrophils (square) and DOX induced MDCK-mCherry cells with adhering neutrophils (triangle). DOX induced MDCK-mCherry cells with adhered neutrophils had the greatest adenovirus susceptibility. Statistical significance was evaluated using one way ANOVA and Bonferroni post hoc test, *P<.05, ***P<.001,

MDCK-CAR^{Ex8} cells, yet there was no significant difference in the presence of DOX. This data strongly suggests that neutrophils increase adenoviral entry and the presence of increased CAR^{Ex8}, which results in increased neutrophil adhesion, is further amplified.

5.2. Neutrophil adhesion does not decreases transepithelial resistance

5.2.1. Rationale:

The previous experiments do not indicate how neutrophils promote adenoviral infection. Previous studies have shown that neutrophil adhesion at the apical surface of the gut epithelium increased the epithelial cell paracellular permeability in order to promote neutrophil transmigration. There are two measures of epithelial permeability 1) the ability for a current to move through the epithelium, which can be measured by transepithelial resistance, and 2) the ability of small substances to migrate within the paracellular space through the tight junctions and between adjacent cells. Both of these measures frequently correlate, therefore, I first sought to determine the transepithelial resistance in the presence of apically adhered neutrophils.

5.2.2. Results:

Neutrophil adhesion at the epithelial apical surface does not decrease the transepithelial resistance

Neutrophil adhesion assay was performed on polarized MDCK-CAR^{Ex8} cells that were either uninduced or induced with DOX. Polarized epithelia with bound neutrophils were submerged and TER measured. Interestingly, we did not observe a decrease in the transepithelial resistance when compared to MDCK-

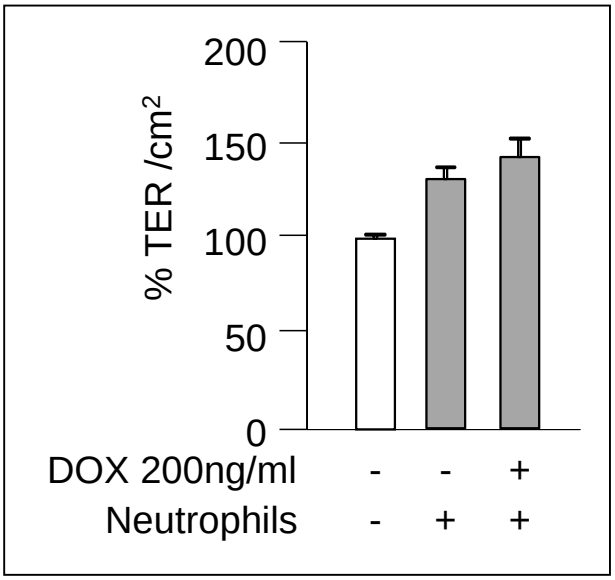

Figure 33: Neutrophil adhesion does not decrease the transepithelial resistance of MDCK-CAR^{Ex8} cells. TER was measured in MDCK-CAR^{Ex8} cells that were not induced with or without neutrophils or DOX-induced MDCK-CAR^{Ex8} cells with tethered neutrophils

CAR^{Ex8} without apically adhered neutrophils (Figure 33). Although there was a trend towards increased TER, this was not significant by one-way ANOVA.

5.3. Discussion:

In this study we have demonstrated a novel function for the apical adenoviral receptor, CAR^{Ex8}. CAR^{Ex8} tethers the infiltrating neutrophils at the epithelial apical surface. Although neutrophils are critical for fighting invading pathogens, the importance of apically adhered neutrophils is not yet well established. It is speculated that under physiological conditions, the apically adhered neutrophils are crucial to enable a close encounter with, and ultimately eradication of, the pathogen. For example, it is known that a threshold number of neutrophils are required to eradicate bacteria [124, 125]. However, apical neutrophil adhesion may be detrimental under pathological conditions. Accumulation of neutrophils at the epithelial cell surface can cause adverse effects on the surrounding tissue. These cells can release inflammatory cytokines which exacerbate the situation. In this study, I show yet another repercussion of accumulated neutrophils at the epithelial apical surface. I have demonstrated that neutrophils promote adenovirus entry into the airway epithelia, which is expected to further contribute to pathology (Figures 29 and 30). Taken together, our data suggests that the adenovirus may have evolved to co-opt the innate immune response of the host, which may have been initiated by the virus. In addition it is possible that under pathological conditions, such as CF, where excess neutrophils accumulate on the cell surface, the adenoviral entry may be further augmented. There could be several mechanisms by which the neutrophils might be promoting

viral infection. For example: 1) as shown with intestinal epithelial cells, it is possible that the apically adhered neutrophils, cause epithelial cell signaling which culminates in the loosening of the junctions to enable increased neutrophil recruitment. This is not likely given that there is no change in TER (Figure 32), 2) apically adhered neutrophils may themselves stimulate apical CAR^{Ex8} localization. While this would accommodate additional infiltrating neutrophils, adenovirus is able to take advantage of the additional receptors to enter the epithelium, 3) the apically adhered neutrophils may release inflammatory mediators that alter the fluid phase endocytosis that occurs at the apical surface. 4) Neutrophil-produced inflammatory mediators may alter epithelial barrier integrity. Future experiments will focus on elucidating the exact mechanism(s) behind enhance viral entry. Understanding this may lead to novel therapies to inhibit adenovirus infection or reduce the toxic effects of chronic inflammation.

Rhinovirus, another viral respiratory pathogen, might be using a similar mechanism as adenovirus to enter into the host epithelial cell from the apical surface of epithelia. Rhinovirus uses ICAM-1 to bind and enter airway epithelial cells. Similar to CAR^{Ex8}, the apical expression and localization of ICAM-1 is regulated by TNF-α and IFN-γ. The expression of ICAM-1 is tightly regulated and usually kept very low. However, when the epithelium is exposed to TNF-α or IFN-γ, ICAM-1 expression is augmented and focused at the apical surface where it can tether neutrophils. Rhinovirus that might have gained entry into airway can take advantage of this host response to enter the epithelium. Therefore, decoding the

mechanism of viral entry will help design novel interventions that may prevent the infections of other viruses, which currently have no specific treatments.

Chapter 6: Global Discussion

CAR is the primary receptor for most adenovirus types. The apical isoform of CAR (CAR^{Ex8}) is identical to the basolateral isoform of CAR (CAR^{Ex7}) except for the C-terminal 13 or 26 amino acids that are unique to CAR^{Ex8} or CAR^{Ex7}, respectively. This seemingly minor difference in C-termini has a tremendous effect on the subcellular localization of the two isoforms. Understanding the molecular mechanism of apical CAR^{Ex8} regulation is important because both increasing and decreasing the concentration of apical viral receptor will have direct implications in the development of interventions for both augmenting adenoviral based vector entry and reducing susceptibility to wild type adenovirus in the event of an outbreak.

IL-8 is a proinflammatory cytokine and neutrophil chemoattractant secreted at the time of pathogenic intrusion. IL-8 is secreted by the epithelium itself and by resident macrophages in the lung [126]. A polarized secretion of IL-8 at the epithelial apical surface generates the chemotactic gradient that facilitates neutrophil recruitment [127]. In this study, we show that IL-8 increases CAR^{Ex8} expression and localization on the apical surface of Calu-3 cells as well as in primary human airway epithelia (Figures 7, 9 and 11). It is also demonstrated that IL-8, via differential activation of AKT/S6K (Figures 15 and 16) and inactivation of GSK3β (Figure 18), stimulates CAR^{Ex8} protein synthesis without altering mRNA

levels. While the pathway IL-8/AKT/S6K in CAR regulation is novel and exciting, the involvement of other signaling proteins in the pathway cannot be ruled out and is yet to be determined. This data suggested that CAR^{Ex8} might have a role in the host innate immune response. Therefore, I sought to determine the biological function of CAR^{Ex8}. Neutrophils are typically found at the epithelial apical surface after the transmigrating through epithelial paracellular space. This is an essential step to obtain the critical neutrophil concentration required to clear invading pathogens and other pro-inflammatory molecules efficiently.

Therefore, I hypothesized that apical CAR^{Ex8} tethers infiltrating neutrophils at the epithelial apical surface. In agreement with the hypothesis, I was able to demonstrate that CAR^{Ex8} binds neutrophils at the apical surface (Figure 24). Moreover, CAR^{Ex8} adheres neutrophils infiltrating from the basolateral surface to the apical surface of the epithelium (Figure 28C and D). It was also demonstrated that IL-8 augments neutrophil adhesion coincident with stimulating CAR^{Ex8} apical localization (Figure 26). Additionally, previous studies have shown that CAR^{Ex7} (basolateral CAR) interacts with neutrophil expressed JAML and that this interaction is important for the proper transmigration of neutrophils across the epithelium. In agreement with this, I have shown that overexpressing CAR^{Ex7} stimulates neutrophil transmigration across the polarized epithelium (Figure 28E and F).

Taken together, these data strongly suggest that a biological function of CAR^{Ex8} is to tether infiltrating neutrophils at the epithelial apical surface. The present study has found a novel function of CAR^{Ex8} as a mediator of the innate

immune response. While I found that this is an IL-8-mediated effect, it is also very likely that this might be a general mechanism used by other pro-inflammatory cytokines, such as IL-1β and IL-6, and opens a new area of research in the field.

We next considered the fate of the invading adenovirus that may have gained entry into the airway. Adenovirus, via its protruding fiber knob, binds to CAR at the same extracellular region, which CAR uses to interact with JAML. Therefore I asked whether the apically bound neutrophils protect the epithelium from the invading adenovirus, or if invading adenovirus is able to outcompete the neutrophils for the extracellular binding site on CAR^{Ex8}. Surprisingly, it was found that apically adhered neutrophils increased adenoviral entry (Figures 29 and 30). I first hypothesized that the neutrophils were destroying the tight junctions of the epithelium allowing the virus access to basolateral CAR^{Ex7}. However, there was no drop in the transepithelial resistance of the polarized epithelium (Figure 33), an event that is required for the virus to access basolateral CAR^{Ex7}. It could be possible that adhered neutrophil-mediated signaling at the apical surface stimulates CAR^{Ex8} apical localization, thus promoting infection. Therefore, it is important in the future to determine the exact mechanism of increased adenovirus entry.

Taking all of these data together, it is envisioned that, IL-8 augments the expression of CAR^{Ex8} at the apical surface of the epithelia to tether the infiltrating neutrophils. However, if adenovirus happens to gain entry into the airway through a droplet, it can hijack the innate host immune response to gain entry into the cell by attaching to the CAR^{Ex8} recruited to the apical surface (Figure 34). Previously,

it was assumed that adenovirus must breach the barrier to access its primary receptor. My data provides a mechanism and an explanation as to how the virus might infect the intact epithelium without breaching the barrier. Under pathological conditions, like in the case of CF where resident bacterial biofilms constantly cause inflammation, this reaction might be amplified leading to secondary infection with the virus.

A similar mechanism may be used by rhinovirus as well. Rhinovirus is the most common human cold virus. ICAM-1 is the primary receptor for rhinovirus [128]. The apical expression of ICAM-1 is induced by proinflammatory cytokines TNF-α and IFN-γ [10, 53]. ICAM-1 can tether neutrophils on the apical surface of both airway and intestinal epithelia [52, 110]. Different cytokines use different receptors to trigger cellular signaling cascades. Therefore, the kind of cytokine plays a critical role in the type of response initiated [129]. In the future it will be interesting to test if IL-8 has an effect on ICAM-1 and if TNF-α/IFN-γ can regulate the expression of CAR^{Ex8}. It appears that both adenovirus and rhinovirus have evolved to take advantage of the innate immune response to other pathogens.

CF is characterized by the accumulation of neutrophils at the mucus surface of the epithelium. Viral infections are one of the major causes for the exacerbation of CF and acute respiratory distress in CF patients [130]. My data suggests that the neutrophils accumulated at the apical surface favors adenoviral infection. Our study has generated a platform for understanding the mechanisms for viral infection in inflammatory diseases and could ultimately aid in the development of novel therapeutics for inflammatory diseases and to reduce viral-mediated

exacerbation of disease. Yet, there are many questions that remain to be answered, such as whether this scenario is observed in healthy individuals. If so, why do neutrophils promote adenoviral entry while they are for the protection of the host? One possible explanation could be that *in vivo*, the effect of IL-8 mediated increase in CAR^{Ex8} expression, localization, and adhesion of neutrophils is counteracted by other cytokines, or other factors, which are missing when using *in vitro* models.

Our lab is currently working on designing drugable peptides that can either increase or decrease the expression of CAR^{Ex8} at the apical surface of polarized epithelium. In future, we hope to test these peptides for their ability to augment or reduce the epithelial susceptibility to adenoviral infection and retain, recruit or release neutrophils, based on patient needs.

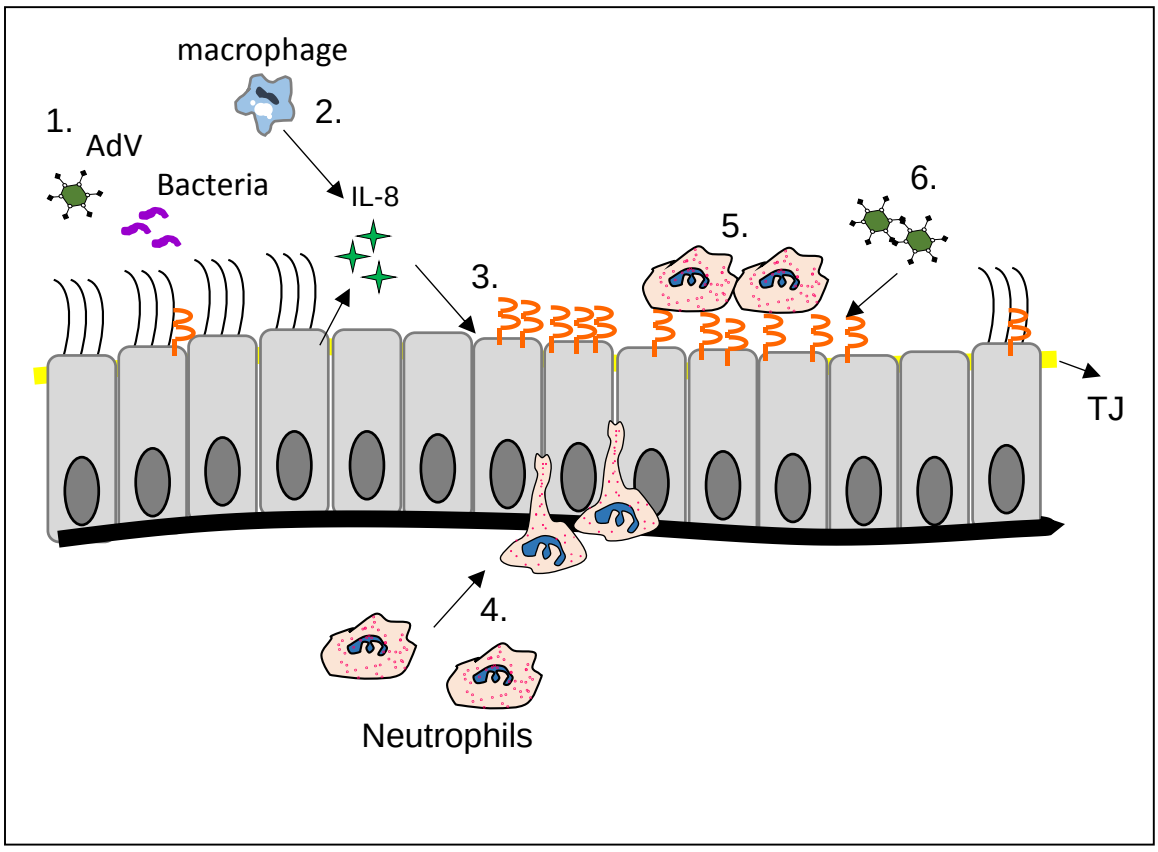

Figure 34: Schematic for the evolution of apical adenovirus infection 1) pathogenic invasion of the airway causes 2) both the resident macrophages and the epithelial cells to secrete IL-8. 3) IL-8 augments the protein synthesis and apical localization of CAR^{Ex8}. 4) In addition, IL-8 also recruits neutrophils that transmigrate through the epithelium from the basal surface to the apical surface. 5) On the epithelial apical surface, the neutrophils adhere in a CAR^{Ex8} dependent manner. 6) At the same time, adenovirus that has gained entry into the airway can hijack the host innate immune response to gain entry into the host cell. TJ – Tight junction

References:

1. Chin, A.C. and C.A. Parkos, *Pathobiology of neutrophil transepithelial migration: implications in mediating epithelial injury.* Annu Rev Pathol, 2007. **2**: p. 111-43.
2. Furuse, M., *Molecular basis of the core structure of tight junctions.* Cold Spring Harb Perspect Biol, 2010. **2**(1): p. a002907.
3. Coyne, C.B. and J.M. Bergelson, *CAR: a virus receptor within the tight junction.* Adv Drug Deliv Rev, 2005. **57**(6): p. 869-82.
4. Walters, R.W., et al., *Adenovirus fiber disrupts CAR-mediated intercellular adhesion allowing virus escape.* Cell, 2002. **110**(6): p. 789-99.
5. Brasch, J., et al., *Thinking outside the cell: how cadherins drive adhesion.* Trends Cell Biol, 2012. **22**(6): p. 299-310.
6. Vincent, T., et al., *Cytokine-mediated downregulation of coxsackievirus-adenovirus receptor in endothelial cells.* J Virol, 2004. **78**(15): p. 8047-58.
7. Coyne, C.B., et al., *Regulation of airway tight junctions by proinflammatory cytokines.* Mol Biol Cell, 2002. **13**(9): p. 3218-34.
8. Bruewer, M., et al., *Interferon-gamma induces internalization of epithelial tight junction proteins via a macropinocytosis-like process.* FASEB J, 2005. **19**(8): p. 923-33.
9. Ivanov, A.I., A. Nusrat, and C.A. Parkos, *Endocytosis of the apical junctional complex: mechanisms and possible roles in regulation of epithelial barriers.* Bioessays, 2005. **27**(4): p. 356-65.
10. Parkos, C.A., et al., *Expression and polarization of intercellular adhesion molecule-1 on human intestinal epithelia: consequences for CD11b/CD18-mediated interactions with neutrophils.* Mol Med, 1996. **2**(4): p. 489-505.
11. Guglielmi, K.M., et al., *Reovirus binding determinants in junctional adhesion molecule-A.* J Biol Chem, 2007. **282**(24): p. 17930-40.
12. Benedicto, I., et al., *The tight junction-associated protein occludin is required for a postbinding step in hepatitis C virus entry and infection.* J Virol, 2009. **83**(16): p. 8012-20.
13. Muhlebach, M.D., et al., *Adherens junction protein nectin-4 is the epithelial receptor for measles virus.* Nature, 2011. **480**(7378): p. 530-3.
14. Mapoles, J.E., D.L. Krah, and R.L. Crowell, *Purification of a HeLa cell receptor protein for group B coxsackieviruses.* J Virol, 1985. **55**(3): p. 560-6.
15. Bergelson, J.M., et al., *Isolation of a common receptor for Coxsackie B viruses and adenoviruses 2 and 5.* Science, 1997. **275**(5304): p. 1320-3.
16. Coyne, C.B. and J.M. Bergelson, *Virus-induced Abl and Fyn kinase signals permit coxsackievirus entry through epithelial tight junctions.* Cell, 2006. **124**(1): p. 119-31.
17. Danthi, P., et al., *Reovirus receptors, cell entry, and proapoptotic signaling.* Adv Exp Med Biol, 2013. **790**: p. 42-71.
18. Excoffon, K.J., et al., *Isoform-specific regulation and localization of the coxsackie and adenovirus receptor in human airway epithelia.* PLoS One, 2010. **5**(3): p. e9909.
19. Kolawole, A.O., et al., *The PDZ1 and PDZ3 domains of MAGI-1 regulate the eight-exon isoform of the coxsackievirus and adenovirus receptor.* J Virol, 2012. **86**(17): p. 9244-54.
20. Sharma, P., et al., *Sidestream smoke exposure increases the susceptibility of airway epithelia to adenoviral infection.* PLoS One, 2012. **7**(11): p. e49930.
21. Hayashi, S. and J.C. Hogg, *Adenovirus infections and lung disease.* Curr Opin Pharmacol, 2007. **7**(3): p. 237-43.
22. Nazir, S.A. and J.P. Metcalf, *Innate immune response to adenovirus.* J Investig Med, 2005. **53**(6): p. 292-304.

23. Hall, K., M.E. Blair Zajdel, and G.E. Blair, *Unity and diversity in the human adenoviruses: exploiting alternative entry pathways for gene therapy.* Biochem J, 2010. **431**(3): p. 321-36.
24. van Raaij, M.J., et al., *Dimeric structure of the coxsackievirus and adenovirus receptor D1 domain at 1.7 A resolution.* Structure, 2000. **8**(11): p. 1147-55.
25. Meier, O. and U.F. Greber, *Adenovirus endocytosis.* J Gene Med, 2004. **6 Suppl 1**: p. S152-63.
26. Wolfrum, N. and U.F. Greber, *Adenovirus signalling in entry.* Cell Microbiol, 2013. **15**(1): p. 53-62.
27. Cohen, C.J., et al., *Multiple regions within the coxsackievirus and adenovirus receptor cytoplasmic domain are required for basolateral sorting.* J Biol Chem, 2001. **276**(27): p. 25392-8.
28. Hong, S.S., et al., *Adenovirus type 5 fiber knob binds to MHC class I alpha2 domain at the surface of human epithelial and B lymphoblastoid cells.* EMBO J, 1997. **16**(9): p. 2294-306.
29. Arnberg, N., et al., *Adenovirus type 37 uses sialic acid as a cellular receptor.* J Virol, 2000. **74**(1): p. 42-8.
30. Doronin, K., et al., *Coagulation factor X activates innate immunity to human species C adenovirus.* Science, 2012. **338**(6108): p. 795-8.
31. Ashbourne Excoffon, K.J., T. Moninger, and J. Zabner, *The coxsackie B virus and adenovirus receptor resides in a distinct membrane microdomain.* J Virol, 2003. **77**(4): p. 2559-67.
32. Meier, O., et al., *Adenovirus triggers macropinocytosis and endosomal leakage together with its clathrin-mediated uptake.* J Cell Biol, 2002. **158**(6): p. 1119-31.
33. Henaff, D., S. Salinas, and E.J. Kremer, *An adenovirus traffic update: from receptor engagement to the nuclear pore.* Future Microbiol, 2011. **6**(2): p. 179-92.
34. Carson, S.D., N.N. Chapman, and S.M. Tracy, *Purification of the putative coxsackievirus B receptor from HeLa cells.* Biochem Biophys Res Commun, 1997. **233**(2): p. 325-8.
35. Tomko, R.P., R. Xu, and L. Philipson, *HCAR and MCAR: the human and mouse cellular receptors for subgroup C adenoviruses and group B coxsackieviruses.* Proc Natl Acad Sci U S A, 1997. **94**(7): p. 3352-6.
36. Freimuth, P., L. Philipson, and S.D. Carson, *The coxsackievirus and adenovirus receptor.* Curr Top Microbiol Immunol, 2008. **323**: p. 67-87.
37. Asher, D.R., et al., *Coxsackievirus and adenovirus receptor is essential for cardiomyocyte development.* Genesis, 2005. **42**(2): p. 77-85.
38. Mirza, M., et al., *Essential role of the coxsackie- and adenovirus receptor (CAR) in development of the lymphatic system in mice.* PLoS One, 2012. **7**(5): p. e37523.
39. Nagai, M., et al., *Coxsackievirus and adenovirus receptor, a tight junction membrane protein, is expressed in glomerular podocytes in the kidney.* Lab Invest, 2003. **83**(6): p. 901-11.
40. Okegawa, T., et al., *The mechanism of the growth-inhibitory effect of coxsackie and adenovirus receptor (CAR) on human bladder cancer: a functional analysis of car protein structure.* Cancer Res, 2001. **61**(17): p. 6592-600.
41. Bewley, M.C., et al., *Structural analysis of the mechanism of adenovirus binding to its human cellular receptor, CAR.* Science, 1999. **286**(5444): p. 1579-83.
42. Sharma, P., et al., *Accessibility of the coxsackievirus and adenovirus receptor and its importance in adenovirus gene transduction efficiency.* J Gen Virol, 2012. **93**(Pt 1): p. 155-8.

43. Moog-Lutz, C., et al., *JAML, a novel protein with characteristics of a junctional adhesion molecule, is induced during differentiation of myeloid leukemia cells.* Blood, 2003. **102**(9): p. 3371-8.
44. Zen, K., et al., *Neutrophil migration across tight junctions is mediated by adhesive interactions between epithelial coxsackie and adenovirus receptor and a junctional adhesion molecule-like protein on neutrophils.* Mol Biol Cell, 2005. **16**(6): p. 2694-703.
45. Witherden, D.A., et al., *The junctional adhesion molecule JAML is a costimulatory receptor for epithelial gammadelta T cell activation.* Science, 2010. **329**(5996): p. 1205-10.
46. Luissint, A.C., et al., *JAM-L-mediated leukocyte adhesion to endothelial cells is regulated in cis by alpha4beta1 integrin activation.* J Cell Biol, 2008. **183**(6): p. 1159-73.
47. Verdino, P., et al., *The molecular interaction of CAR and JAML recruits the central cell signal transducer PI3K.* Science, 2010. **329**(5996): p. 1210-4.
48. Kirby, I., et al., *Identification of contact residues and definition of the CAR-binding site of adenovirus type 5 fiber protein.* J Virol, 2000. **74**(6): p. 2804-13.
49. Moutsopoulos, N.M., et al., *Defective neutrophil recruitment in leukocyte adhesion deficiency type I disease causes local IL-17-driven inflammatory bone loss.* Sci Transl Med, 2014. **6**(229): p. 229ra40.
50. Del Rio, L., et al., *CXCR2 deficiency confers impaired neutrophil recruitment and increased susceptibility during Toxoplasma gondii infection.* J Immunol, 2001. **167**(11): p. 6503-9.
51. Zemans, R.L., S.P. Colgan, and G.P. Downey, *Transepithelial migration of neutrophils: mechanisms and implications for acute lung injury.* Am J Respir Cell Mol Biol, 2009. **40**(5): p. 519-35.
52. Sumagin, R., et al., *Transmigrated neutrophils in the intestinal lumen engage ICAM-1 to regulate the epithelial barrier and neutrophil recruitment.* Mucosal Immunol, 2014. **7**(4): p. 905-15.
53. Konno, S., et al., *Interferon-gamma enhances rhinovirus-induced RANTES secretion by airway epithelial cells.* Am J Respir Cell Mol Biol, 2002. **26**(5): p. 594-601.
54. Edens, H.A., et al., *Neutrophil transepithelial migration: evidence for sequential, contact-dependent signaling events and enhanced paracellular permeability independent of transjunctional migration.* J Immunol, 2002. **169**(1): p. 476-86.
55. Zen, K. and C.A. Parkos, *Leukocyte-epithelial interactions.* Curr Opin Cell Biol, 2003. **15**(5): p. 557-64.
56. Chin, A.C., et al., *Neutrophil-mediated activation of epithelial protease-activated receptors-1 and -2 regulates barrier function and transepithelial migration.* J Immunol, 2008. **181**(8): p. 5702-10.
57. Zen, K., et al., *JAM-C is a component of desmosomes and a ligand for CD11b/CD18-mediated neutrophil transepithelial migration.* Mol Biol Cell, 2004. **15**(8): p. 3926-37.
58. Lawrence, D.W., et al., *Antiadhesive role of apical decay-accelerating factor (CD55) in human neutrophil transmigration across mucosal epithelia.* J Exp Med, 2003. **198**(7): p. 999-1010.
59. Brazil, J.C., et al., *Neutrophil migration across intestinal epithelium: evidence for a role of CD44 in regulating detachment of migrating cells from the luminal surface.* J Immunol, 2010. **185**(11): p. 7026-36.
60. Persson, C.G. and L. Uller, *Resolution of cell-mediated airways diseases.* Respir Res, 2010. **11**: p. 75.
61. O'Donnell, R., et al., *Inflammatory cells in the airways in COPD.* Thorax, 2006. **61**(5): p. 448-54.

62. Rowe, S.M., S. Miller, and E.J. Sorscher, *Cystic fibrosis.* N Engl J Med, 2005. **352**(19): p. 1992-2001.
63. Peters, S., *Cystic fibrosis: a review of pathophysiology and current treatment recommendations.* S D Med, 2014. **67**(4): p. 148-51, 153.
64. Clunes, M.T. and R.C. Boucher, *Cystic Fibrosis: The Mechanisms of Pathogenesis of an Inherited Lung Disorder.* Drug Discov Today Dis Mech, 2007. **4**(2): p. 63-72.
65. Ehre, C., C. Ridley, and D.J. Thornton, *Cystic fibrosis: An inherited disease affecting mucin-producing organs.* Int J Biochem Cell Biol, 2014. **52C**: p. 136-145.
66. Burns, J.L., et al., *Respiratory viruses in children with cystic fibrosis: viral detection and clinical findings.* Influenza Other Respi Viruses, 2012. **6**(3): p. 218-23.
67. Frickmann, H., et al., *Spectrum of viral infections in patients with cystic fibrosis.* Eur J Microbiol Immunol (Bp), 2012. **2**(3): p. 161-175.
68. Rosenecker, J., et al., *Adenovirus infection in cystic fibrosis patients: implications for the use of adenoviral vectors for gene transfer.* Infection, 1996. **24**(1): p. 5-8.
69. Downey, D.G., S.C. Bell, and J.S. Elborn, *Neutrophils in cystic fibrosis.* Thorax, 2009. **64**(1): p. 81-8.
70. Gern, J.E., et al., *Rhinovirus enters but does not replicate inside monocytes and airway macrophages.* J Immunol, 1996. **156**(2): p. 621-7.
71. Lutschg, V., et al., *Chemotactic antiviral cytokines promote infectious apical entry of human adenovirus into polarized epithelial cells.* Nat Commun, 2011. **2**: p. 391.
72. Walters, R.W., et al., *Basolateral localization of fiber receptors limits adenovirus infection from the apical surface of airway epithelia.* J Biol Chem, 1999. **274**(15): p. 10219-26.
73. Majhen, D., et al., *Increased expression of the coxsackie and adenovirus receptor downregulates alphavbeta3 and alphavbeta5 integrin expression and reduces cell adhesion and migration.* Life Sci, 2011. **89**(7-8): p. 241-9.
74. Excoffon, K.J., et al., *Functional effects of coxsackievirus and adenovirus receptor glycosylation on homophilic adhesion and adenoviral infection.* J Virol, 2007. **81**(11): p. 5573-8.
75. Liu, X., et al., *ROCK inhibitor and feeder cells induce the conditional reprogramming of epithelial cells.* Am J Pathol, 2012. **180**(2): p. 599-607.
76. Rheinwald, J.G. and H. Green, *Serial cultivation of strains of human epidermal keratinocytes: the formation of keratinizing colonies from single cells.* Cell, 1975. **6**(3): p. 331-43.
77. Foster, K.A., et al., *Characterization of the Calu-3 cell line as a tool to screen pulmonary drug delivery.* Int J Pharm, 2000. **208**(1-2): p. 1-11.
78. Tseng, C.T., et al., *Apical entry and release of severe acute respiratory syndrome-associated coronavirus in polarized Calu-3 lung epithelial cells.* J Virol, 2005. **79**(15): p. 9470-9.
79. Karp, P.H., et al., *An in vitro model of differentiated human airway epithelia. Methods for establishing primary cultures.* Methods Mol Biol, 2002. **188**: p. 115-37.
80. Greber, U.F., et al., *Stepwise dismantling of adenovirus 2 during entry into cells.* Cell, 1993. **75**(3): p. 477-86.
81. Zhu, Y., A. Chidekel, and T.H. Shaffer, *Cultured human airway epithelial cells (calu-3): a model of human respiratory function, structure, and inflammatory responses.* Crit Care Res Pract, 2010. **2010**.
82. Harcourt, J.L., et al., *Evaluation of the Calu-3 cell line as a model of in vitro respiratory syncytial virus infection.* J Virol Methods, 2011. **174**(1-2): p. 144-9.

83. MacManus, C.F., et al., *Interleukin-8 signaling promotes translational regulation of cyclin D in androgen-independent prostate cancer cells.* Mol Cancer Res, 2007. **5**(7): p. 737-48.
84. Grimes, C.A. and R.S. Jope, *The multifaceted roles of glycogen synthase kinase 3beta in cellular signaling.* Prog Neurobiol, 2001. **65**(4): p. 391-426.
85. Rommel, C., et al., *Mediation of IGF-1-induced skeletal myotube hypertrophy by PI(3)K/Akt/mTOR and PI(3)K/Akt/GSK3 pathways.* Nat Cell Biol, 2001. **3**(11): p. 1009-13.
86. Wang, X., et al., *Eukaryotic initiation factor 2B: identification of multiple phosphorylation sites in the epsilon-subunit and their functions in vivo.* EMBO J, 2001. **20**(16): p. 4349-59.
87. Welsh, G.I., et al., *Regulation of eukaryotic initiation factor eIF2B: glycogen synthase kinase-3 phosphorylates a conserved serine which undergoes dephosphorylation in response to insulin.* FEBS Lett, 1998. **421**(2): p. 125-30.
88. Welsh, G.I. and C.G. Proud, *Glycogen synthase kinase-3 is rapidly inactivated in response to insulin and phosphorylates eukaryotic initiation factor eIF-2B.* Biochem J, 1993. **294 (Pt 3)**: p. 625-9.
89. Woods, Y.L., et al., *The kinase DYRK phosphorylates protein-synthesis initiation factor eIF2Bepsilon at Ser539 and the microtubule-associated protein tau at Thr212: potential role for DYRK as a glycogen synthase kinase 3-priming kinase.* Biochem J, 2001. **355**(Pt 3): p. 609-15.
90. Welsh, G.I., C. Wilson, and C.G. Proud, *GSK3: a SHAGGY frog story.* Trends Cell Biol, 1996. **6**(7): p. 274-9.
91. Cross, D.A., et al., *Inhibition of glycogen synthase kinase-3 by insulin mediated by protein kinase B.* Nature, 1995. **378**(6559): p. 785-9.
92. Liang, M.H. and D.M. Chuang, *Regulation and function of glycogen synthase kinase-3 isoforms in neuronal survival.* J Biol Chem, 2007. **282**(6): p. 3904-17.
93. Fulcher, M.L., et al., *Well-differentiated human airway epithelial cell cultures.* Methods Mol Med, 2005. **107**: p. 183-206.
94. Pezzulo, A.A., et al., *The air-liquid interface and use of primary cell cultures are important to recapitulate the transcriptional profile of in vivo airway epithelia.* Am J Physiol Lung Cell Mol Physiol, 2011. **300**(1): p. L25-31.
95. Wessler, S. and S. Backert, *Molecular mechanisms of epithelial-barrier disruption by Helicobacter pylori.* Trends Microbiol, 2008. **16**(8): p. 397-405.
96. Braum, O., M. Klages, and H. Fickenscher, *The cationic cytokine IL-26 differentially modulates virus infection in culture.* PLoS One, 2013. **8**(7): p. e70281.
97. Schaller, M., et al., *Respiratory viral infections drive chemokine expression and exacerbate the asthmatic response.* J Allergy Clin Immunol, 2006. **118**(2): p. 295-302; quiz 303-4.
98. Stroobant, J., *Viral infection in cystic fibrosis.* J R Soc Med, 1986. **79 Suppl 12**: p. 19-22.
99. Gern, J.E., et al., *Comparison of the etiology of viral respiratory illnesses in inner-city and suburban infants.* J Infect Dis, 2012. **206**(9): p. 1342-9.
100. Waugh, D.J. and C. Wilson, *The interleukin-8 pathway in cancer.* Clin Cancer Res, 2008. **14**(21): p. 6735-41.
101. Sabroe, I., et al., *Chemoattractant cross-desensitization of the human neutrophil IL-8 receptor involves receptor internalization and differential receptor subtype regulation.* J Immunol, 1997. **158**(3): p. 1361-9.
102. Magnuson, B., B. Ekim, and D.C. Fingar, *Regulation and function of ribosomal protein S6 kinase (S6K) within mTOR signalling networks.* Biochem J, 2012. **441**(1): p. 1-21.
103. Acosta-Jaquez, H.A., et al., *Site-specific mTOR phosphorylation promotes mTORC1-mediated signaling and cell growth.* Mol Cell Biol, 2009. **29**(15): p. 4308-24.

104. Pullen, N., et al., *Phosphorylation and activation of p70s6k by PDK1.* Science, 1998. **279**(5351): p. 707-10.
105. Rayasam, G.V., et al., *Glycogen synthase kinase 3: more than a namesake.* Br J Pharmacol, 2009. **156**(6): p. 885-98.
106. Yamaguchi, H., J.L. Hsu, and M.C. Hung, *Regulation of ubiquitination-mediated protein degradation by survival kinases in cancer.* Front Oncol, 2012. **2**: p. 15.
107. Wang, H., et al., *Desmoglein 2 is a receptor for adenovirus serotypes 3, 7, 11 and 14.* Nat Med, 2011. **17**(1): p. 96-104.
108. Krakauer, T., *Stimulant-dependent modulation of cytokines and chemokines by airway epithelial cells: cross talk between pulmonary epithelial and peripheral blood mononuclear cells.* Clin Diagn Lab Immunol, 2002. **9**(1): p. 126-31.
109. Barker, J.N., et al., *Modulation of keratinocyte-derived interleukin-8 which is chemotactic for neutrophils and T lymphocytes.* Am J Pathol, 1991. **139**(4): p. 869-76.
110. Tabary, O., et al., *Adherence of airway neutrophils and inflammatory response are increased in CF airway epithelial cell-neutrophil interactions.* Am J Physiol Lung Cell Mol Physiol, 2006. **290**(3): p. L588-96.
111. Huang, G.T., et al., *Infection of human intestinal epithelial cells with invasive bacteria upregulates apical intercellular adhesion molecule-1 (ICAM)-1) expression and neutrophil adhesion.* J Clin Invest, 1996. **98**(2): p. 572-83.
112. Osawa, Y., et al., *Tumor necrosis factor alpha-induced interleukin-8 production via NF-kappaB and phosphatidylinositol 3-kinase/Akt pathways inhibits cell apoptosis in human hepatocytes.* Infect Immun, 2002. **70**(11): p. 6294-301.
113. Decramer, M., et al., *COPD as a lung disease with systemic consequences--clinical impact, mechanisms, and potential for early intervention.* COPD, 2008. **5**(4): p. 235-56.
114. Sethi, S., et al., *Inflammation in COPD: implications for management.* Am J Med, 2012. **125**(12): p. 1162-70.
115. Snelgrove, R.J., A. Godlee, and T. Hussell, *Airway immune homeostasis and implications for influenza-induced inflammation.* Trends Immunol, 2011. **32**(7): p. 328-34.
116. Franz, A., et al., *Correlation of viral load of respiratory pathogens and co-infections with disease severity in children hospitalized for lower respiratory tract infection.* J Clin Virol, 2010. **48**(4): p. 239-45.
117. Antunes, H., et al., *Etiology of bronchiolitis in a hospitalized pediatric population: prospective multicenter study.* J Clin Virol, 2010. **48**(2): p. 134-6.
118. Calvo, C., et al., *Detection of new respiratory viruses in hospitalized infants with bronchiolitis: a three-year prospective study.* Acta Paediatr, 2010. **99**(6): p. 883-7.
119. Stempel, H.E., et al., *Multiple viral respiratory pathogens in children with bronchiolitis.* Acta Paediatr, 2009. **98**(1): p. 123-6.
120. Berk, A., *Adenoviridae: The Viruses and Their Replication*. 5th ed. Fields Virology, ed. D.K.a.P. Howley. Vol. 2. 2007, Philadelphia: Lippincott Williams and Wilkins.
121. Gern, J.E., et al., *Effects of viral respiratory infections on lung development and childhood asthma.* J Allergy Clin Immunol, 2005. **115**(4): p. 668-74; quiz 675.
122. Hogg, J.C., *Role of latent viral infections in chronic obstructive pulmonary disease and asthma.* Am J Respir Crit Care Med, 2001. **164**(10 Pt 2): p. S71-5.
123. Currie, A.J., D.P. Speert, and D.J. Davidson, *Pseudomonas aeruginosa: role in the pathogenesis of the CF lung lesion.* Semin Respir Crit Care Med, 2003. **24**(6): p. 671-80.
124. Li, Y., et al., *Determination of the critical concentration of neutrophils required to block bacterial growth in tissues.* J Exp Med, 2004. **200**(5): p. 613-22.

125. Malka, R., et al., *Evidence for bistable bacteria-neutrophil interaction and its clinical implications.* J Clin Invest, 2012. **122**(8): p. 3002-11.
126. Conese, M., et al., *Neutrophil recruitment and airway epithelial cell involvement in chronic cystic fibrosis lung disease.* J Cyst Fibros, 2003. **2**(3): p. 129-35.
127. Chow, A.W., et al., *Polarized secretion of interleukin (IL)-6 and IL-8 by human airway epithelia 16HBE14o- cells in response to cationic polypeptide challenge.* PLoS One, 2010. **5**(8): p. e12091.
128. Staunton, D.E., et al., *A cell adhesion molecule, ICAM-1, is the major surface receptor for rhinoviruses.* Cell, 1989. **56**(5): p. 849-53.
129. Mayer, G. *Cytokines and immunoregulation*. 2010; Available from: http://pathmicro.med.sc.edu/bowers/imm-reg-ver2.htm.
130. Wat, D. and I. Doull, *Respiratory virus infections in cystic fibrosis.* Paediatr Respir Rev, 2003. **4**(3): p. 172-7.